

VIRULENCE-ASSOCIATED PROTEINS OF TYPE III SECRETION SYSTEMS

**CHARACTERIZATION OF VIRULENCE-ASSOCIATED PROTEINS OF THE
TYPE III SECRETION SYSTEMS IN ENTERIC PATHOGENS**

By SARAH E. ALLISON, B.Sc., M.Sc.

A Thesis Submitted to the School of Graduate Studies in Partial Fulfilment of the
Requirement for the Degree Doctor of Philosophy

McMaster University © Copyright by Sarah E. Allison, September 2014

McMaster University DOCTOR OF PHILOSOPHY (2014) Hamilton, Ontario
(Biochemistry and Biomedical Sciences)

TITLE: Characterization of Virulence-Associated Proteins of the Type III Secretion
Systems in Enteric Pathogens

AUTHOR: Sarah E. Allison, B.Sc., M.Sc. (McMaster University)

SUPERVISOR: Dr. Brian K. Coombes

NUMBER OF PAGES: xi, 150

ABSTRACT

Enteric pathogens have a substantial impact on human health as they can cause outbreaks and severe disease outcomes. These pathogens employ many virulence strategies to evade host defenses and cause disease. While some virulence strategies have been carefully studied, other mechanisms remain largely uncharacterized. In addition, there are a number of putative virulence factors that have yet to be phenotypically or biochemically characterized. In order to facilitate the development of novel and effective treatment strategies for enteric pathogens, an understanding of how these putative virulence-associated proteins contribute to pathogenesis is required. In this work, the characterizations of two proteins implicated in the processes of motility and type III secretion are presented. The *Escherichia coli* O157:H7 protein Z0021 is found in an O-island unique to the most virulent serotypes of Shiga-toxin producing *E. coli*. Z0021 was found to encode for a repressor of motility that exerted its regulatory effect prior to the activation of class II promoters in the flagellar cascade. This work provided the first identification and characterization of a fimbrial operon-encoded motility repressor in *E. coli* O157:H7. The second protein, SsaN, from *Salmonella enterica* is a putative type III secretion system ATPase. This work examined the role of SsaN in virulence and effector secretion, and moreover provided insight into the mechanism by which SsaN binds to a chaperone to facilitate effector secretion. Together, these findings contribute to the understanding of the virulence strategies of two enteric pathogens that have had, and continue to have, significant impacts on human health worldwide.

ACKNOWLEDGMENTS

First and foremost, I must extend my most sincere thanks to my supervisor, Dr. Brian K. Coombes. I thank you for letting me be a part of your phenomenal research group for the past few years and for your continued support throughout all of my endeavors. Your mentorship, vast scientific knowledge, professionalism, and passion for your work have made it truly joyful learning from you. Thank you. I must also extend my gratitude to my wonderful committee members, Dr. Lori Burrows and Dr. Marie Elliot, who have provided support and great scientific insight into my projects over the years.

To the Coombes lab members, it has been a true pleasure working alongside you. Thank you for your discussions, both academic and non-academic, and for all of your kindness. I have realized that one cannot undervalue the importance of enjoying the company of those that you work with, and I could not have been surrounded by a better group of people. A particular thanks to Brian Tuinema, David Mulder, Sarah Reid-Yu, Cherrie Small, Joseph McPhee, Ellen Everson and Ana Berube for making my time in the Coombes lab so enjoyable. I must also thank the many collaborators that have had a profound impact on the projects that I have undertaken during my graduate studies. A particular thanks to the fantastic Dr. Murray Junop who was always willing to discuss science with me and who played a critical role in the success of the SsaN project. I also extend my appreciation to the other collaborators, some of whom I have met and some of whom I have not, but who have nonetheless contributed to the projects described herein.

I would like to thank my parents for their love and support over the years for which I am forever grateful. As well, I extend a heartfelt thanks to my brothers who have

always been supportive of me. And of course, I thank my husband Sean who I met on this this crazy journey of graduate school. I am truly appreciative of your support, love, and understanding over the years and I am so happy with the family of pets we have surrounded ourselves with. I must give a special mention to Gibson who spent many hours curled up beside me while I wrote this thesis.

TABLE OF CONTENTS

ABSTRACT	iii
ACKNOWLEDGMENTS	iv
TABLE OF CONTENTS	vi
LIST OF TABLES	viii
LIST OF FIGURES	ix
LIST OF ABBREVIATIONS	x
CHAPTER ONE – INTRODUCTION	1
The Impact of Disease Significance of Enteric Pathogens	2
Horizontal Gene Transfer and Pathogenicity Islands.....	5
The Pathogenesis of Enterohemorrhagic <i>Escherichia coli</i> and <i>Salmonella enterica</i>	10
Flagellar Regulation and Assembly	13
Structure and Regulation of <i>Escherichia coli</i> Type I Fimbriae.....	16
The Virulence-Associated Type III Secretion Systems of <i>Salmonella enterica</i>	18
The Link amongst Motility, Adherence, and Type III Secretion Systems.....	30
Purpose and Aims of this Work	32
CHAPTER TWO – Novel Repressor of <i>Escherichia coli</i> O157:H7 Motility Encoded in the Putative Fimbrial Cluster OI-1	38
Co-authorship Statement.....	39
Title Page and Author List.....	40
Abstract	41
Introduction	42
Materials and Methods	45
General methods	45
Construction of mutants and HA-tagged variants	45
Motility assays.....	45
Transmission electron microscopy	46
Western blot analysis	46
Transcriptional reporter assays	47
Quantitative RT-PCR analysis	47
Construction of pFLAG- <i>Z0021</i> and pFLAG- <i>Z0021-flhDC</i>	48
Sequencing <i>Z0021</i> from a STEC strains collection.....	48
Results	50
Deletion of OI-1 increases motility and flagellin production in <i>E. coli</i> O157:H7.....	50
Over-expression of Z0021 inhibits motility in <i>E. coli</i> O157:H7.....	51
Deletion of <i>Z0021</i> increases the transcription of class II and class III promoters.....	51
FlhDC is a high-copy suppressor of the non-motile phenotype associated with over-expression of <i>Z0021</i>	53
Prevalence of <i>Z0021</i> among STEC.....	54
Discussion	55
Acknowledgments	59

CHAPTER THREE – Identification of the Docking Site between a Type III Secretion System ATPase and a Chaperone for Effector Cargo	77
Co-authorship Statement	78
Title Page and Author List	79
Abstract	80
Introduction	81
Materials and Methods	84
Competitive infections	84
Construction of mutant strains	84
<i>Salmonella</i> secretion assays	85
Protein interaction studies	86
Protein purification, activity assays, and circular dichroism	87
Crystallization, data collection and structure determination	87
Results	89
SsaN is essential for virulence in an animal model of infection and for secretion of a subset of SPI-2 effectors	89
Crystal structure of SsaN	90
Placement of SrcA onto hexameric SsaN	92
Experimental validation of the chaperone-T3SS ATPase interface	93
Discussion	97
Acknowledgments	101
CHAPTER FOUR – DISCUSSION	122
Summary of Main Conclusions	123
Future Directions for OI-1 and Z0021-Mediated Repression of Motility	125
Future Directions Addressing the Role of SsaN in Type III Secretion and Beyond	127
Concluding Remarks	130
REFERENCES	132

LIST OF TABLES

Table 2.1	Strains, plasmids and oligonucleotides used in this study.....	74
Table 3.1	Data collection and model refinement statistics.....	116
Table 3.2	SPI-2 effector secretion in $\Delta ssaN$ and $\Delta ssaN\Delta invC$ strains.....	117
Table 3.3	Conservation of chaperone binding domain amongst T3SS ATPases in Gram-negative pathogens.....	118
Table 3.S1	Strains, plasmids and oligonucleotides used in this study.....	119

LIST OF FIGURES

Figure 1.1	Overall structure of the T3SS-2 from <i>Salmonella enterica</i>	34
Figure 1.2	Linking the Flagellar, Fimbrial, and T3SS Assembly Pathways.....	36
Figure 2.1	Genetic organization of O-island 1 in <i>E. coli</i> O157:H7 strain EDL933...	60
Figure 2.2	Deletion of OI-1 increases swimming motility.....	62
Figure 2.3	Deletion of <i>Z0021</i> increases flagellum production in <i>E. coli</i> O157:H7 ...	64
Figure 2.4	Over-expression of <i>Z0021</i> represses swimming motility in <i>E. coli</i> O157:H7 strain EDL933.....	66
Figure 2.5	Deletion of <i>Z0021</i> impacts the flagellar cascade prior to class II/III activation	68
Figure 2.6	Increased expression of <i>flhDC</i> suppresses the non-motile phenotype associated with over-expression of <i>Z0021</i>	70
Figure 2.7	Prevalence of <i>Z0021</i> in Shiga-toxin producing <i>E. coli</i>	72
Figure 3.1	<i>ssaN</i> contributes to pathogenesis in a murine model of typhoid and is required for the secretion of only a subset of SPI-2 effectors.....	102
Figure 3.2	The structure of SsaN _{Δ1-89}	104
Figure 3.3	Structural differences between SsaN and EscN.....	106
Figure 3.4	Structural model of the SrcA-SsaN interaction.....	108
Figure 3.5	Identification of the chaperone binding region on SsaN	110
Figure 3.6	Key residues on SrcA that contribute to the chaperone-T3SS interface.	112
Figure 3.7	Conservation of the putative chaperone binding domain between SsaN and EscN	114

LIST OF ABBREVIATIONS

A/E	Attaching and effacing
bp	Base pair
CCCP	Carbonyl cyanide <i>m</i> -chlorophenylhydrazone
cDNA	Complementary deoxyribonucleic acid
CFU	Colony forming units
CI	Competitive index
Cm	Chloramphenicol
DAEC	Diffusely-adherent <i>E. coli</i>
<i>E. coli</i>	<i>Escherichia coli</i>
EAEC	Enteroaggregative <i>E. coli</i>
EAST1	Enteroaggregative <i>E. coli</i> heat-stable toxin 1
ECP	<i>E. coli</i> common pilus
EDTA	Ethylenediaminetetraacetic acid
Efa-1	EHEC factor for adherence
EHEC	Enterohemorrhagic <i>E. coli</i>
EIEC	Enteroinvasive <i>E. coli</i>
EPEC	Enteropathogenic <i>E. coli</i>
ETEC	Enterotoxigenic <i>E. coli</i>
G + C	Guanine and cytosine
Gb3	Globotriaosylceramide
HA	Hemagglutinin
HGT	Horizontal gene transfer
HUS	Hemolytic uremic syndrome
IPTG	Isopropyl- β -D-1-thiogalactopyranoside
LB	Luria broth
LEE	Locus of enterocyte effacement
Lpf	Long polar fimbriae
LPM medium	Low phosphate and magnesium medium
LT	Heat-labile enterotoxin
M cells	Microfold cells
MAT	Meningitis-associated and temperature-regulated
NF- κ B	Nuclear factor- κ B
OD	Optical density
OI	O-island
OmpA	Outer membrane protein A

Paa	Porcine attaching-effacing associated protein
PAI	Pathogenicity island
PBS	Phosphate buffered saline
PCR	Polymerase chain reaction
qRT-PCR	Quantitative reverse transcription PCR
<i>S. Typhimurium</i>	<i>Salmonella enterica</i> serovar Typhimurium
Saa	STEC autoagglutinating adhesin
SCV	<i>Salmonella</i> -containing vacuole
SDS-PAGE	Sodium dodecyl sulfate-polyacrylamide gel electrophoresis
ShET1	<i>Shigella</i> enterotoxin 1
Sif	<i>Salmonella</i> induced filaments
SILAC	Stable isotope labeling of amino acids in cell culture
SKIP	SifA and kinesin interacting protein
SNPs	Single nucleotide polymorphisms
SPI	<i>Salmonella</i> pathogenicity island
ST	Heat-stable enterotoxin
STEC	Shiga-toxin producing <i>E. coli</i>
Stx	Shiga toxin
TCEP	Tris-(2-carboxyethyl)-phosphine
T3SS	Type III secretion system
TEM	Transmission electron microscopy

CHAPTER ONE
INTRODUCTION

INTRODUCTION

1. The Impact and Disease Significance of Enteric Pathogens

There are a number of bacteria, both commensal and pathogenic, that colonize the gastrointestinal tract of humans (1). Enteric pathogens are of particular clinical significance as they can cause gastroenteritis, and infections can lead to the development of more severe disease outcomes. While a vast number of enteric pathogens are Gram-negative bacteria, this work specifically focuses on the impact and virulence mechanisms of *Escherichia coli* and *Salmonella*.

1.1 – The Impact of Pathogenic *Escherichia coli*

Escherichia coli (*E. coli*) are Gram-negative, facultative anaerobes that are of great importance to human health. The commensal *E. coli* strains that colonize the gastrointestinal tract represent a large component of the intestinal microbiota and are often beneficial to humans, while other species of *E. coli* have evolved to cause disease (1,2). There are a number of pathogenic strains of *E. coli* that are associated with intestinal diseases and these strains can be divided into six main classes: enteropathogenic *E. coli* (EPEC), enterohemorrhagic *E. coli* (EHEC), enteroaggregative *E. coli* (EAEC), enteroinvasive *E. coli* (EIEC), enterotoxigenic *E. coli* (ETEC), and diffusely-adherent *E. coli* (DAEC) (1,2).

The first report of EPEC came from a 1945 outbreak of infantile diarrhea in the United Kingdom, and even today this pathogen remains one of the leading causes of

infantile diarrhea, particularly in developing countries (1). EPEC is also believed to be the ancestor of EHEC (3,4), a pathogen that has been responsible for a number of foodborne and waterborne outbreaks of bloody diarrhea (hemorrhagic colitis) and hemolytic syndrome (HUS) worldwide (3-5). HUS is a potentially fatal complication that results from the production of toxins by EHEC, and is characterized by hemolytic anemia and renal failure (1). There are over 200 serotypes of EHEC (6), identified on the basis of their O (lipopolysaccharide) and H (flagellar) antigens (2), which cause outbreaks and disease to varying extents. Serotypes are classified into five seropathotype groupings (A-E) depending on their association with outbreaks and disease severity (6). The O157:H7 serotype of EHEC, which falls within the seropathotype A category and has a particularly low infectious dose (6), has had a profound impact on North America (1). Specifically, *E. coli* O157:H7 has caused numerous multi-state outbreaks, and is responsible for tens of thousands of illnesses annually that result in hospitalizations and deaths (7). The cost associated with the O157:H7 serotype is 700 million dollars per year in the United States alone (7).

The four remaining pathogenic classes of *E. coli* that colonize the gastrointestinal tract (DAEC, EAEC, EIEC, and ETEC) all cause diarrhea. While DAEC may only contribute to instances of childhood diarrhea in infants over one year of age (8), EAEC are associated with persistent cases of diarrhea and this class has been implicated in numerous outbreaks worldwide (1,2). One of the most recent outbreaks linked to this class was the 2011 outbreak of diarrhea and HUS in Germany (9,10). This particular strain of EAEC was unique compared to other strains of EAEC because it produced

Shiga-toxin, a toxin that is most often associated with EHEC (9,10). Although EAEC do not typically produce Shiga-toxins, this class is known to secrete a number of other toxins, such as *Shigella* enterotoxin 1 (ShET1) and the enteroaggregative *E. coli* heat-stable toxin 1 (EAST1) (1). ETEC, the leading cause of travelers' diarrhea (11), colonizes the small intestine and can produce heat-labile (LT) and heat-stable (ST) enterotoxins (1,2). Similar to all other classes of diarrheagenic *E. coli*, ETEC is transmitted by the fecal-oral route through the consumption of contaminated water and food sources (11). In comparison to most classes of diarrheagenic *E. coli*, EIEC is able to survive and replicate within macrophages and epithelial cells (1). The disease outcomes caused by EIEC are similar to those caused by *Shigella*, and while they are often limited to watery diarrhea, EIEC can cause more severe conditions such as dysentery (1,2). Altogether, these six classes of pathogenic *E. coli* have a significant and global impact on human health.

1.2 – The Impact of *Salmonella enterica*

Salmonella are Gram-negative, facultative anaerobes that can be divided into two main species, *Salmonella bongori* and *Salmonella enterica* (12). There are over 2500 serovars of *Salmonella enterica* that are further subdivided into six subspecies (12). A number of *Salmonella enterica* serovars are of particular importance to human populations as they can cause gastroenteritis (13), and serovars such as *S. Typhi* and *S. Paratyphi* can cause typhoid fever. Similar to *E. coli* infections, *Salmonella* is transmitted by the fecal-oral route often through contaminated food sources (14). The impact of gastroenteritis due to *Salmonella enterica* infections is significant with 93.8 million cases

annually, 155, 000 deaths per year, and associated costs in the billions of dollars (13).

Typhoid fever, a potentially life-threatening illness, is most common in south-central and south-east regions of Asia while there are lower incidence rates in developed countries (15). Globally, there are estimated to be 21.7 million cases of typhoid illnesses annually that result in over 216, 000 deaths (15). Thus, the global health and economic burdens caused by enteric pathogens are profound.

2. Horizontal Gene Transfer and Pathogenicity Islands

2.1 – Defining Characteristics of Horizontal Gene Transfer

Horizontal gene transfer (HGT), the movement of DNA between cells through a process that is separate from cell division (16), is of particular importance for pathogenic bacteria because it enables the acquisition of genomic regions that can encode for virulence factors (17). These genomic regions, referred to as pathogenicity islands (PAIs), have some defining characteristics that have been summarized by Schmidt and Hensel (18) as follows: (1) they are large regions (10-200 kb) that contain one or more virulence-associated genes; (2) their G + C content and codon usage vary from the core genome; (3) they are found next to tRNA genes or are flanked by direct repeat sequences; and (4) they are often associated with mobile elements and mobility-related genes (18).

HGT can occur by three mechanisms: transformation, transduction, and conjugation. Transformation occurs with the uptake of DNA from the surrounding

environment (17), and in order for this process to happen, bacteria must have become competent (19). Transduction is the movement of genetic material between a donor and a recipient bacterium and it involves bacteriophages (17). Donor DNA from a bacterium that has been infected with a bacteriophage is packaged into a phage capsid, and this genetic material is then transferred to a recipient bacterium upon infection. The bacteriophage receptor-binding proteins that attach to receptors on the recipient bacterial cell surface dictate the extent to which DNA can be transferred by this process (17). Conjugation involves the movement of donor DNA to a recipient bacterium through a pilus and it is the only process of HGT that requires cell-to-cell contact (19). Although conjugation is often associated with the transfer of plasmids (19), some chromosomal elements can also be moved by this process (17). Altogether, these mechanisms of HGT allow for bacteria to acquire and incorporate new genetic material into their genomes.

2.2 – Pathogenicity Islands in *Enterohemorrhagic Escherichia coli*

Sequencing efforts on *E. coli* O157:H7 outbreak strains have identified 177 potential genomic islands (20,21), referred to as O-islands (OIs), that are specific to this pathogen and most of which were acquired through HGT by bacteriophages (21). Of the genes that are unique to O157:H7, approximately 130 genes are presumed to encode for proteins with diverse virulence-related functions such as iron-transport, toxins, fimbriae and proteins required for survival within phagosomes (21). These virulence-associated genes are located in both the bacterial chromosome as well as on two large plasmids (21). The two most extensively characterized virulence-associated genomic regions of EHEC

are the locus of enterocyte effacement (LEE) and the Stx-encoding phage regions that are responsible for the production of Shiga toxins (Stx). The pathogenicity island, LEE, is responsible for the attaching and effacing (A/E) lesion phenotype characteristic of both EPEC and EHEC (1,22,23). A/E lesion formation involves adherence of the pathogen to intestinal epithelial cells, followed by disruption of the brush border microvilli, and rearrangement of the host cytoskeleton to produce pedestal-like structures (1,2,24). The ability of these pathogens to produce A/E lesions relies on the gene products encoded by LEE: a type III secretion system (T3SS) and a subset of effectors; the adhesin, intimin, and its translocated receptor, Tir; and a positive regulator of LEE known as Ler (24). The second distinguishing phenotype of EHEC is the production of Shiga toxins, Stx1 and Stx2, which are responsible for the development of the potentially fatal HUS (1). Stx1 and Stx2, located in late prophage genes, have been acquired by Shiga-toxin producing *E. coli* (STEC) via transduction and have subsequently integrated into the bacterial chromosome (21,25,26).

Many of the OIs in STEC are related to fimbrial biosynthesis (21). Of the fourteen genomic islands that were originally identified as encoding for putative fimbriae, most are conserved or are partially conserved with a reference *E. coli* K12 strain while only four are unique to EHEC (21,27). Two more genomic islands associated with fimbrial biosynthesis have also been identified, one related to the meningitis-associated and temperature-regulated (MAT) fimbrial operon and a putative type IV fimbrial gene cluster (27). The four OIs that are specific to the O157:H7 serotype (OI-1, OI-47, OI-141, and OI-154) have been studied to varying extents. OI-1, which is predicted to encode for

a type 1-like fimbria on the basis of its similarity to the *E. coli* type 1 fimbrial locus (5), remains phenotypically and functionally uncharacterized. OI-47 has also yet to be studied but it may encode for long polar fimbria (LPF), similar to that found in *Salmonella*, as well as additional virulence factors (5). By contrast, the long polar fimbriae produced by OI-141 and OI-154 have been investigated and facilitate adherence to epithelial cells (28,29). Although there has been limited work examining the contribution of these four OIs to STEC pathogenesis, they may account for the greater virulence of seropathotype A strains over other seropathotypes (5). In comparison to other pathogenicity islands that have been clearly acquired by HGT, the evidence for HGT for the four putative fimbrial-encoding OIs is limited (5). These four OIs may therefore have been acquired by HGT early in the evolution of this enteric pathogen (5).

2.3 – Pathogenicity Islands in *Salmonella*

Salmonella species have acquired a number of pathogenicity islands, known as *Salmonella* pathogenicity islands (SPIs), which encode for a variety of virulence-associated gene products. A total of twenty-one SPIs have been found in *Salmonella* serotypes; however, not all serotypes have each SPI (30). A defining characteristic of all *Salmonella* is the presence of a 40 kb genomic island known as SPI-1. SPI-1 encodes for a type III secretion system that is needed for the invasion of non-phagocytic cells, and it also contains an iron-transport system that is encoded by the *sit* gene cluster (30-32). The genes in SPI-1 are activated within the host intestine and assembly of the T3SS-1 allows for virulence proteins, encoded both within the SPI-1 locus and elsewhere in the genome,

to be translocated into host cells (14). These virulence proteins, known as effectors, promote membrane ruffling and engulfment, which enables *Salmonella* to gain entry into host cells and colonize the intestine (14). The acquisition of SPI-1 approximately 25-40 million years ago allowed for *Salmonella* to evolve into an intracellular pathogen in cold-blooded animals (33).

The subsequent acquisition of another 40 kb genomic island by HGT, SPI-2, allowed for the divergence of *Salmonella enterica* species from *Salmonella bongori* (33). SPI-2 encodes for a type III secretion system that translocates effectors necessary for intracellular survival and replication within macrophages (34,35). The genes in SPI-2 are activated following entry of *Salmonella* into the host cell (14,36), and this genomic island has enabled *Salmonella enterica* species to infect a wide range of warm-blooded animals and cause disease (33). In addition to encoding for a type III secretion system, the SPI-2 locus also contains a *ttr* gene cluster (37). The *ttr* gene cluster encodes for a tetrathionate reductase system and it is not required for *Salmonella* virulence (37,38).

The distribution of the remaining SPIs varies amongst different serovars. For instance, there are 11 SPIs that are present in both *S. Typhimurium* and *S. Typhi*, while SPI-14 is unique to *S. Typhimurium* and four SPIs are unique for *S. Typhi* (30). The functions of the remaining SPIs are also diverse and include genes for magnesium transport (SPI-3), type I secretion systems (SPI-4 and SPI-9), effectors (SPI-5), type VI secretion systems (SPI-6), fimbrial (SPI-6) and capsule biosynthesis (SPI-7), and so on (reviewed in (30,39)). There are also a number of SPI genes whose functions have yet to be elucidated.

3. The Pathogenesis of Enterohemorrhagic *Escherichia coli* and *Salmonella enterica*

3.1 – Pathogenesis of Enterohemorrhagic *Escherichia coli*

EHEC infections begin following the consumption of contaminated food or water sources. From here, EHEC survives passage through the stomach due to its acid resistance systems and then travels to the large intestine where it specifically colonizes the terminal ileum and colon (40,41). Colonization is mediated by a number of adherence factors; however, the exact repertoire of adhesins and mechanisms of colonization have yet to be determined. Fimbriae have a demonstrated role in facilitating adherence to epithelial cells (1), and the genomes of *E. coli* O157:H7 strains contain at least 16 putative fimbrial clusters (27). Four of these fimbria-encoding clusters were shown through subtractive hybridization to be specific for seropathotype A strains and may therefore play an important role in specifically mediating *E. coli* O157:H7 colonization (5). These four clusters are either predicted to encode, or have been shown to produce, type 1 fimbriae and long polar fimbriae (5,28,29). Other adhesin factors of EHEC include, but are not limited to (summarized in 1,42): intimin, Efa-1 (EHEC factor for adherence), Saa (STEC autoagglutinating adhesin), ECP (*E. coli* common pilus) (43), ToxB (a pO157 encoded adherence factor) (44), Paa (porcine attaching-effacing associated protein), and OmpA (outer membrane protein A) (45).

Once EHEC has adhered to intestinal epithelial cells, the LEE-encoded type III secretion system translocates effector proteins into the host cells. Two important LEE-encoded components are the large outer membrane protein, intimin, and the translocated

intimin receptor, Tir (1,2). Intimin, encoded by *eaeA*, consists of a highly conserved N-terminal domain that serves as a membrane anchor and a variable C-terminal region that interacts with Tir once Tir has been inserted into the host-cell membrane (46,47). The interaction between intimin and Tir mediates the intimate attachment of both EPEC and EHEC to epithelial cells and promotes formation of the A/E lesion (1,40). The A/E lesion is characterized by extensive host cytoskeleton rearrangement and actin polymerization, which results in the formation of a pedestal-like structure that serves as a docking site for these pathogens (1,2). In addition to Tir, an extensive number of putative effectors secreted by the LEE-encoded T3SS have also been identified, largely through proteomics approaches (48,49). A number of these effectors have been implicated in modulating host cytoskeleton and signaling pathways; however, many of the effectors still require functional characterization (48).

A key factor of EHEC pathogenesis is the production of Shiga-toxins. The production of these toxins is largely responsible for the disease outcomes associated with EHEC infections (1). The Stx family can be divided into two classes, Stx1 and Stx2, which share approximately 56 % nucleotide sequence identity (2,26). These toxins are composed of two subunits: the A subunit, an *N*-glycosidase that modifies the ribosomal RNA of the 60S subunit (50); and a B subunit that as a pentamer facilitates binding to the glycolipid globotriaosylceramide (Gb3) receptor on host cells (2,26). Although these toxins are produced in the colon, they exert their effects on the kidney where damage can be substantial and can lead to the development of the potentially fatal condition, HUS (1). While most individuals infected with EHEC recover within 5-10 days, more severe

infections can require hospitalization and intravenous fluid treatments (51). The use of antibiotics is strongly discouraged for EHEC infections as sub-inhibitory levels of antibiotics have been shown to increase toxin production, thereby worsening the disease outcome (51,52).

3.2 – Pathogenesis of *Salmonella enterica*

Similar to EHEC infections, an infection with *Salmonella enterica* commences with the consumption of a contaminated food source, from which point *Salmonella* will travel to the small intestine and reach the intestinal epithelial layer (14). While *Salmonella enterica* species also use fimbriae to adhere to epithelial cells, a critical aspect of *Salmonella* pathogenesis is its ability to invade host cells and survive intracellularly. As such, *Salmonella* species have developed a number of mechanisms to access the intestinal epithelium (summarized in 14). *Salmonella* can invade specialized cells of Peyer's patches, known as microfold (M) cells, which function in ushering bacteria and antigens to immune cells (53). *Salmonella* can also enter non-phagocytic cells through bacterial-mediated endocytosis (14). This invasion of non-phagocytic cells requires the SPI-1 encoded T3SS to translocate effectors into the host cell that alter the host cytoskeleton and promote membrane ruffling (54). *Salmonella* can also cross the intestinal epithelial layer by disrupting tight junctions, a mechanism which likely results in the onset of diarrhea (14,55). Once *Salmonella* has crossed the intestinal epithelial barrier, it can enter macrophages and reside within a specialized compartment known as the *Salmonella* containing vacuole (SCV) (14). The SPI-2 encoded T3SS is required at

this stage of infection to translocate effectors across the membrane of the SCV to ensure intracellular survival and replication of *Salmonella* within macrophages (56-58). While most *Salmonella* infections are limited to the intestine and resolve within 5-7 days (14), some infections can become systemic and require hospitalization and treatment with antibiotics (59-61).

4. Flagellar Regulation and Assembly

4.1 – Regulation of the Flagellar Cascade

Prior to adherence to host cells, bacteria must first reach their site of colonization. Flagella-mediated motility is thus an important aspect of bacterial pathogenesis. *E. coli* and *Salmonella* species have numerous flagella distributed over their cell surfaces, known as peritrichous flagella (62), which enables these pathogens to access essential nutrients and their colonization sites along the intestinal epithelium (63-65). In addition to these motility functions, flagella are also involved in biofilm formation and play a role in adherence (66-69). Flagella are composed of three main structures: the basal-body complex, hook, and filament (62). The basal-body forms the flagellar motor that generates torque from the proton motive force to drive rotation of the hook and filament (62,70,71). The basal-body structure is composed of three rings located within the cytoplasmic membrane (MS ring), peptidoglycan (P-ring) and lipopolysaccharide (L-ring) layers (70,71). The hook serves to connect the basal-body complex to the filament (71).

The completed filament, which is 10 – 15 μm in length, comprises up to 20,000 – 30,000 flagellin subunits and can be spun at hundreds of revolutions per second (70).

Given that flagellar synthesis and assembly is an energetically costly event, the expression of these appendages is tightly controlled (71). The over fifty genes involved in flagellar biosynthesis are distributed throughout at least seventeen operons and are divided into three classes – the early, middle, and late genes which are transcribed from the class I, II, and III promoters, respectively (reviewed in (72)). The class I promoter drives the expression of only the *flhDC* operon which encodes for the master transcriptional regulator of the flagellar cascade, the FlhD₄C₂ complex (73,74). FlhD₄C₂ activates expression of the middle genes from class II promoters located in eight operons (72). The gene products from these operons include those responsible for the synthesis of the hook-basal-body complex (71), as well as the alternative sigma factor σ^{28} (encoded by *fliA*) that is required for the expression of the late genes from class III promoters (75,76). The anti- σ^{28} factor, FlgM, is transcribed by both class II and III promoters and it interacts with FliA to prevent transcription from class III promoters until the hook-basal-body complex is assembled (72,77). Once construction of the hook-basal-body is complete, FlgM is secreted thereby allowing for σ^{28} -dependent expression of the late genes that encode for the stator proteins, the flagellin subunits, and the proteins of the chemotaxis system (71,72,78). This transcriptional hierarchy, along with post-transcriptional regulatory mechanisms, ensures efficient flagellar assembly (72). Since activation of the *flhDC* operon determines whether flagellar biosynthesis occurs, the class I promoter is subject to the greatest number of regulatory inputs. The expression of the *flhDC* operon

can be affected by numerous environmental cues and several transcription factor binding sites have been mapped within the class I promoter region (reviewed in (72)).

4.2 – The Mechanism of Flagellar Assembly

Once the flagellar cascade is activated, flagellar assembly begins with formation of the MS-ring in the cytoplasmic membrane and incorporation of three C-ring proteins (70). The C-ring proteins, FliM and FliN, form the flagellar switch complex, a component which dictates the direction of filament rotation based upon signals that are transduced through the chemotaxis system (79). The other C-ring protein, FliG, serves to connect FliM and FliN to the MS-ring and is a rotor component of the flagellar motor (71,80). The stator components of the flagellar motor, MotA and MotB, are also incorporated once the late genes have been expressed (70).

There are nine proteins that comprise the export apparatus, six of which are located in the inner membrane and three of which form a soluble cytoplasmic complex (62,70,81). The assembly of the export apparatus is critical as this structure facilitates the secretion of a number of flagellar components, such as the proximal rod and distal rod components (62,70). The P-ring and L-ring then form in the peptidoglycan and lipopolysaccharide layers of the membrane, respectively, to complete formation of the basal-body-complex (62). The export of the P-ring and L-ring components does not depend on the flagellar export apparatus, but instead relies on the Sec-dependent pathway (62,70). The remaining flagellar substrates, however, are secreted by the flagellar T3SS and include components of the second main structure of the flagellum, the hook. The

hook is composed of FlgE subunits and its length is regulated by the molecular ruler protein, FliK (82-84).

Once the hook has been assembled the hook-associated proteins are incorporated, and the final structure is built (62,70,71). The filament is the propeller of the flagellum and it is composed of numerous flagellin subunits (70,71). The assembly and function of virulence-associated T3SS components, which will be discussed in subsequent sections, have largely been proposed based upon work on the flagellar T3SS.

5. Structure and Regulation of *Escherichia coli* Type I Fimbriae

Fimbriae are important cell surface structures of bacteria, particularly of pathogenic bacteria, as they have an established role in colonization and biofilm formation (68,85,86). While there is a diverse range of fimbriae, the classical fimbriae of the chaperone-usher assembly pathway are type I fimbriae (85-87). Type I fimbriae are 0.2 – 2 μm in length and facilitate binding to mannose-containing receptors on host cells (85,87). These fimbriae are encoded by the *fim* operon that consists of *fimAICDFGH* (88). FimA is the major structural subunit while FimF, FimG, and FimH are the minor fimbrial subunits (89,90). FimH is present at the distal ends of fimbriae and this adhesin mediates binding to host mannose-containing receptors (89,91). In addition to these structural components, the *fim* operon also encodes for the assembly proteins FimC and FimD. FimC is a chaperone that captures the structural subunits in the periplasm and targets them to the outer membrane usher protein, FimD, so that the subunits can be incorporated

into the growing fimbria (92-94). In contrast to the other fimbrial components, the precise function of FimI is unknown. Strains that lack *fimI* are unable to assemble fimbriae at the cell surface, suggesting that this protein plays a critical role in fimbrial biosynthesis (95). P fimbriae, which also belong to the chaperone-usheer assembly pathway, have a structural organization similar to that of type I fimbriae (86). The adhesin, PapG, facilitates binding to specific glycolipid receptors on host cells, thereby allowing P fimbriae to play an important role in the establishment of urinary tract infections by uropathogenic *E. coli* (86,92,96).

The expression of the *fim* operon is controlled by an invertible region containing the *fimA* promoter, known as *fimS* (97,98). The *fimS* region is also surrounded by two inverted repeat sequences (98). In the ON position, the *fimA* promoter is oriented such that it is able to drive the expression of the *fim* operon while in the OFF position the *fim* operon cannot be transcribed (98). This phase variation is regulated by two site-specific recombinases, FimB and FimE, which bind to the inverted repeat sequences. FimB is capable of orienting the *fimS* region in either the ON or OFF position while FimE can largely only regulate the expression of the *fim* operon from the ON to OFF state (98-100). In addition to environmental cues such as temperature (101), there are a number of regulators of the *fim* operon. Many of these regulators function by controlling the expression of the recombinases, FimB and FimE (98). However, some regulators such as H-NS, which also modulates the expression of the flagellar cascade and the T3SSs in *Salmonella enterica*, can interact directly with the *fimS* region (102,103). This mechanism of type I fimbriae regulation in *E. coli* is different than that in *S. Typhimurium* (104). *S.*

Typhimurium does not contain homologues of FimB and FimE, and is incapable of the typical phase variation (104,105). The FimY, FimZ, and FimW proteins are involved in modulating type I fimbrial expression in *S. Typhimurium* (104); FimY and FimZ activate expression while FimW functions as a negative regulator (104,106).

While fimbriae of the chaperone-usher assembly class have an established role in the pathogenesis of uropathogenic *E. coli*, the roles of specific fimbriae in EHEC pathogenesis are unknown. The O157:H7 serotype of EHEC is unable to express type I fimbriae despite possessing the *fim* operon because of a 16 bp deletion in the *fim* invertible element (107). Thus, novel type I-like fimbriae, such as that predicted to be encoded by OI-1 (5), may facilitate EHEC colonization (27).

6. The Virulence-Associated Type III Secretion Systems of *Salmonella enterica*

6.1 – Regulation of the SPI-1 and SPI-2 Type III Secretion Systems

The two T3SSs of *Salmonella enterica* species, encoded by SPI-1 and SPI-2, are required at different points during the course of an infection and are assembled upon activation by specific regulatory cues (14). The SPI-1 locus of *Salmonella enterica* is activated within the intestinal lumen, under environmental conditions such as high osmolarity and low oxygen, and is also expressed during the stationary phase of growth (108,109). These conditions activate the expression of HilC, HilD, and RtsA. All three of these proteins are positive regulators of the master regulator of the SPI-1 locus, HilA

(110,111). HilA is responsible for the activation of other promoters in SPI-1 that drive the expression of the T3SS-1 components and the transcription factor HilF, which is needed for the expression of T3SS-1 effectors (112-114). In addition to these activators of SPI-1, HilA is also repressed by a number of factors. These regulators include the nucleoid associated protein H-NS, which also represses the SPI-2 locus (115,116), and the HilE protein that interacts with HilD to decrease expression from the *hilA* promoter (115,117).

The SPI-2 locus is expressed following the uptake of *Salmonella* by host cells (14), and can be activated *in vitro* with media containing low concentrations of phosphate and magnesium and an acidic pH (118,119). The SPI-2 locus is composed of four main operons that encode a two-component regulatory system, T3SS-2 structural components, chaperones, and some effector substrates (120). The main regulator of SPI-2 is the SsrA/SsrB two-component regulatory system. SsrA is a sensor kinase, which upon activation by a currently unknown environmental signal phosphorylates the response regulator, SsrB (115,121). In its phosphorylated state, the C-terminal region of SsrB binds SPI-2 promoters at a defined 18 bp palindrome sequence thereby activating the expression of other T3SS-2 components (122,123). Similar to the main regulator of SPI-1, the SsrA/SsrB two component system is subject to a number of regulatory inputs. The two-component regulatory systems, PhoP/PhoQ and EnvZ/OmpR, are known to be positive regulators of the SPI-2 locus (124,125). The SlyA transcription factor also activates the SPI-2 locus by binding to the *ssrA* promoter, and the nucleoid-associated protein Fis has been shown to bind to and increase expression from both the *ssrA* and *ssaG* promoters (115,126-128). In addition to these positive regulators, three nucleoid-

associated proteins have a demonstrated role in repressing the SPI-2 locus: H-NS, YdgT, and Hha (115,129,130). This fine-tuning of the expression of the SPI-1 and SPI-2 master regulators ensures that T3SS assembly and effector secretion occur at appropriate stages during the course of infection.

6.2 – Assembly of Virulence-Associated Type III Secretion Systems

The putative functions of a number of virulence-associated T3SS components have been assigned based upon homology to proteins in the flagellar T3SS. The flagellar T3SS is believed to be the ancestor of virulence-associated T3SSs which have subsequently evolved to translocate effector proteins into host cells (131). The overall architecture of the *Salmonella enterica* T3SS-2 is shown in Figure 1.1. There are four main components to virulence-associated T3SSs: the export apparatus, the needle and translocon pore, chaperones, and effectors. While the precise order of assembly has not been fully elucidated, work on the *Yersinia* T3SS indicates that assembly likely occurs in an outside-to-inside order wherein the outer membrane secretin forms first followed by incorporation of the inner membrane components (132). From here, the C-ring proteins and the export apparatus are assembled prior to needle construction (132). In contrast to this work on *Yersinia*, other studies on T3SS assembly in *Salmonella* instead suggest an inside-to-outside assembly order (133,134).

The export apparatus is composed of eight proteins that are widely conserved amongst all T3SSs (135,136). In the *Salmonella enterica* T3SS-2, the export apparatus is predicted to consist of the five inner membrane proteins SsaR, SsaS, SsaT, SsaU, and

SsaV; and a three-membered cytoplasmic complex of SsaK, SsaN, and SsaO (120). These proteins have remained largely uncharacterized and the precise arrangement of the five proteins within the inner membrane has yet to be determined. Despite this, work from other virulence-associated T3SSs provides insight into the potential role of these proteins in the *Salmonella enterica* T3SS-2. For instance, as a member of the YscV family, the cytoplasmic domain of SsaV may play a role in substrate recognition and binding, while the cytoplasmic domain of SsaU may interact with other T3SS-related proteins to facilitate the transition from early to late substrate secretion (136-138). To date, the most extensively studied substrate switch for the SPI-2 encoded T3SS is the SsaB/SsaM/SsaL complex (139). This complex is a pH-dependent switch that coordinates the secretion of translocon and effector substrates (139).

The export apparatus is connected to the IM rings, likely composed of SsaJ and SsaD, and the C-ring protein SsaQ (120). In contrast to a number of T3SS-2 structural proteins, SsaQ has been the subject of investigation (140). The *ssaQ* gene encodes for two proteins by tandem translation, the products of which include a full-length SsaQ product (SsaQ_L) that is required for proper T3SS-2 function and a shorter product (SsaQ_S) which stabilizes SsaQ_L (140). The IM rings are associated with the OM secretin that is predicted to be composed of SsaC subunits (132,136,141). The OM secretin forms the platform for the inner rod and needle components that may be composed of SsaG/SsaH/SsaI (142). Needle length is regulated by members of the YscP protein family (136,143). This family of proteins, unlike other components of the T3SS, is weakly conserved amongst pathogens. The prediction that SsaP is the needle length regulation protein for the

Salmonella enterica T3SS-2 is based upon recent work on EscP from enteropathogenic *E. coli* (144). A long filament extends outward from the base of T3SSs and is connected to a translocon pore. The SseB, SseC, and SseD proteins have been shown to be localized to the cell surface and function as the translocon (145,146); however, SseB may function as the filament based upon its similarity to other characterized needle filament proteins (147). The translocon pore is a critical component of T3SS assembly because without this structure effectors would be unable to cross the eukaryotic cell membrane and thus would not be injected into the host cell cytosol (148). In addition to these structural components, chaperones and effector substrates play an important role in type III secretion and function as discussed in Sections 6.4 and 6.5.

6.3 – The Importance of the Type III Secretion System ATPase

T3SS ATPases are widely conserved amongst all T3SSs and a number of these proteins have been subject to extensive structural and biochemical investigation: EscN from enteropathogenic *E. coli* (149,150); YscN from *Yersinia* (151); InvC from the *Salmonella* T3SS-1 (152); CdsN from *Chlamydia* (153,154); HrcN from the plant pathogen *Xanthomonas* (155,156); and FliI from the flagellar T3SS (157-159). T3SS ATPases are structurally related to the catalytic β subunit of the F_0F_1 ATPase and form hexameric rings that are peripherally associated with the membrane (157,158,160). T3SS ATPases are cooperative enzymes and their catalytic activity can be increased by acidic phospholipids (158). Structural insight into these T3SS ATPases has been provided by the determination of the structures of monomeric FliI and EscN (150,157). While models

have been proposed for the hexameric form of T3SS ATPases, electron microscopy work has allowed for the visualization of the ring structures formed by these proteins (158,161,162).

The interactions of T3SS ATPases with other components of the secretion system have been investigated, and work on the *Yersinia* T3SS using the yeast two-hybrid system provides evidence for a YscN-YscK-YscL-YscQ complex (163). The YscN, YscK, and YscL proteins form a complex in the bacterial cytoplasm (151,163). YscL family members, including the flagellar component FliH, bind to the N-terminal region of T3SS ATPases and act as negative regulators of ATPase activity (151,164,165). In contrast, YscK family members (FliJ homologues) bind to the C-terminal region of T3SS ATPases and promote their oligomerization (162). The YscL protein is believed to bridge the T3SS ATPase to the C-ring protein (151). SsaO is the putative YscL family member protein for the *Salmonella* T3SS-2, although this assignment has not been validated (166). The most recent characterization of a YscL homologue comes from work on the EPEC protein, EscO (166). In addition to these interactions, bacterial two-hybrid system analysis and immunoprecipitation experiments have shown that T3SS ATPases interact with chaperones, effectors, and chaperone-effector complexes (153,167-169). The interaction of T3SS ATPases with these components occurs most efficiently when the T3SS ATPase is in its hexameric form (167).

T3SS ATPases were long believed to provide the energy for effector secretion until it was observed that the flagellar and virulence-associated T3SSs in *Yersinia* could be inhibited using the protonophore, carbonyl cyanide *m*-chlorophenylhydrazone (CCCP)

(170). The finding that the proton motive force provided the energy for effector secretion was further substantiated by careful work on the *Salmonella* flagellar T3SS showing that strains lacking the ATPase, FliI, are still weakly motile and can assemble a limited number of flagella (171). The dispensability of ATP hydrolysis for effector secretion was surprising; however, it is now known that the catalytic activity of these enzymes is required to dissociate chaperones from their effector substrates and to promote effector unfolding for passage of these substrates through the secretion apparatus (167). Mutations in T3SS ATPases result in severe effector secretion defects that translate into pronounced virulence attenuation phenotypes (150,152,168,172,173). Interestingly, the defects associated with the loss of the flagellar T3SS ATPase can be overcome by compensatory mutations in the export gate proteins, FlhA and FlhB (171). The mutations in FlhA and FlhB have been proposed to increase the likelihood that secretion substrates enter the export gate and are subsequently secreted in the absence of FliI (171).

6.4 – The Role of Chaperones in Type III Secretion

T3SS chaperones play a critical role in ensuring that effector substrates are delivered to the base of the T3SS for secretion (174). While the complete repertoire of chaperones has yet to be elucidated, particularly for the *Salmonella* T3SS-2, these proteins have a few defining characteristics such as their low molecular weight (10-20 kDa), an often acidic pI (often 4-5), and their ability to form and act as dimers (reviewed in (174)). Chaperones, which bind to an N-terminal chaperone binding domain on the effector substrate, are classified based upon the number of their effector substrates and

their location within the genome (174). Class IA chaperones bind to only one effector and are often encoded adjacent to it while class 1B chaperones can bind multiple effectors and their genomic location is more varied (174). A prime example of a class IA chaperone is the SPI-1 associated chaperone SicP that is required for the secretion of its effector cargo, SptP (175). The multi-cargo chaperone associated with the *Salmonella* T3SS-2, SrcA, is classified as a class IB chaperone as it can bind both PipB2 and SseL (176). The class II designation is used for chaperones that bind translocon components while chaperones that bind to needle and filament proteins of the T3SS are classified as class III (174). The recently characterized T3SS-2 chaperone SscA that is required for the secretion of the translocon pore protein, SseC, is classified as a class II chaperone (177). There are a limited number of chaperones that have been identified as class III chaperones, but examples include the PscG and PscE chaperones in *Pseudomonas* that bind the needle protein, PscF (178). While chaperones have a demonstrated role in effector secretion, they have also been implicated in other roles (reviewed in (179)). For instance, chaperones can be involved in transcriptional regulation, determining the hierarchy of effector secretion, maintaining effectors in an unfolded ‘secretion-competent’ state, ensuring that effectors are targeted to the correct T3SS apparatus, and acting as anti-aggregation factors (179).

Despite the abundance of SPI-2 effectors, only a subset of chaperones has been identified for the T3SS-2. SseA was the first chaperone identified for the T3SS-2, and it is needed for binding and the secretion of the needle and translocon components, SseB and SseD, respectively (180,181). Subsequent work on the SPI-2 encoded gene, *ssaE*, showed

that SsaE also chaperones SseB and can interact with SsaN at the base of the T3SS-2 (182). SscB was shown to be the chaperone for the only effectors encoded within the SPI-2 locus, SseF and SseG (183). SrcA was the first chaperone identified that was encoded outside of the SPI-2 locus and its absence was shown to result in a secretion defect of PipB2 and SseL (176). Additional phenotypic work and stable isotope labeling of amino acids in cell culture (SILAC) coupled with mass spectrometry confirmed a role for SrcA as the chaperone for these two effectors (176). Finally, although SscA has long been implicated as the chaperone for the translocon protein SseC, this assignment was only validated recently through secretion analysis and immunoprecipitation experiments (177). Given the large repertoire of effector substrates associated with the T3SS-2, it is likely that additional chaperones have yet to be identified.

6.5 – The Function of SPI-1 and SPI-2 Effectors

Effectors are the virulence proteins that bacteria inject into host cells with the aim of promoting bacterial invasion, survival, and replication. The translocation of effector proteins into host cells is a highly coordinated process that must occur at the appropriate stage during infection (14). A vast number of effector substrates have been identified for the *Salmonella* T3SSs – there are approximately twenty effectors for the T3SS-1 and nearly thirty effectors associated with the T3SS-2 (58,184). Effector proteins contain a weakly conserved N-terminal secretion signal within the first 20 amino acids that is required for targeting to T3SSs, and effectors often possess an additional N-terminal chaperone binding domain within the first 140 residues (185). Given the lack of

conservation within the N-terminal region of effector substrates, a precise secretion signal has not yet been defined and there has been debate as to whether it is encoded at the mRNA or amino acid level (186-191). While the secretion signal is required to ensure that the effector protein exits the bacterial cytoplasm, it is the chaperone binding domain that confers specificity and dictates to which T3SS the effector is targeted (185). For instance, Lee and Galan have shown that if the SPI-1 effectors SptP and SopE lack their encoded chaperone binding domains, they can be secreted by the flagellar T3SS (185).

Effector proteins often have redundant functions, which can highlight the importance of disrupting a particular aspect of host physiology, but this also makes it difficult to elucidate their precise role. Despite this, many studies are beginning to uncover the host pathways and functions that are targeted by bacterial virulence proteins (reviewed in (14,58,192)). For the SPI-1 encoded T3SS, at least five proteins are required for the initial stages of invasion (14). SopE, SopE2, and SopB manipulate host cytoskeleton dynamics, which leads to membrane ruffling and bacterial uptake (14,193-195). This process of *Salmonella* engulfment is further mediated by the effectors SipA and SipC (14,196,197). The roles of SopE, SopE2, and SopB also extend beyond that of modulating actin dynamics, as the activation of host Rho GTPases by these effectors has many effects on several transcription factors and signaling pathways (14). Several other SPI-1 effectors also modulate host signaling pathways and impact pro-inflammatory responses. For instance, AvrA is a member of the cysteine protease family and it prevents activation of the transcription factor, nuclear factor (NF)- κ B (14,198). SipB plays a critical role in the *Salmonella* infection process by activating caspase-1 and causing

macrophage apoptosis (14,199,200). SopA is proposed to have E3 ubiquitin ligase activity and is thus likely also involved in disrupting host responses (14,201). Altogether, SPI-1 effectors induce actin rearrangement and modulate host transcription factors and pathways, ensuring the successful invasion of host cells by *Salmonella* (14).

The functions of many SPI-2 effectors are unknown, but for those that have been characterized, a substantial number are involved in *Salmonella* induced filament (Sif) formation and maintaining the integrity of the SCV (58,192). Sifs are structures that protrude from the SCV (202), and while their exact role in *Salmonella* pathogenesis is not known (202), the effector SifA is recognized as an important contributor to Sif formation (203). In addition to this role, SifA also interacts with the host protein, SKIP (SifA and kinesin interacting protein), to maintain positioning of the SCV near the host nucleus (204). The SPI-2 encoded effectors, SseF and SseG, have also been implicated in Sif formation along with PipB2 and SopD2 (14,58). While the absence of these effectors does impact Sif formation, their exact roles in the production of these structures have not yet been elucidated (14). PipB2 displays sequence similarity with PipB and these effectors are found in particular within lipid rafts of the SCV and Sif membranes (205). Subsequent work has revealed that PipB2 interacts with kinesin-1, which is involved in anterograde transport, and links kinesin-1 to the SCV membrane (206). SopD2 has been shown to act antagonistically to SifA and causes SCV instability (207).

While effectors have a weakly conserved N-terminal domain, there are a group of SPI-2 effectors that have similar secretion signals (58,208). SseJ is encoded outside of the SPI-2 locus and possesses a secretion signal similar to that of SspH1, SspH2, SlrP, SseI,

SifB and SifA (208,209). The C-terminal region of SseJ contains a glycerophospholipid-cholesterol acyltransferase domain and a role for SseJ in cholesterol esterification has been described, supporting a role for this effector in maintaining the integrity of the SCV membrane (14, 209). SspH1, SspH2, and SlrP have been implicated in ubiquitin modification and function as E3 ubiquitin ligases (58). SspH1 has been implicated in modulating the NF- κ B pathway while SlrP modifies the redox protein, thioredoxin, which is involved in host cell apoptosis (58,210,211). SspH2 has been found to interact with host actin-binding proteins, and may impact the rate of actin polymerization (58,212). In addition to these effectors that possess similar secretion signals, other effectors such as SseK1, SseK2 and SseK3 have also been identified. The identification of these effectors was facilitated by their conservation with one another and their similarity to the *E. coli* T3SS-associated effector protein, NleB (58,213,214). The absence of all three SseK effectors together impairs *Salmonella* virulence; however, their exact function in *Salmonella* pathogenesis is not yet known (58,214). As stated, the redundancy of effector functions often makes it difficult to elucidate the host cell target of a particular effector. Future work is required to determine the host cell targets of many SPI-2 effectors and to determine the precise mechanisms by which these effectors enable *Salmonella* survival and replication within the host.

7. The Link amongst Motility, Adherence and Type III Secretion Systems in *Salmonella*

The pathways that govern the synthesis and assembly of flagella, fimbriae, and T3SSs in *Salmonella* are complex and are subject to a number of regulatory inputs. The cross-talk that occurs between these three pathways adds yet another layer of complexity, as highlighted in Figure 1.2 (also summarized in (215,216)). Given the opposing roles of motility and adherence, it is not surprising that bacteria have evolved mechanisms to reciprocally regulate these processes. In *S. Typhimurium*, FliZ is a positive regulator of flagellar expression that has been shown to repress the expression of type I fimbriae by regulating FimZ (215,217); however, at times when flagellar synthesis must be repressed, FimZ can exert an effect on the class I promoter and decrease expression of the *flhDC* operon (217,218). In addition to FimZ, other fimbrial operon-encoded motility regulators have been identified, such as MrpJ from *Proteus mirabilis* and PapX from uropathogenic *E. coli* (219-221). Both of these regulators repress flagellar synthesis by decreasing the level of *flhDC* transcription (219-221).

There are examples of cross-talk between the SPI-1 encoded T3SS and the flagellar cascade (reviewed in (112)). For instance, RtsB, which is encoded in the *rtsAB* operon alongside the positive regulator of HilA, can repress *flhDC* expression by binding to the flagellar class I promoter (111). The flagellar gene products can also modulate SPI-1 expression by a number of mechanisms, most of which rely on the FliZ-mediated activation of HilD activity (222). Since FliZ is a main regulator of HilD, the levels of FliZ can indirectly affect SPI-1 expression. For example, the RcsCDB system, which plays a

role in regulating a number of cell envelope genes (223), represses *hilA* expression by preventing flagellar gene activation (224). This repression of the flagellar cascade ultimately leads to a decrease in *fliZ* expression and prevents the FliZ-mediated activation of HilD (112,216,222). Additional examples of regulators that modulate the flagellar cascade and FliZ levels, which ultimately impacts SPI-1 expression, are shown in Figure 1.2. These regulators include, but are not limited to: DsbA (216), the ClpXP protease (225), and the Lon protease (222,226). In addition to these links between flagellar and SPI-1 expression, there is also a direct link between type I fimbriae and the expression of the SPI-1 T3SS. FimZ has been shown to induce the expression of HilE, a repressor of HilD, and thus prevents the activation of HilA (227).

Finally, in *Salmonella* there is also a link between the SPI-1 and SPI-2 encoded T3SSs. The link between the T3SS-1 and T3SS-2 is expected since the expression and assembly of these systems must be coordinated with the stages of *Salmonella* infection (14). The SPI-1 activator of HilA, HilD, counteracts the repression exerted on the *ssrAB* operon by H-NS (228). Furthermore, mutations in SPI-2 genes have been shown to reduce SPI-1 gene expression (229). Despite these examples, the evidence linking the two T3SSs in *Salmonella* is limited. A number of SPI-2 effectors have been found to be secreted by both the T3SS-1 and T3SS-2, and some SPI-1 effectors may be involved during the later intracellular stages of infection (14). As such, there may be a greater interplay between the T3SS-1 and T3SS-2 than previously anticipated.

8. Purpose and Aims of this Work

The purpose of this work was to study uncharacterized gene products in pathogenicity islands of the enteric pathogens, *Escherichia coli* O157:H7 and *Salmonella enterica*, in order to gain a deeper understanding of the virulence mechanisms employed by these pathogens. Previous research on the pathogenesis of STEC led to the identification of four O-islands that are unique to seropathotype A strains (5). Of the four O-islands identified, OI-1 and its gene products had yet to be phenotypically characterized. In contrast to the limited work on the unique STEC OIs, the T3SS encoded by SPI-2 in *S. Typhimurium* has been extensively studied. However, the function of a number of SPI-2 gene products has been inferred from work on other T3SSs and there has been limited biochemical or phenotypic evidence to support these assignments. Since combating pathogens can rely on a mechanistic understanding of their virulence strategies, and valuable insights into host-pathogen relationships can be provided by elucidating the roles of gene products in pathogenicity islands, a detailed characterization of the gene products of both OI-1 and SPI-2 is warranted.

The hypotheses at the time this work was undertaken were: (1) a component(s) of OI-1 represses motility in *E. coli* O157:H7; and that (2) SsaN is the putative SPI-2 encoded T3SS ATPase in *S. Typhimurium* and it is essential for effector secretion. As such, the aims of this work were to understand how the gene product(s) in OI-1 represses motility and to provide a molecular understanding of how SsaN facilitates effector secretion. The aims of this work are discussed in detail in the following chapters:

1. A Novel Repressor of *Escherichia coli* O157:H7 Motility Encoded in the Putative Fimbrial Cluster OI-1

- This study identified *Z0021* as a motility repressor in *E. coli* O157:H7 and demonstrated that *Z0021* exerts its regulatory effects on flagellar class II promoters.

2. Identification of the Docking Site between a Type III Secretion System ATPase and a Chaperone for Effector Cargo

- This study elucidated the molecular basis by which SsaN engages a chaperone to facilitate effector secretion and showed that the chaperone-T3SS ATPase interaction is important for *Salmonella* pathogenesis.

An underlying theme of this work is to study uncharacterized gene products in pathogenicity islands and provide mechanistic insight into their potential role in virulence. The identification of a novel repressor of motility encoded in an O-island that is found almost exclusively in the *E. coli* O157:H7 serotype aids in understanding the basis of the unique pathogenesis of these strains. The elucidation of the molecular interface for the chaperone-T3SS ATPase interaction – an interaction that is essential for *Salmonella* pathogenesis – gives insight into the mechanism of effector secretion by T3SSs. Together, these studies have expanded our understanding of virulence properties and mechanisms of enteric pathogens.

Figure 1.1. Overall structure of the T3SS-2 from *Salmonella enterica*. There are four main components to type III secretion systems: the export apparatus, the needle and translocon pore, chaperones, and effectors. An important component of the export apparatus is the T3SS ATPase, SsaN, which assembles into a hexamer on the cytoplasmic face of the bacterial inner membrane. The precise interactions of SsaN at the membrane with other components of the export apparatus are not entirely known; however, the YscL homologue, SsaK, may serve to link SsaN to the C-ring protein, SsaQ, based upon work on the *Yersinia* T3SS (163). The energy derived from ATP hydrolysis is used to facilitate chaperone dissociation and effector unfolding (167). The transition from translocon to effector secretion is regulated by the pH-dependent switch complex, SsaB/L/M (shown in red) (139). This figure was adapted and modified from work by Kuhle and Hensel (230).

Figure 1.1

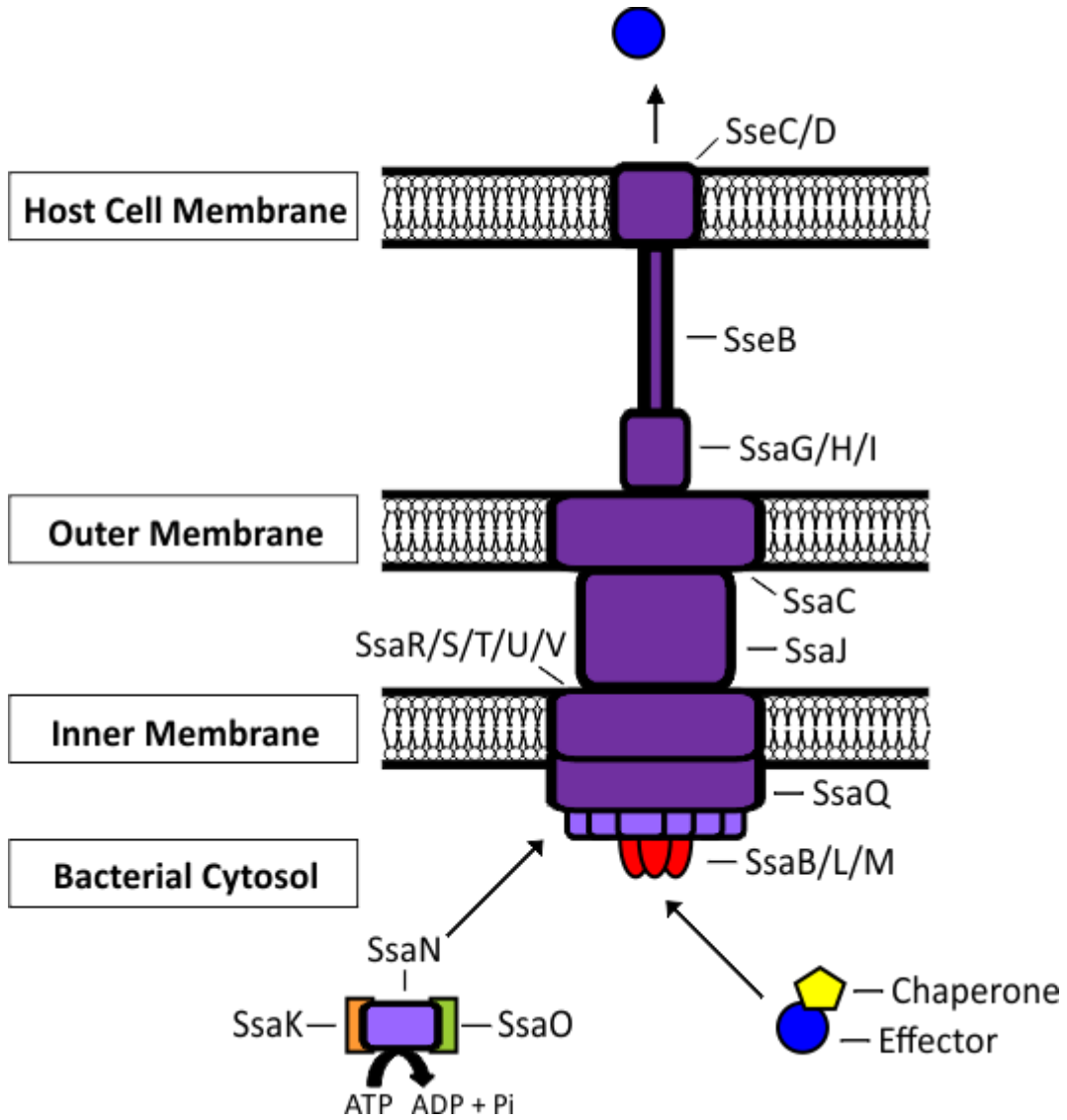
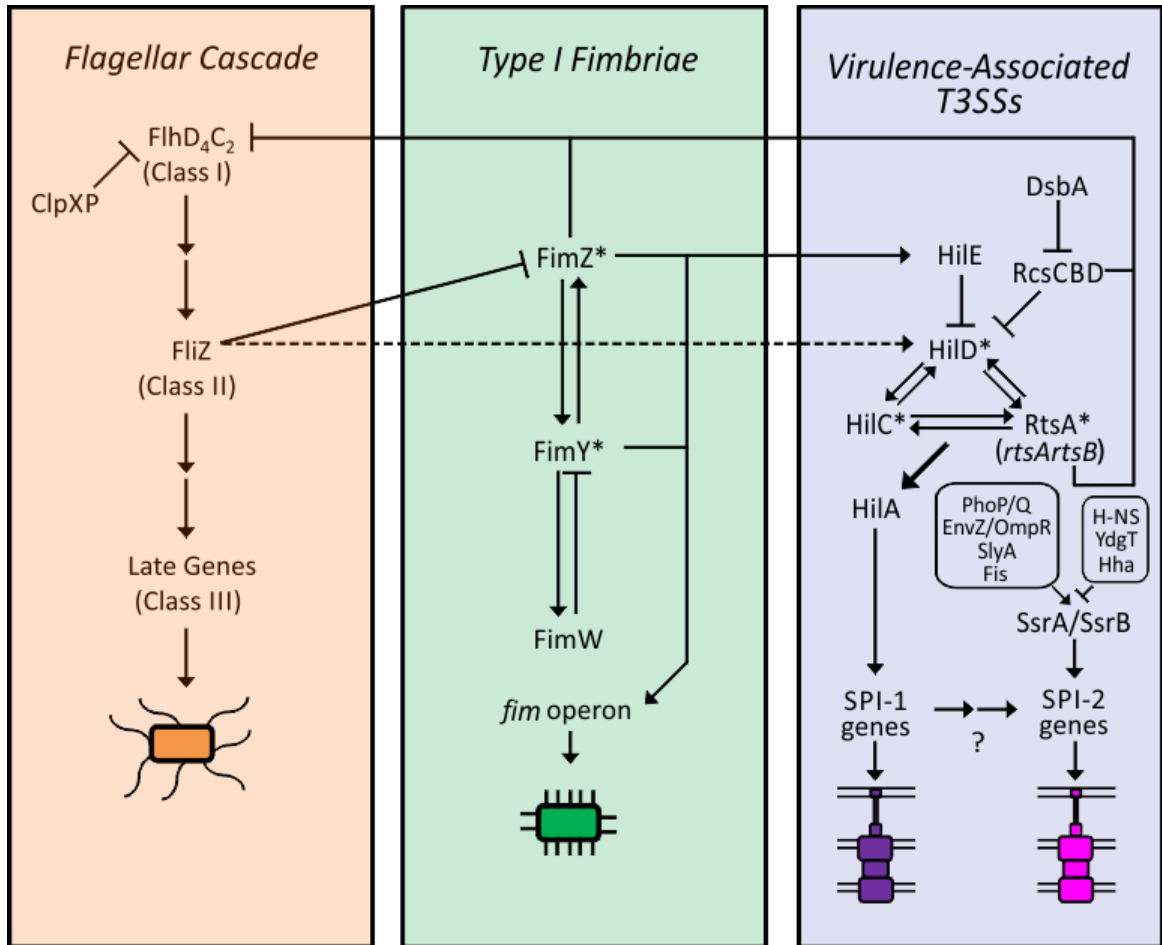


Figure 1.2. Linking the Flagellar, Type I Fimbrial, and T3SS Assembly Pathways in

Salmonella. There are a number of regulatory mechanisms that govern the processes of motility, adherence, and type III secretion in *Salmonella*. Adding to this complexity are the layers of regulation and cross-talk that occur between the three processes, some of which are shown in this figure. The asterisk denotes that a protein can regulate its own expression and the question mark between the SPI-1 and SPI-2 genes indicates that there are likely a number of regulatory effects that have yet to be uncovered between these two T3SSs. This figure was based upon and adapted from the following works (216,217,227).

Figure 1.2



CHAPTER TWO

A Novel Repressor of *Escherichia coli* O157:H7 Motility Encoded in the Putative Fimbrial Cluster OI-1

CO-AUTHORSHIP STATEMENT

The chapter herein has been adapted from material that has been published in the *Journal of Bacteriology*. The complete citation for the published work is as follows:

Allison, S.E., Silphaduang, U., Mascarenhas, M., Konczy, P., Quan, Q., Karmali, M., and Coombes, B.K. (2012). Novel Repressor of *Escherichia coli* O157:H7 Motility Encoded in the Putative Fimbrial Cluster OI-1. *J. Bacteriol.* **194**, 5343-5352

The contributions by each author to the project are described below:

1. Strains and plasmids were created by S.E.A. and U.S.
2. Motility assays were conducted by S.E.A. and U.S.
3. Transmission electron microscopy and FliC Western blot experiments were conducted by U.S.
4. Transcriptional reporter analysis was performed by S.E.A. and U.S.
5. Quantitative RT-PCR was conducted by U.S.
6. Western blot and multi-copy suppression experiments were performed by S.E.A.
7. Sequencing and *Z0021* prevalence analysis was done by M.M., P.K., Q.Q., M.K. and B.K.C.
8. S.E.A., U.S., and B.K.C. contributed to the writing of the manuscript

*Note that references in the following data chapters have been compiled into one reference list at the end of the thesis in order to avoid any redundancy between sections.

**Novel Repressor of *Escherichia coli* O157:H7 Motility Encoded in the Putative
Fimbrial Cluster OI-1**

Sarah E. Allison^{1,2*}, Uma Silphaduang^{1*}, Mariola Mascarenhas³, Paulina Konczy³, Quyen
Quan³, Mohamed Karmali³, and Brian K. Coombes^{1,2}

¹ Department of Biochemistry and Biomedical Sciences, McMaster University, Hamilton,
Ontario, Canada

² Michael G. DeGroot Institute for Infectious Disease Research, Hamilton, Ontario,
Canada

³ Laboratory for Foodborne Zoonoses, Public Health Agency of Canada, Guelph, Ontario,
Canada

* These authors contributed equally to this work

Address correspondence to BKC (coombes@mcmaster.ca):

1280 Main Street West, Health Sciences Centre Room 4H17, Hamilton, ON L8S 4K1

ABSTRACT

Escherichia coli O157:H7 is a gastrointestinal pathogen that has become a serious public health concern as it is associated with outbreaks and severe diseases such as hemolytic-uremic syndrome. The molecular basis for its enhanced virulence compared to other serotypes is not completely known. OI-1 is a putative fimbria-encoding genomic island that is found almost exclusively in the O157:H7 serotype of Shiga toxin-producing *E. coli* and it may be associated with the enhanced pathogenesis of these strains. In this study, we identified and characterized a novel repressor of flagellar synthesis encoded by OI-1. We showed that deletion of *Z0021* increased the motility of *E. coli* O157:H7, which correlated with an increase in flagellin production and enhanced assembly of flagella on the cell surface. By contrast, over-expression of *Z0021* inhibited motility. We demonstrated that *Z0021* exerted its regulatory effects downstream of the transcription and translation of *flhDC* but prior to the activation of class II/III promoters. Furthermore, the master regulator of flagellar synthesis, FlhD₄C₂, was shown to be a high copy suppressor of the non-motile phenotype associated with elevated levels of *Z0021* – a finding consistent with *Z0021*-FlhD₄C₂ being a potential regulatory complex. This work provides insight into the mechanism by which *Z0021*, which we have named *fmrA*, represses flagellar synthesis, and is the first report of a fimbrial operon-encoded inhibitor of motility in *E. coli* O157:H7.

INTRODUCTION

Shiga toxin-producing *Escherichia coli* (STEC) are foodborne and waterborne pathogens that have been implicated in outbreaks worldwide and can cause hemorrhagic colitis and the potentially fatal hemolytic-uremic syndrome (HUS) (2,231-234). The O157:H7 serotype of enterohemorrhagic STEC (EHEC), classified as a seropathotype A strain, is known for its prevalence and high virulence in humans (2,235-237). A genomic comparison of *E. coli* O157:H7 with serotype O26:H11, which is less frequently associated with human outbreaks and disease, revealed the presence of four fimbria-encoding genomic islands that are unique to seropathotype A strains: O-island (OI)-1, OI-47, OI-141, and OI-154 (5). Although the mechanisms underlying the unique pathogenesis of *E. coli* O157:H7 compared to that of other STEC strains are not fully known, these four O-islands may enable O157:H7 serotypes to colonize humans and cause disease more readily than other serotypes do (5).

Fimbriae-mediated adherence of *E. coli* O157:H7 to intestinal epithelial cells is an important and early step in the colonization process. The sequencing of two *E. coli* O157:H7 outbreak strains led to the identification of at least 16 fimbrial operons (20,21,27). Of the four fimbria-encoding OIs that are specific for seropathotype A strains, two of these regions have been the subject of investigation. OI-141 and OI-154 encode for long polar fimbriae (Lpf) which were first described in *Salmonella enterica* serovar Typhimurium and are similar to type I fimbriae (238). Torres and colleagues showed that the Lpf1 cluster of *E. coli* O157:H7, located in OI-141, increases fimbrial expression and adherence to tissue culture cells when introduced into a non-fimbriated *E. coli* K12 strain

(28). Furthermore, the Lpf1 cluster has a demonstrated role in microcolony formation (28). The second *lpf* cluster of *E. coli* O157:H7, located in OI-154, is implicated in the initial stages of adhesion and a similar region in *E. coli* O113:H21 mediates adherence to epithelial cells (29,239). In contrast to OI-141 and OI-154, OI-1 and OI-47 have yet to be characterized. The major fimbrial proteins encoded by OI-47 are similar to *Salmonella* Lpf and this OI is also predicted to encode putative virulence factors (5). OI-1 is distinct from these three Lpf related clusters and is predicted to encode for type 1-like fimbriae. The arrangement of the putative fimbrial genes in OI-1 are shown in Figure 2.1 (5).

In addition to fimbriae, flagella also play an important role in *E. coli* O157:H7 pathogenesis as they enable the bacteria to breach the intestinal mucous layer to access the intestinal epithelium. Flagellar synthesis is a tightly regulated and highly energetic three-tier process (240). The early genes, *flhD* and *flhC*, encode for the master regulator FlhD₄C₂ that is required for the transcription of the middle genes from class II promoters (72). The middle genes encode for the structural and assembly proteins required for the synthesis of the hook-basal body complex, the alternative sigma factor FliA (σ 28), and its anti-sigma factor FlgM (anti- σ 28). Once the hook-basal body complex has been assembled, FlgM is secreted, thereby allowing FliA to activate the transcription of the late genes that encode the filament subunits, motor proteins, and the proteins of the chemotaxis system (62). Given that adherence and motility represent antagonistic functions, bacteria use mechanisms to reciprocally regulate these processes. For instance, the BvgAS two-component signal transduction system in *Bordetella pertussis* activates adhesin genes while repressing those involved in motility (241). There are also proteins

encoded within fimbrial operons that have been shown to regulate motility. In *Proteus mirabilis*, MrpJ of the MR/P fimbrial cluster inhibits swimming and swarming motility by repressing the transcription of *flhDC* (219). The MrpJ homologue in uropathogenic *E. coli*, PapX, has been shown to repress motility by binding directly to the *flhDC* promoter (220,221). To date, there have been no fimbrial operon-encoded regulators of motility identified in *E. coli* O157:H7.

We turned our attention to the OI-1 genomic island as a potential source of virulence determinants associated with the O157:H7 serotype of EHEC. In this work, we identified and characterized a novel repressor of motility in *E. coli* O157:H7, Z0021. We show that deletion of *Z0021* leads to an increase in swimming motility and flagellar production in *E. coli* O157:H7 compared to the parental strain while over-expression of Z0021 inhibits motility. Using a transcriptional reporter system, we demonstrate that Z0021 regulates motility prior to middle and late gene transcription but downstream of the master regulator, FlhD₄C₂. In addition, we show that FlhD₄C₂ is a high-copy suppressor of the non-motile phenotype associated with over-expression of Z0021. Given its role in motility regulation, we propose that *Z0021* be renamed *fmrA* (fimbrial-operon-encoded motility regulator A). This study reports on a novel fimbrial operon-encoded regulator of flagellar synthesis in *E. coli* O157:H7 and provides insight into the mechanism by which Z0021/FmrA represses motility.

MATERIALS AND METHODS

General methods

Table 2.1 lists the strains, plasmids and oligonucleotides used in this work. *E. coli* strains were grown in Luria broth (LB) medium and when necessary antibiotics were used at the following concentrations: ampicillin, 100 µg/ml; kanamycin, 50 µg/ml; and chloramphenicol, 34 µg/ml. Gel extraction and plasmid mini-prep kits were purchased from Qiagen (Mississauga, ON, Canada). Vent polymerase was from New England Biolabs (Beverly, MA, U.S.A) and restriction enzymes were purchased from Fermentas (Burlington, ON, Canada).

Construction of mutants and HA-tagged variants

The deletion of single or multiple genes within OI-1 was carried out as described by Datsenko and Wanner (242). Linear DNA was amplified from pKD4 using the primers listed in Table 2.1. *E. coli* O157:H7 strain EDL933 harbouring pKD46 was transformed with concentrated PCR product and plated onto LB-agar plates containing kanamycin. All strains generated were confirmed by PCR. A similar strategy using pSU315 was employed to create strains in which *flhC* had been HA-tagged at its C-terminus.

Motility assays

Swimming motility was assessed using 0.25 % LB-agar plates. Overnight cultures were diluted to an OD₆₀₀ of 1.0 and 2 µL of culture was stabbed onto agar plates. Ampicillin was added to the plates when required to maintain plasmids, and IPTG and arabinose

were added to the plates for induction when necessary. The plates were incubated for 6 h at 37 °C and then the diameter of the swimming zone around the inoculation site was measured.

Transmission electron microscopy

Wild-type EDL933, Δ OI-1 and Δ Z0021 strains were cultured in motility agar for 6 h at 37°C. Bacteria were absorbed to carbon-stabilized Formvar supports on 200-mesh copper transmission electron microscopy (TEM) grids by floating the Formvar side down on a drop of culture for 30 sec, followed by a rapid wash with water. Bacteria on TEM grids were stained by submerging the grids for 10 sec in 0.1 % (wt/vol) uranyl acetate and then examined with a Philips CM10 transmission electron microscope at an operating voltage at 80 kV. Digital images of bacteria were captured with a SIS/OLYPUS, Morada, 11 megapixel CCD camera (Biophysics Interdepartment Group, University of Guelph).

Western blot analysis

To examine the levels of H7 flagellin in wild-type EDL933, Δ OI-1 and Δ Z0021 strains cultures were grown in LB medium for 3, 6 and 24 h at 37 °C. Whole cell lysates were resolved on a 10 % sodium dodecyl sulfate-polyacrylamide gel and transferred to a polyvinylidene difluoride membrane (Immobilon-P; Millipore Corp.). The blots were incubated with a 1:2000 dilution of rabbit polyclonal antiserum to H7 flagellin, followed by a 1:2000 dilution of peroxidase conjugated mouse anti-rabbit immunoglobulin G, and developed using a chemiluminescent detection system (Pierce Chemical Company,

Rockford, IL, USA). For Western blot analysis of FlhC-HA levels in wild-type EDL933 and $\Delta Z0021$ strains, cultures were grown in LB medium at 37 °C to an OD₆₀₀ of ~ 0.5. Bacteria were then pelleted and whole cell lysates were probed with anti-HA (1:2000) and anti-DnaK (1:10000) antibodies. DnaK was used as a loading control.

Transcriptional reporter assays

Luciferase reporter constructs for class I, II, and III promoters were created by PCR amplifying the promoter regions from *E. coli* O157:H7 strain EDL933 genomic DNA using the primers listed in Table 2.1. The PCR products were then cloned into pCS26 (243) and transformed into wild-type EDL933 and $\Delta Z0021$ strains. The sequences of all constructs were confirmed by sequencing at MOBIX (McMaster University, Hamilton, ON, Canada). Overnight cultures were sub-cultured into LB medium to a starting OD₆₀₀ of 0.005 and were then grown for 6 h with shaking. Luminescence and OD₆₀₀ values were recorded directly (EnVision, Perkin-Elmer) and the relative light units were normalized to OD₆₀₀ readings. All experiments were performed in triplicate.

Quantitative RT-PCR analysis

Wild-type and $\Delta Z0021$ strains were grown in LB medium at 37 °C to an OD₆₀₀ ~ 0.6 and then RNA was isolated using a High Pure RNA Isolation Kit (Roche, Laval, PQ, Canada). RNA was treated with DNase I (Ambion, TURBO DNA-free Kit, Applied Biosystems, Foster City, CA) and first strand cDNA was synthesized from 500 ng total RNA using the Transcriptor First Stand cDNA Synthesis Kit (Roche). Real-time PCR amplification was

performed on 5 µL cDNA in a reaction containing 1X LightCycler 480 CYBR Green I Master (Roche) and 500 nM each of the forward and reverse primers in a 20 µL reaction volume. Relative quantification was performed using the Light Cycler 480 Relative Quantification software (Roche) to compare the relative expression of selected gene targets to the *icdA* control gene. Primers designed to amplify regions of *flhD*, *flgM*, *motA*, *fliC*, and *icdA* were validated by generating standard curves and are listed in Table 2.1. Assays were performed in triplicate with the Lightcycler 480 II (Roche) instrument.

Construction of pFLAG-Z0021 and pFLAG-Z0021-*flhDC*

Z0021 and *flhDC* were amplified from the chromosomal DNA of *E. coli* O157:H7 strain EDL933 using primers *Z0021*-F and *Z0021*-R and *flhDC*-F and *flhDC*-R, respectively. *Z0021* was cloned into the HindIII/KpnI sites of pFLAG-CTC to create pFLAG-*Z0021* while *flhDC* was cloned into pBAD33 (244) at the KpnI/HindIII sites. A fragment containing *araC*-P_{BAD}-*flhDC* was amplified from pBAD33-*flhDC* using primers *araC*-*flhDC*-F and *araC*-*flhDC*-R and was then cloned into the BglII/SalI sites of pFLAG-*Z0021*. The resulting plasmid, pFLAG-*Z0021*-*flhDC*, had an IPTG-inducible copy of *Z0021* and a tightly regulated copy of *flhDC* under arabinose control.

Sequencing *Z0021* from a STEC strains collection

The gene encoding *Z0021* was amplified from purified chromosomal DNA by PCR using forward primer 5'- AAG CGG ACG CTA TTA CAA TTA G-3' and reverse primer 5'- GTC CCG ATG GTT CGC CAT TAA C-3' to generate a 721 bp product. DNA was

purified through Sephadex and sequenced using a BigDye® Terminator sequencing kit (Applied Biosystems, Life Technologies, Carlsbad, CA) and an ABI 3730XL automated sequencer (Applied Biosystems). Sequencing of amplified fragments was performed in both directions and in duplicate. A consensus sequence was generated from four sequence reads per strain using Discovery Studio Gene software (Accelrys Software Inc., San Diego, CA).

RESULTS

Deletion of OI-1 increases motility and flagellin production in *E. coli* O157:H7

Given the existence of flagellar regulatory proteins encoded within fimbrial clusters in other bacteria (219,220,245), we sought to determine whether the putative fimbrial genomic island, OI-1, encoded for any repressors of motility. We created a Δ OI-1 strain in which genes *Z0020-Z0025* had been replaced by a kanamycin resistance cassette and examined the swimming motility of the resulting mutant. In a standard soft-agar motility assay, the Δ OI-1 strain was highly motile compared to the wild-type EDL933 strain (Figure 2.2A and 2B). To elucidate which gene(s) was responsible for this phenotype, a series of single and multiple deletion mutants was constructed and assayed for motility. The Δ *Z0021* strain showed enhanced swimming motility similar to deletion of the entire OI-1, while the motility of the Δ *Z0020* and Δ *Z0022-Z0025* mutants was comparable to that of wild-type EDL933 (Figure 2.2A and 2.2B). All strains exhibited similar growth kinetics to the wild-type parental strain. The enhanced motility phenotype of the Δ *Z0021* strain was eliminated upon complementation with *Z0021* on a plasmid (Figure 2.2C). These data indicate that deletion of *Z0021* is responsible for the increased swimming phenotype of the Δ OI-1 strain.

We then investigated whether the enhanced motility of the Δ OI-1 and Δ *Z0021* mutants was due to an increase in flagellar function or due to an increase in flagellar biosynthesis. Bacteria were harvested from motility plates and the surface flagella were examined by transmission electron microscopy (TEM). While the majority of wild-type EDL933 bacteria were either non-flagellated or possessed a limited number of surface

flagella, the Δ OI-1 and Δ Z0021 mutants had a greater number of flagella on their surface (Figure 2.3A-C), suggesting that loss of Z0021 de-represses the biosynthesis of flagella under these conditions. To further confirm this, the amount of flagellin produced by the Z0021 and OI-1 deletion mutants was compared to the wild-type strain at 3, 6 and 24 h of growth. As shown in Figure 2.3F, the Δ OI-1 and Δ Z0021 mutants showed higher levels of flagellin production at every time point examined compared to wild-type. Taken together, these data are consistent with the OI-1-encoded Z0021 acting as a repressor of motility in *E. coli* O157:H7 strain EDL933.

Over-expression of Z0021 inhibits motility in *E. coli* O157:H7

Having identified Z0021 as a potential negative regulator of flagellar-based motility, we investigated whether elevated expression of Z0021 would repress the motility of *E. coli* O157:H7 strain EDL933. Z0021 was cloned under the control of the *tac* promoter in pFLAG-CTC and the motility of wild-type EDL933 carrying pFLAG-Z0021 was assessed at various concentrations of IPTG. Increasing inducer concentrations from 0.05 to 1 mM led to a marked decrease in swimming motility of *E. coli* O157:H7 strain EDL933 that was completely abolished at 1 mM IPTG (Figure 2.4). Western blot analysis confirmed that these motility patterns correlated with elevated levels of Z0021.

Deletion of Z0021 increases the transcription of class II and class III promoters

The enhanced swimming motility of the Δ Z0021 mutant was associated with an increase in flagellum production. To examine where in the flagellar activation cascade

this point of regulation occurred, we cloned promoter regions corresponding to each of the three promoter classes as transcriptional fusions to *luxCDABE* and measured luciferase activity in wild-type EDL933 and $\Delta Z0021$ strains. While *flhDC* promoter activity in the $\Delta Z0021$ mutant was comparable to that of the wild-type strain, there was a significant increase in the activity of the transcriptional reporters for all class II and class III promoters tested in the $\Delta Z0021$ strain compared to the wild-type strain (Figure 2.5A). These data suggest that Z0021 acts downstream of the transcription of *flhDC* and prior to the activation of the middle genes. To elucidate whether the increase in class II/III promoter expression was due to an increase in FlhD and FlhC production, we first used quantitative reverse-transcription PCR to measure *flhD*, *flgM*, *motA* and *fliC* transcript levels in wild-type and $\Delta Z0021$ strains. Deletion of *Z0021* led to a substantial increase in all middle and late flagellar gene transcripts but did not alter the level of the *flhD* transcript (Figure 2.5B). We then replaced the chromosomal copy of *flhC* in the *flhDC* operon with a C-terminal HA-tagged variant and determined the levels of FlhC-HA in wild-type and $\Delta Z0021$ backgrounds by western blot analysis. As expected from the reporter data, the levels of FlhC in the $\Delta Z0021$ mutant were comparable to the levels in the wild-type strain (Figure 2.5C). These results suggest that Z0021 regulates flagellar synthesis after translation of the FlhD and FlhC subunits.

FlhDC is a high-copy suppressor of the non-motile phenotype associated with over-expression of Z0021

Since Z0021 exerts its regulatory effect on class II flagellar promoters without altering the levels of the master regulator, we considered whether Z0021 was inhibiting the action of a functional FlhD₄C₂ complex. If this were the case, over-expression of *flhDC* should suppress the non-motile phenotype associated with elevated levels of Z0021. To investigate this idea, we tested whether increasing the expression of *flhDC* would restore motility to *E. coli* O157:H7 expressing Z0021. *E. coli* O157:H7 carrying pFLAG-Z0021-*flhDC* has a tightly regulated copy of *flhDC* under arabinose control and an IPTG-inducible copy of Z0021. The motility of this strain was assayed over varying concentrations of arabinose and at a fixed concentration of 0.1 mM IPTG – a concentration which we showed impairs the motility of *E. coli* O157:H7 strain EDL933 harbouring pFLAG-Z0021 (Figure 2.4). In our soft-agar motility assay, an arabinose concentration of 0.002 % restored motility of *E. coli* O157:H7 strain EDL933 harbouring pFLAG-Z0021-*flhDC* to that of the empty vector control while arabinose concentrations of 0.02 % and greater increased the motility of *E. coli* O157:H7 strain EDL933 harbouring pFLAG-Z0021-*flhDC* beyond that of the empty vector control (Figure 2.6). Taken together, these data show that the motility defects caused by Z0021 can be suppressed by increasing *flhDC* expression, implying a genetic link between Z0021 and the FlhD₄C₂ regulatory complex.

Prevalence of *Z0021* among STEC

O157:H7 was previously identified in seropathotype A strains of STEC. To examine the distribution of *Z0021* among the other four seropathotypes comprising non-O157:H7 STEC, we screened the 69 strains from the original seropathotype collection of Shiga toxin-containing *E. coli* (6) by PCR and sequenced the positive *Z0021* gene products. Only the O157:H7 strains from the seropathotype A group had the same *Z0021* sequence as the EDL933 reference strain with 100 % conservation (Figure 2.7). Although strains from the other seropathotypes harboured the *Z0021* gene, the gene contained either a frameshift mutation at nucleotide position 148 resulting in a downstream premature stop codon at position 73, or a deletion mutation at position 299 resulting in a frameshift starting at amino acid position 100 (Figure 2.7). Interestingly, these two gene variants appear to have evolved a number of times independently in different serotypes that assort to different seropathotype classes. Only seven other strains in the collection had a *Z0021* sequence similar to that of the EDL933 reference strain; however, in all cases these sequences had at least one non-synonymous substitution. Thus, only the O157:H7 strains in our collection had a *Z0021* sequence that was identical to the enterohemorrhagic *E. coli* reference strain. This *Z0021* sequence from all seropathotypes A strains was distinguished from all other serotypes by unique frame shifts or non-synonymous substitutions.

DISCUSSION

Many regulators of the flagellar transcriptional hierarchy have been identified and some of these are encoded within fimbrial clusters, presumably to control the opposing processes of adherence and motility. In the *E. coli* O157:H7 genome, the majority of the putative fimbrial clusters are uncharacterized and no fimbrial operon-encoded regulators of motility have been identified to date. In this work, we have reported on a novel repressor of *E. coli* O157:H7 motility encoded in the putative type 1-like fimbrial cluster, OI-1, and have shown that Z0021 regulates flagellar synthesis through its influence on class II promoters via FlhD₄C₂.

E. coli type 1 fimbriae play a role in facilitating adherence to host cells and establishing disease (96,246,247). Since *E. coli* O157:H7 strains are unable to produce type 1 fimbriae because of a deletion in the *fim* regulatory element (248), novel type 1-like fimbriae may play a role in the process of intestinal colonization (5,27). OI-1 is one of four fimbria-encoding OIs that is found in seropathotype A strains of O157 STEC and may be a key determinant of the unique virulence of such strains (5). OI-1 may encode for a type 1-like fimbria based on its similarity to the *E. coli* type 1 fimbrial locus. By comparison to the Lpf clusters in OI-141 and OI-154, which contain mutations in their export machinery (27), Z0022 and Z0023 of OI-1 may encode for functional usher and chaperone proteins, respectively. These gene products of OI-1 may therefore be able to assemble fimbriae at the cell surface. The putative adhesin gene in OI-1, Z0020, is different from characterized adhesin genes suggesting that it may encode for a novel adhesin or that other components of the fimbria produced by OI-1 confer binding

specificity (27). Future studies are required to structurally and functionally characterize the fimbriae produced by OI-1 and to determine the importance of this OI to O157:H7 STEC pathogenesis.

In an expression analysis of the 16 putative fimbrial clusters in *E. coli* O157:H7, OI-1 showed no or minimal expression under the *in vitro* conditions tested (27). While the expression of OI-1 *in vivo* has not been examined, our work has shown that expression of OI-1, and in particular *Z0021*, is important for repressing flagellar synthesis in *E. coli* O157:H7. The expression of flagella varies during the course of an infection: flagella are produced to a great extent by attaching bacterial cells in the early stages of infection, but are not present at later time points (249). We therefore speculate that the gene products of OI-1 may be of significance following the early stages of infection at a time when flagella expression is decreased.

Z0021 was found to exert its regulatory effects on class II flagellar promoters downstream of *flhDC* transcription and translation. It is therefore conceivable that *Z0021* could regulate flagellar synthesis by: (1) targeting FlhD and/or FlhC for degradation or (2) preventing a functional FlhD₄C₂ complex from binding to class II promoters. The ClpXP protease has been shown to degrade FlhD₄C₂ in both *Salmonella enterica* serovar Typhimurium and *E. coli* O157:H7 (250,251). Given that the transcript and protein levels of FlhD and FlhC were unchanged in the wild-type and $\Delta Z0021$ strains, this suggests that *Z0021* regulates flagellar synthesis through a mechanism independent of ClpXP. The mechanism of action of *Z0021* may be more similar to that of *Salmonella enterica* serovar Typhimurium YdiV, which in addition to repressing flagellar synthesis via a ClpXP-

dependent pathway (252), also acts via a ClpXP-independent pathway by interacting with the FlhD₄C₂ complex and preventing its binding to class II promoters (253). However, we have been unable to identify motifs shared by Z0021 and YdiV and the two proteins lack sequence conservation at the amino acid level. The latter proposed mechanism for Z0021-mediated repression is supported by the ability of *flhDC* to suppress the non-motile phenotype associated with expression of *Z0021*, indicating that the effects of Z0021 are reversible and dependent on the levels of the FlhD and/or FlhC subunits.

Comparative sequence analysis of the *Z0021* gene in STEC strains from our collection revealed a high degree of nucleotide sequence conservation among seropathotype A strains, including those which are non-motile. In addition to its role as the master regulator of the flagellar cascade, FlhD₄C₂ can also bind to and activate non-flagellar genes (254). Z0021 may therefore be conserved amongst these non-motile strains to regulate non-flagellar genes through an interaction with FlhD₄C₂ or the individual subunits, FlhD and FlhC. A highly conserved *Z0021* is also present in some seropathotype B-E strains. Although OI-1 is found predominantly in seropathotype A strains, there is evidence for OI-1 in other seropathotypes which may account for the wider distribution of *Z0021* in non-O157 STEC (5).

In summary, we identified a novel repressor of motility in *E. coli* O157:H7 and showed that Z0021 negatively regulates flagellar synthesis at a stage prior to the transcription of the middle and late genes. The characterization of Z0021 is the first report of a fimbrial operon-encoded gene product that represses flagellar synthesis in *E. coli* O157:H7, and consistent with this role we propose that *Z0021* be renamed *fmrA*. Most

importantly, our work has provided insight into the function of an OI that may be associated with the enhanced virulence of seropathotype A strains of STEC.

ACKNOWLEDGMENTS

This work was funded by an operating grant to B.K.C. from the Canadian Institutes of Health Research (MOP-82704), an infrastructure grant from the Canada Foundation for Innovation, and the Canada Research Chairs Program from the Government of Canada. S.E.A. is the recipient of a Canada Graduate Scholarship from the CIHR. U.S. was supported by NSERC Visiting Fellowship. B.K.C. is the Canada Research Chair in Infectious Disease Pathogenesis.

Figure 2.1. Genetic organization of O-island 1 in *E. coli* O157:H7 strain EDL933.

Arrows refer to open reading frames and the colour key for putative functions of open reading frames based on BLAST similarity is shown.

Figure 2.1

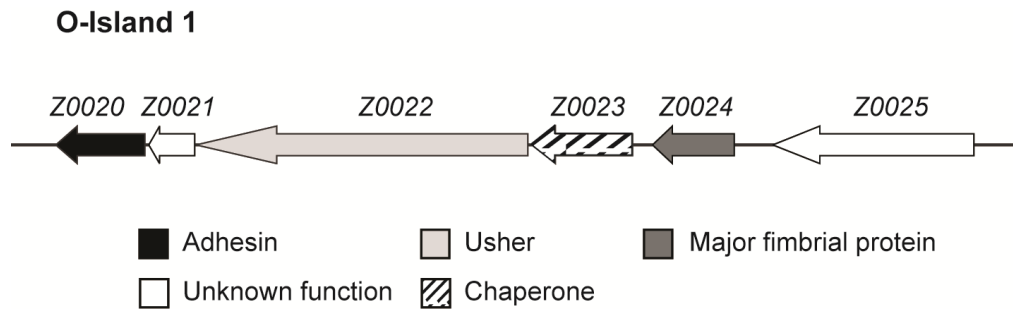


Figure 2.2. Deletion of OI-1 increases swimming motility. (A) Wild-type, Δ OI-1, Δ Z0020, Δ Z0021 and Δ Z0022-Z0025 mutant strains were examined for their swimming motility by a standard motility assay. (B) Migration distances of indicated strains in motility LB-agar plates were measured after 6 h at 37 °C. The asterisk denotes a *P*-value of < 0.001 compared to the wild-type strain. (C) Complementation of the Z0021 deletion strain restores the non-motile phenotype. The asterisk denotes a *P*-value of < 0.001 compared to the wild-type strain. All data are the means reported with standard deviations from at least three independent experiments.

Figure 2.2

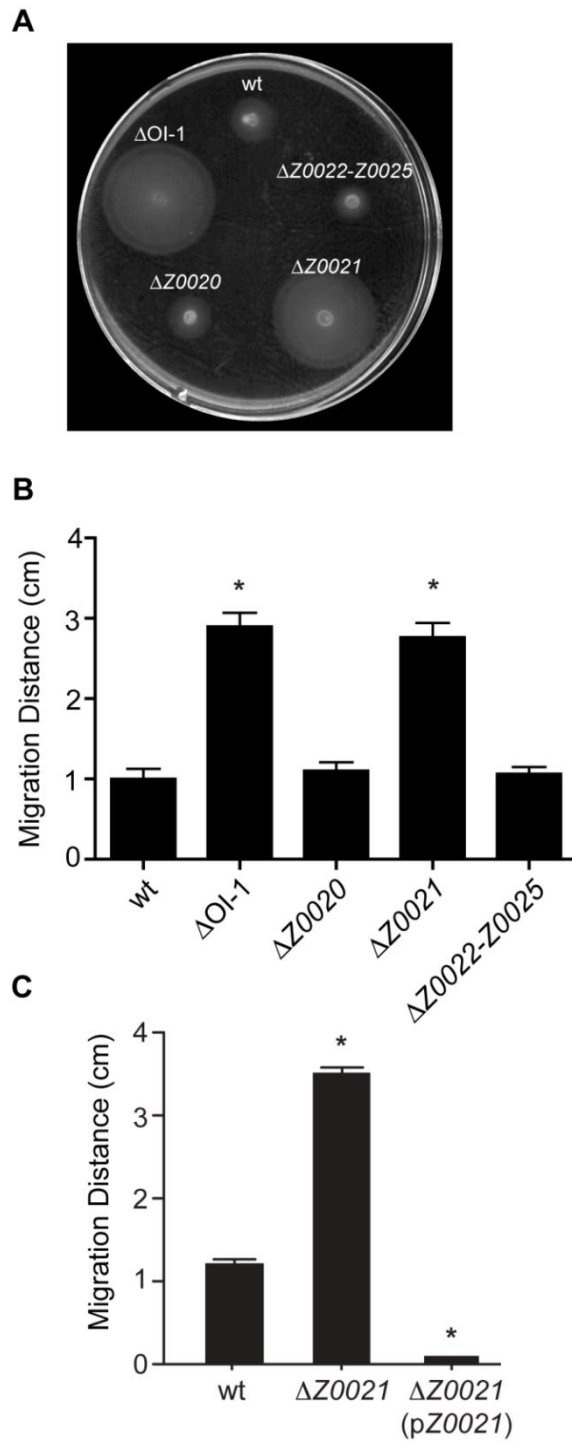


Figure 2.3. Deletion of *Z0021* increases flagellum production in *E. coli* O157:H7. (A-E) Transmission electron micrographs of: (A) wild-type *E. coli* O157:H7 strain EDL933 (scale bar of 1 μm); (B) $\Delta\text{OI-1}$ mutant strain (scale bar of 2 μm); (C) ΔZ0021 strain (scale bar of 2 μm); (D) $\Delta\text{OI-1}$ mutant strain carrying p*Z0021* (scale bar of 1 μm); and (E) ΔZ0021 strain complemented with p*Z0021* (scale bar of 1 μm). Cells were harvested from motility LB-agar plates after 6 h at 37 °C, were stained with 0.1% uranyl acetate, and were then viewed by TEM. (F) Western blot analysis of flagellin (FliC) levels in whole cell lysates of wild-type, $\Delta\text{OI-1}$, and ΔZ0021 strains. Asterisks indicate non-specific cross-reacting bands which were used as loading controls.

Figure 2.3

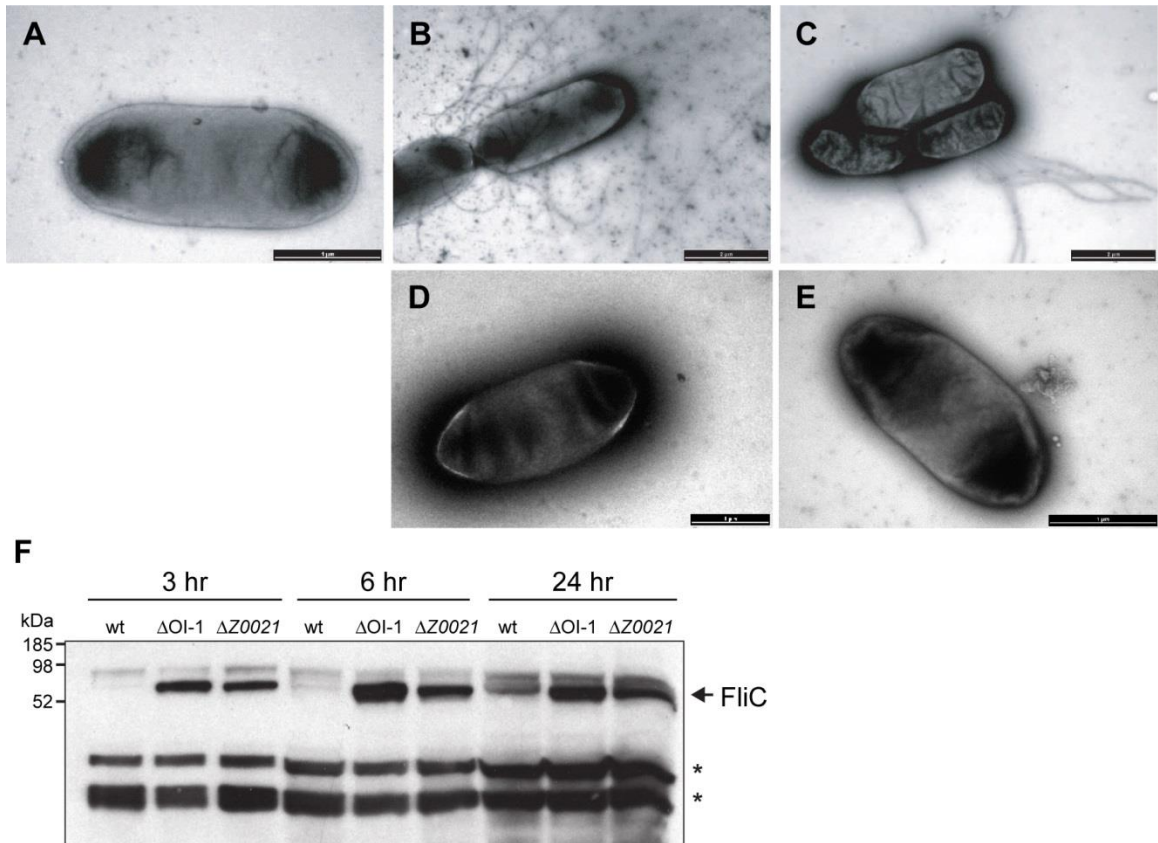


Figure 2.4. Over-expression of Z0021 represses swimming motility in *E. coli*

O157:H7 strain EDL933. Motility of *E. coli* O157:H7 harbouring an empty pFLAG or pFLAG-*Z0021* vector was assessed at varying concentrations of IPTG as shown. The migration distances on motility LB-agar plates were measured after 6 h at 37 °C and the data represent means with standard deviations. The * denotes a *P*-value of < 0.01 while ** indicates a *P*-value of < 0.001 compared to the pFLAG-empty control.

Figure 2.4

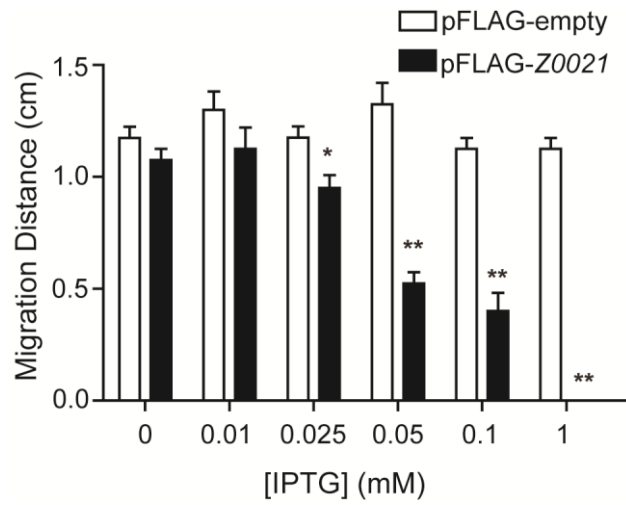


Figure 2.5. Deletion of *Z0021* impacts the flagellar cascade prior to class II/III

activation. (A) Transcriptional reporter activity for the indicated class I, II, and III promoters was examined in wild-type and $\Delta Z0021$ mutant strain backgrounds.

Luminescence was measured after 6 h of growth at 37 °C and was then normalized to the OD₆₀₀ readings. Data reported are means with standard deviations. The asterisk denotes a *P*-value of < 0.001 compared to the wild-type strain. (B) qRT-PCR analysis of *flhD*,

flgM, *motA* and *fliC* in wild-type and $\Delta Z0021$ mutant strain backgrounds. The levels of all transcripts were normalized to *icdA* mRNA. Shown are the means with standard

deviations from two independent experiments with three technical replicates (C) Whole

cell lysates from wild-type and $\Delta Z0021$ mutant strains were subjected to western blotting with anti-HA and anti-DnaK antibodies to determine the levels of FlhC-HA. DnaK served as a loading control.

Figure 2.5

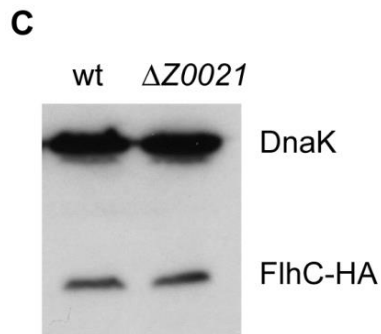
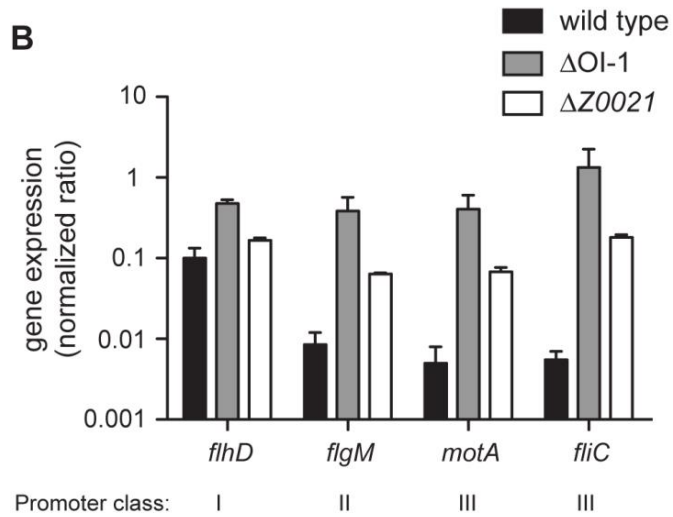
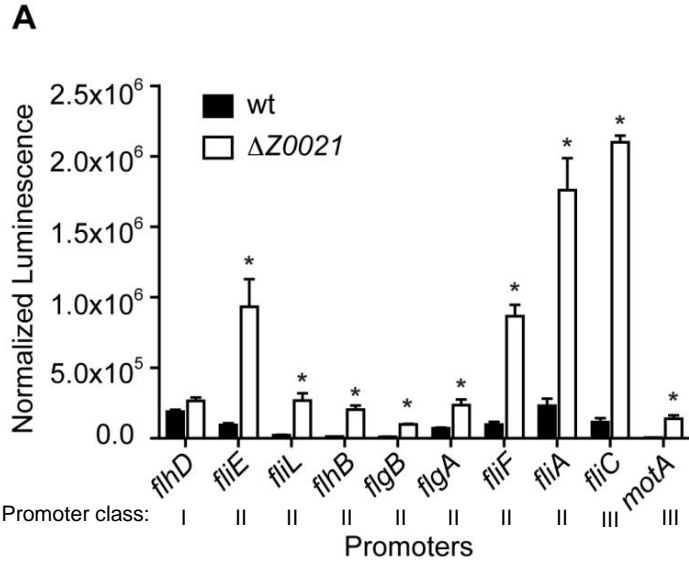


Figure 2.6. Increased expression of *flhDC* suppresses the non-motile phenotype associated with over-expression of Z0021. Motility of *E. coli* O157:H7 strain EDL933 harbouring an empty pFLAG vector, pFLAG-Z0021-*araC*-P_{BAD} or pFLAG-Z0021-*flhDC* was assessed in 0.25 % LB-agar containing ampicillin and 0.1 mM IPTG. Arabinose was varied from 0 – 0.2 % and migration distance was measured after 6 h of growth at 37°C. Data represent means with standard deviations, and the asterisk denotes a *P*-value of < 0.01 compared to the pFLAG-empty strain.

Figure 2.6

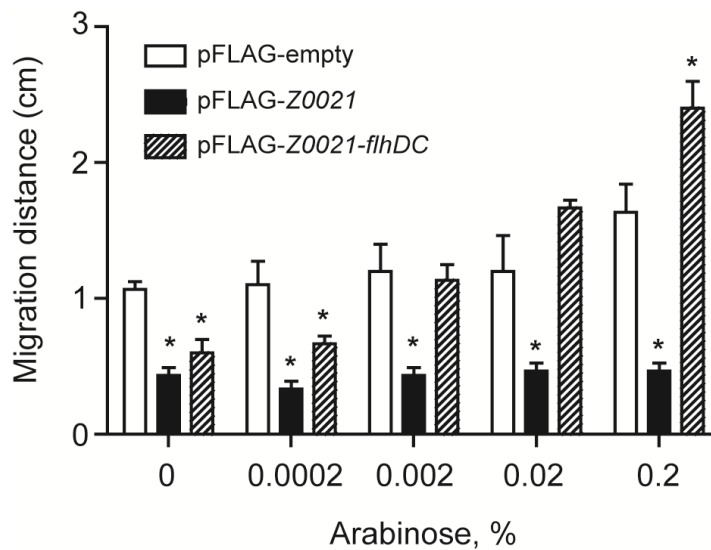


Figure 2.7. Prevalence of Z0021 in Shiga-toxin producing *E. coli*. Z0021 genes were amplified from 69 STEC strains, including non-O157 STEC from all seropathotypes. Nucleotide sequences were translated *in silico* and the amino acid sequences were aligned. Strain names are given to the left of the sequence and are grouped into seropathotypes. The alignment is shown as a heat-map according to the conservation at each position, with darker blue representing higher conservation and light blue representing lower conservation among all the sequences.

Figure 2.7

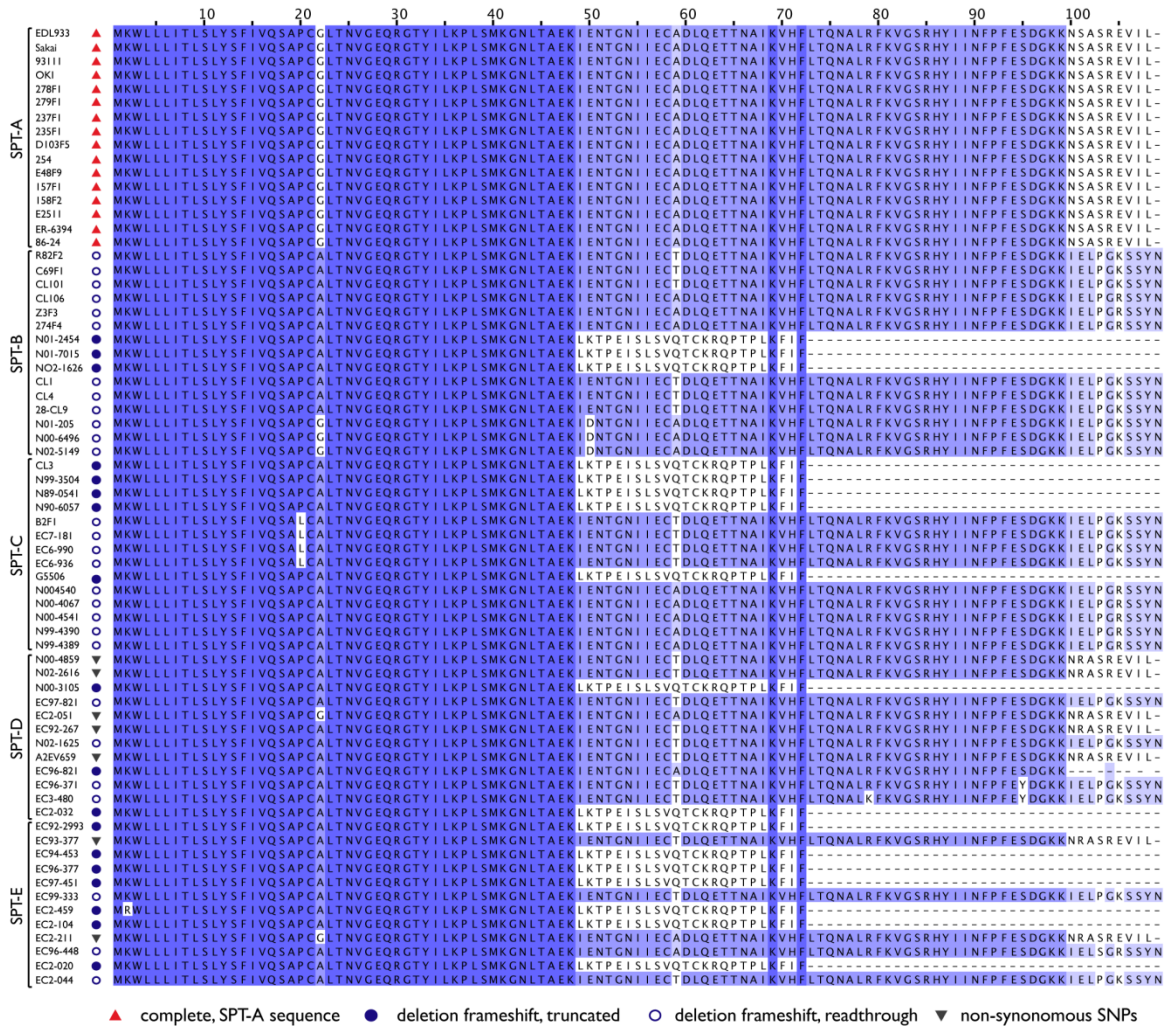


Table 2.1. Strains, plasmids and oligonucleotides used in this study.

Strain, plasmid or oligonucleotide	Description ^{a, b}	Reference or source
Strains		
BKC15-1	Enterohemorrhagic <i>E. coli</i> serotype O157:H7, wild-type strain EDL933	20
BKC19-79	EDL933 with deletion of O-island 1 (Δ OI-1:: <i>Kan</i>)	This study
BKC19-81	EDL933 Δ Z0020, Kan ^R	This study
BKC20-1	EDL933 Δ Z0021, Kan ^R	This study
BKC15-3	EDL933 Δ Z0021; kan cassette excised	This study
BKC20-7	EDL933 Δ Z0022 Δ Z0023 Δ Z0024 Δ Z0025, Kan ^R	This study
BKC30-74	EDL933 with pCS26- <i>flhD</i>	This study
BKC30-75	EDL933 with pCS26- <i>fliE</i>	This study
BKC30-76	EDL933 with pCS26- <i>fliL</i>	This study
BKC30-77	EDL933 with pCS26- <i>flhB</i>	This study
BKC30-78	EDL933 with pCS26- <i>flgB</i>	This study
BKC30-79	EDL933 with pCS26- <i>flgA</i>	This study
BKC30-80	EDL933 with pCS26- <i>fliF</i>	This study
BKC30-81	EDL933 with pCS26- <i>fliA</i>	This study
BKC31-1	EDL933 with pCS26- <i>fliC</i>	This study
BKC31-2	EDL933 with pCS26- <i>motA</i>	This study
BKC31-3	EDL933 Δ Z0021 (BKC15-3) with pCS26- <i>flhD</i>	This study
BKC31-4	EDL933 Δ Z0021 (BKC15-3) with pCS26- <i>fliE</i>	This study
BKC31-5	EDL933 Δ Z0021 (BKC15-3) with pCS26- <i>fliL</i>	This study
BKC31-6	EDL933 Δ Z0021 (BKC15-3) with pCS26- <i>flhB</i>	This study
BKC31-7	EDL933 Δ Z0021 (BKC15-3) with pCS26- <i>flgB</i>	This study
BKC31-8	EDL933 Δ Z0021 (BKC15-3) with pCS26- <i>flgA</i>	This study
BKC31-9	EDL933 Δ Z0021 (BKC15-3) with pCS26- <i>fliF</i>	This study
BKC31-10	EDL933 Δ Z0021 (BKC15-3) with pCS26- <i>fliA</i>	This study
BKC31-11	EDL933 Δ Z0021 (BKC15-3) with pCS26- <i>fliC</i>	This study
BKC31-12	EDL933 Δ Z0021 (BKC15-3) with pCS26- <i>motA</i>	This study
BKC16-15	EDL933 <i>flhD</i> :: <i>flhD</i> -HA	This study
BKC16-16	EDL933 <i>flhC</i> :: <i>flhC</i> -HA	This study
BKC31-14	EDL933 Δ Z0021 <i>flhC</i> :: <i>flhC</i> -HA	This study
BKC31-15	EDL933 harbouring pFLAG-CTC	This study
BKC31-16	EDL933 harbouring pFLAG-Z0021	This study
BKC31-17	EDL933 harbouring pFLAG-Z0021- <i>araC</i> -P _{BAD}	This study
BKC31-18	EDL933 harbouring pFLAG-Z0021- <i>flhDC</i>	This study
BKC1-14	DH5 α (<i>hsdR recA lacZYA</i> ϕ 80 <i>lacZ</i> Δ M15)	Lab collection
Plasmids		
pKD4	ori γ , Kan ^R cassette flanked by FRT sites (FLP recombinase target)	242
pKD46	RepA1019(Ts), λ , γ , β and <i>exo</i> expressed from <i>ParaBAD</i> , Ap ^R	242
pCS26	pSC101 <i>ori</i> , <i>luxCDABE</i> , Kan ^R	243
pCS26- <i>flhD</i>	<i>flhD</i> promoter from EDL933 fused to <i>luxCDABE</i> in pCS26, Kan ^R	This study

pCS26- <i>fliE</i>	<i>fliE</i> promoter from EDL933 fused to <i>luxCDABE</i> in pCS26, Kan ^R	This study
pCS26- <i>fliL</i>	<i>fliL</i> promoter from EDL933 fused to <i>luxCDABE</i> in pCS26, Kan ^R	This study
pCS26- <i>flhB</i>	<i>flhB</i> promoter from EDL933 fused to <i>luxCDABE</i> in pCS26, Kan ^R	This study
pCS26- <i>flgB</i>	<i>flgB</i> promoter from EDL933 fused to <i>luxCDABE</i> in pCS26, Kan ^R	This study
pCS26- <i>flgA</i>	<i>flgA</i> promoter from EDL933 fused to <i>luxCDABE</i> in pCS26, Kan ^R	This study
pCS26- <i>fliF</i>	<i>fliF</i> promoter from EDL933 fused to <i>luxCDABE</i> in pCS26, Kan ^R	This study
pCS26- <i>fliA</i>	<i>fliA</i> promoter from EDL933 fused to <i>luxCDABE</i> in pCS26, Kan ^R	This study
pCS26- <i>fliC</i>	<i>fliC</i> promoter from EDL933 fused to <i>luxCDABE</i> in pCS26, Kan ^R	This study
pCS26- <i>motA</i>	<i>motA</i> promoter from EDL933 fused to <i>luxCDABE</i> in pCS26, Kan ^R	This study
pFLAG-CTC	Cytoplasmic expression of C-terminal FLAG fusion protein under control of the <i>Ptac</i> , Amp ^R	Lab collection
pFLAG-Z0021	pFLAG-CTC carrying Z0021 with native stop codon, Amp ^R	This study
pBAD33	Arabinose-inducible expression vector, Cm ^R	244
pFLAG-Z0021- <i>araC</i> -P _{BAD}	pFLAG-CTC carrying Z0021 with native stop codon at HindIII/KpnI sites and <i>araC</i> -P _{BAD} cloned in at BglII/SalI sites, Amp ^R	This study
pFLAG-Z0021- <i>flhDC</i>	pFLAG-CTC carrying Z0021 with native stop codon and <i>araC</i> -P _{BAD} - <i>flhDC</i> cloned in at BglII/SalI sites, Amp ^R	This study
Primers		
Red-OI-1-F	ggaatggtgaaattatcgcagatagcatttcttctaaattataagatgtgtaggctggagctgcttcg	
Red-OI-1-R	ctcataaattaataataaaaaattcatcaactcaaggactgataatatgaatgtcctccta	
Red-Z0020-F	gcgctccagggagtcatttataatttagaagaagtgtaggctggagctgcttcg	
Red-Z0020-R	cggcagctccccaaagttaaggtgggggagatagacatatgaatatcctccta	
Red-Z0021-F	cgatgaaacaaaacatatatgccagtaaaaggagtgtgtaggctggagctgcttcg	
Red-Z0021-R	gtatggaatggtgaaattatcgcagatagcatttcttctaaacatatgaatatcctccta	
Red-Z0022-F	catagtaaaatcgccgcgagataacaggaaaaagtcgtgtaggctggagctgcttcg	
Red-Z0022-R	tgtgattaataaaaagccactcatagtaaacctcctcatatgaatcctcctta	
Red-Z0022-25-F	taagctaactgactgcacagatcaacaactggcttaagtgtaggctggagctgcttcg	
Red-Z0022-25-R	taaaagaatatagactcaatgtgattaataaaaagccactcactcatatgaatatcctccta	
conf-pKD4-F	ccttcttgacgagttcttct	
Conf-Z0020-R	agttaaggtgggggagatag	
Conf-Z0021-F	cctgtggattgaccaatgc	
Conf-Z0021-R	acgactccgactttaaac	

Conf-Z0022-25-R	gattaataaaagccactca
prom <i>flhD</i> – F	gcgc ggatccc attattcccaccagaataacc
prom <i>flhD</i> – R	gcgc ctcgag gcacacctgaattaactatcaag
prom <i>fliE</i> – F	gcgc ggatcct atcgctgacatttcatctcctg
prom <i>fliE</i> – R	gcgc ctcgagt ggcggtgaatattaccgttacc
prom <i>fliL</i> – F	gcgc ctcgag ggccagcatatttcgctgttcacc
prom <i>fliL</i> – R	gcgc ggatccc gtaatcagtcatgtgttcggggtc
prom <i>flhB</i> – F	gcgc ggatccc ctcgtcagacacgtcgccaatcc
prom <i>flhB</i> – R	gcgc ctcgag agccagtcaggatcagggtggagc
prom <i>flgB</i> – F	gcgc ctcgag gggtggaggtgtgttttggcgcctc
prom <i>flgB</i> – R	gcgc ggatccc ttatcgagcatatctctccgcag
prom <i>flgA</i> – F	gcgc ggatccc tattgccagcattttgcceccag
prom <i>flgA</i> – R	gcgc ctcgag attggcgatgttctgctgccagc
prom <i>fliF</i> – F	gcgc ctcgagt gcggcagtgattcctgcgcacg
prom <i>fliF</i> – R	gcgc ggatccc agtcgattcatcgcgcacctcgtg
prom <i>fliA</i> – F	gcgc ggatccc gagtgaaatcacgataaacagccctg
prom <i>fliA</i> – R	gcgc ctcgag gcaactcctgcgacaaccactccag
prom <i>fliC</i> – F	gcgc ggatccc gacttgtccatgattcgttatcc
prom <i>fliC</i> – R	gggc ctcgag gcgatttctttatcattcgaca
prom <i>motA</i> – F	gcgc ggatccc taagataagcacgacatcatccttc
prom <i>motA</i> – R	gcgc ctcgag cttcgatgttctgtaatgcatgg
qRT- <i>flhD</i> -F	acctccgagttgctgaaacac
qRT- <i>flhD</i> -R	ttgctggagatcgtcaacgc
qRT- <i>flgM</i> -F	ccgtcaaccgcgcgaaacc
qRT- <i>flgM</i> -R	tgctgccgggtgcatcagt
qRT- <i>motA</i> -F	gcgaacagtctggcgtggt
qRT- <i>motA</i> -R	tgtgcgataagcgcceccag
qRT- <i>fliC</i> -F	tgacggtgcctctctgacattc
qRT- <i>fliC</i> -R	aagacttcgcagcatcactgg
qRT- <i>icdA</i> -F	acgtgattgctgatcattcctgc
qRT- <i>icdA</i> -R	accgttcaggtccatacagggcat
pSU315- <i>flhC</i> -F	ccacaactgctggatgaacagagagtacaggctgtttatccgtatgatgttcctg
	at
pSU315- <i>flhC</i> -R	gttaccgctgctggaatgttgcgccacaccgtatcagcatatgaatatacctcctta
	g
conf- <i>flhC</i> -F	cagagccagcagatccatatac
conf- <i>flhC</i> -R	gtttgtgtaatggcgtcgtatgc
Z0021 – F	gcgc caagctt atgaagtggctttattaatc
Z0021 – R	gcgc gaattc ttataagatgacttccctggaag
<i>flhDC</i> – F	gcgc caagctt ttaaacagcctgtactctctgttc
<i>flhDC</i> – R	gcgc ggtaccaataaggaggaaaaaaa gtgggaataatgcatacctccga
	g
<i>araC-flhDC</i> -F	gcgc agatc ttatgacaacttgacggctacatc
<i>araC-flhDC</i> -R	gcgc gtcgac ctgatttaactgtatcaggctg

^A Bolded sequences indicate restriction sites

^B Underlined sequences indicate optimal ribosome binding site (RBS)

CHAPTER THREE

Identification of the Docking Site between a Type III Secretion System ATPase and a Chaperone for Effector Cargo

CO-AUTHORSHIP STATEMENT

At the time that this thesis was written, material within in this chapter was in review at the *Journal of Biological Chemistry*. A modified version of the work has since been accepted at the Journal. The chapter herein has therefore been adapted from the following:

Allison, S.E., Tuinema, B.R., Everson, E.E., Sugiman-Marangos, S., Zhang, K., Junop, M.S., and Coombes B.K. (2014) Identification of the docking site between a type III secretion system ATPase and a chaperone for effector cargo. *J. Biol. Chem.* [In Press]

The contributions by each author to the project are described below:

1. Strains and plasmids were created by S.E.A., B.R.T., and E.E.
2. Secretion assays were performed by S.E.A. and E.E.
3. Mouse infection experiments were conducted by B.R.T.
4. Protein purification, crystallization and structure determinations were done by K.Z., S.S.M., and M.S.J.
5. S.E.A. conducted pull-down and activity experiments, and performed the circular dichroism analysis
6. M.S.J. created the chaperone-T3SS ATPase model
7. S.E.A., B.R.T., S.S.M., M.S.J., and B.K.C. contributed to writing of the manuscript

Identification of the docking site between a type III secretion system ATPase and a chaperone for effector cargo

Sarah E. Allison^{1,2}, Brian R. Tuinema^{1,2}, Ellen S. Everson^{1,2}, Seiji Sugiman-Marangos^{1,2},
Kun Zhang^{1,2}, Murray S. Junop^{1,2} and Brian K. Coombes^{1,2*}

¹ *Department of Biochemistry and Biomedical Sciences, McMaster University, Hamilton, Ontario L8S 4K1, CANADA*

² *Michael G. DeGrootte Institute for Infectious Disease Research, Hamilton, Ontario L8S 4K1, CANADA*

* Address correspondence to BKC (coombes@mcmaster.ca):
1280 Main Street West, Health Sciences Centre Room 4H17, Hamilton, Ontario L8S 4K1

Running Title: Chaperone Recognition by a T3SS ATPase

ABSTRACT

A number of Gram-negative pathogens utilize type III secretion systems (T3SSs) to inject bacterial effector proteins into the host. An important component of T3SSs is a conserved ATPase that captures chaperone-effector complexes and energizes their dissociation to facilitate effector translocation. To date, there has been limited work characterizing the chaperone-T3SS ATPase interaction although it is a fundamental aspect of T3SS function. In this study, we present the 2.1 Å-resolution crystal structure of the *Salmonella enterica* SPI-2 encoded ATPase, SsaN. Our structure revealed a local and functionally important novel feature in helix 10 that we used to define the interaction domain relevant to chaperone binding. We modeled the interaction between the multi-cargo chaperone, SrcA, and SsaN and validated this model using mutagenesis to identify the residues on both the chaperone and ATPase that mediate the interaction. Finally, we quantified the benefit of this molecular interaction on bacterial fitness *in vivo* using chromosomal exchange of wild-type *ssaN* with mutants that retain ATPase activity, but no longer capture the chaperone. Our findings provide insight into chaperone recognition by T3SS ATPases and demonstrate the importance of the chaperone-T3SS ATPase interaction for the pathogenesis of *Salmonella*.

INTRODUCTION

Many Gram-negative pathogens employ a specialized secretion complex known as a type III secretion system (T3SS) for the translocation of bacterial virulence proteins into host cells. These secretion systems, composed of over 20 proteins, span the inner and outer bacterial membranes and cross the eukaryotic cell membrane to form a channel through which largely unfolded effectors pass (255). Effectors, in complex with specific secretion chaperones, are targeted to the base of T3SSs. Here, a highly conserved ATPase aids in chaperone release and effector unfolding (167) and energy derived from the proton motive force drives effector secretion (170,171). Some of the earliest (256,257) and most recent demonstrations (258) of chaperone-T3SS ATPase interactions have come from work on the enteropathogenic *E. coli* T3SS ATPase, EscN, and the chaperones, CesT and CesAB. Despite a crucial role in the secretion process, little is known about how T3SS ATPases recognize their repertoire of chaperones and effector substrates.

Salmonella enterica serovars, a group of pathogens that cause diseases such as gastroenteritis and typhoid fever (259,260), employ two distinct virulence-associated T3SSs for the translocation of unique sets of effector proteins into the host (255). The T3SS encoded by *Salmonella* pathogenicity island 1 (SPI-1) is activated upon contact with intestinal epithelial cells and is required for the invasion of non-phagocytic cells (54). The second T3SS, encoded by SPI-2, translocates effector proteins into the host cell that are necessary for ensuring intracellular survival and replication (34,35). Chaperone-effector interactions have been charted extensively for both the T3SS-1 (261-264) and T3SS-2 (176,177,180,181,183,265), and a number of functions attributed to secretion

chaperones beyond that of effector binding have been demonstrated in *Salmonella* (114,266).

T3SS ATPases share significant structural similarity to the catalytic β subunit of F_0F_1 ATPases (150,157) and form hexameric (150) and dodecameric (161) rings that reside at the interface of the cytoplasmic membrane, likely aligning with the base of the T3SS to form a continuous channel (161,267). Both oligomerization and membrane association enhance the catalytic activity of these enzymes (158,160). At the membrane, T3SS ATPases interact with chaperones and other components of the export apparatus to ensure that effector substrates are delivered to the secretion channel. Loss-of-function mutations in these ATPases result in severe effector secretion defects and strong virulence attenuation phenotypes (152,172,173). One of the most extensively characterized T3SS ATPases is the SPI-1 encoded InvC from *Salmonella enterica* for which particular domains involved in catalytic activity, membrane association and oligomerization have been defined (152). Although recent structural and biochemical work has aided in understanding the role of these T3SS ATPases in effector secretion, the molecular basis for the chaperone-T3SS ATPase interaction has remained elusive.

In this work we used the *Salmonella enterica* SPI-2 encoded ATPase, SsaN, as a model for uncovering fundamental chaperone binding functionality given the large repertoire of chaperones and effectors associated with the T3SS-2. In doing so, we defined the chaperone interaction site on this T3SS ATPase and identified the corresponding residues on the multi-cargo effector chaperone, SrcA, that facilitate binding to SsaN. The high degree of conservation of the chaperone-binding site amongst

T3SS ATPases suggests that insight into the mechanism of substrate recognition provided here likely extends to virulence-associated type III secretion systems in other species.

MATERIALS AND METHODS

Competitive infections

All animal experiments were conducted in accordance with the guidelines set by the Canadian Council on Animal Care and were approved by the McMaster University Animal Review Ethics Board. Female C57BL/6 mice (Charles River, Wilmington, MA) were infected via the peritoneum with 2×10^5 bacteria in 0.1 M HEPES, pH 8.0, and 0.9 % NaCl containing a 1:1 ratio of chloramphenicol-resistant wild-type *S. Typhimurium* (*ushA::Cm*) to an unmarked *ssaN* mutant as described previously (129). At 72 h post-infection the spleen, liver, and cecum were harvested, homogenized in PBS, and plated to determine the total number of colony forming units (CFU). Colonies were replica plated onto LB-agar containing either chloramphenicol or streptomycin to determine the total number of wild-type and mutant CFU and the competitive index (CI) was then calculated as $\text{CFU of (mutant/wild type)}_{\text{output}} / \text{(mutant/wild type)}_{\text{input}}$.

Construction of mutant strains

All strains, plasmids and oligonucleotides used in this study are listed in supplemental Table 3.S1. In-frame deletion strains were constructed using the methods outlined by Datsenko and Wanner (242). Linear DNA was amplified from pKD4 and transformed into SL1344 strains harboring pKD46. Resistance cassettes were removed when necessary using pCP20. All strains generated were confirmed by PCR. To generate His- or FLAG-tagged constructs, genes were cloned into the NdeI/BamHI sites of pET3a or pET28b, the NdeI/KpnI sites of pFLAG-CTC and the XhoI/KpnI sites of pFLAG-MAC,

and confirmed by sequencing. For chromosomal replacements of *ssaN*, 1-kb regions surrounding the chaperone-binding site were cloned into the *Sma*I site of pRE112 and then transformed into *E. coli* S17-1- λ pir. These strains were conjugated with the marked *ssaN* mutant strain and merodiploids were selected on media containing kanamycin and chloramphenicol. Merodiploids were grown overnight in LB containing 5 % (w/v) sucrose and were then plated onto LB-agar. Colonies sensitive to kanamycin and chloramphenicol were confirmed by PCR.

***Salmonella* secretion assays**

Secretion assays were performed as described previously (119). Overnight cultures of strains were washed in low phosphate and magnesium medium (LPM) (pH 5.8), sub-cultured 1:50 into LPM medium containing antibiotics when necessary, and grown to an $OD_{600} \sim 0.6$. Bacteria were pelleted and the supernatant was filtered through a 0.2 μ m filter (Millipore). Supernatant samples were mixed with trichloroacetic acid (10% final concentration) and incubated overnight at 4 °C. Precipitated proteins in the supernatant fractions were centrifuged at $18,000 \times g$ for 45 min and washed with ice-cold acetone prior to suspension in 2x SDS loading buffer based on OD_{600} readings. Bacterial pellets were also resuspended in 2x SDS loading buffer. All samples were resolved by SDS-PAGE and were subjected to western blot analysis using primary antibodies at the following dilutions: mouse anti-HA (1:2000; Covance, MMS-101R), mouse anti-DnaK (1:10000; Stressgen, SPA-880), rabbit anti-SseB or anti-SseD (1:5000; gift from John Brumell), and rabbit anti-SseC (1:15000; gift from Michael Hensel). Secondary

antibodies (1:10000; Sigma, A6154 or A4416) were conjugated to horse radish peroxidase and blots were developed using an enhanced chemiluminescent detection system (Pierce Chemical Company, Rockford, IL, USA).

Protein interaction studies

E. coli BL21(DE3) strains harboring pFLAG or pET vectors were grown at 37 °C in LB medium to an OD₆₀₀ of ~0.5, induced with 1 mM IPTG and grown for an additional 3 h. Cells were harvested by centrifugation (4,850 × g for 10 min) and then resuspended in PBS containing a mini-EDTA protease inhibitor tablet (1 tablet per 40 mL PBS) (Roche, Mississauga, ON). Cells were lysed by sonication (Misonix Sonicator 3000, Misonix, Farmingdale, NY) and the lysate was spun at 4,850 × g for 15 min. The resulting supernatant was filtered through a 0.45 µm filter. During cell lysate preparation, Ni-NTA agarose beads (Qiagen, Valencia, CA) were equilibrated and blocked in PBS with 1 % BSA. Mixed lysates were then incubated with the Ni-NTA agarose beads in binding buffer (PBS with 10 mM imidazole) for 2 h at 4°C with end-on-end mixing. Beads were collected by centrifugation and washed extensively with binding buffer containing 0.01 % Triton X-100. Proteins were then eluted with 500 mM imidazole and subjected to western blot analysis using anti-His (1:20000; GE-Healthcare, GE27471001) and anti-FLAG (1:5000; Sigma, F1804) antibodies.

Protein purification, activity assays, and circular dichroism

SsaN protein was produced and purified as previously described (176). ATPase activity of purified SsaN $_{\Delta 1-89}$ variants was determined by measuring the release of total phosphate at 37 °C in a microplate assay with Biomol Green according to manufacturer's instructions (Enzo Life Sciences). Briefly, purified protein (50 $\mu\text{g}/\text{mL}$) was incubated in reaction buffer (50 mM Tris pH 7.5, 10 mM MgCl_2 , 100 $\mu\text{g}/\text{mL}$ BSA and 1 mM ATP) for 30 mins and then total phosphate release of SsaN variants was measured and normalized to that of wild-type SsaN $_{\Delta 1-89}$.

Circular dichroism spectra of wild-type SsaN $_{\Delta 1-89}$ and variants were collected with an AVIV spectropolarimeter using a quartz cuvette with a path-length of 0.1 cm. Purified protein samples were adjusted to concentrations of 0.11-0.17 mg/mL in buffer containing 5 mM HEPES, pH 7.5. Scans were conducted every nm from 198-260 nm and the temperature was maintained at 25 °C. The spectra reported are the averages of at least three scans and have been corrected for background buffer measurements.

Crystallization, data collection and structure determination

Crystals of SsaN were grown at 20 °C using the hanging-drop vapour diffusion method. SsaN (2 μL of 1.7 mg/mL in 20 mM Tris pH 7.5, 0.1 M potassium chloride, and 0.01 M TCEP) was mixed with 1 μL of crystallization solution (0.5 M ammonium sulphate, 0.1 M sodium citrate tribasic dihydrate pH 5.6, and 10% v/v Jeffamine M-600) and 0.2 μL of 0.1 M L-proline. The drops were initially dehydrated against 500 μL of 1.5 M ammonium sulphate. Following nucleation, the drops were transferred over successively higher

concentrations of well solution to a final concentration of 4 M ammonium sulphate. Diffraction data was collected at a wavelength of 1.1 Å on the X25 beamline of the National Synchrotron Light Source at Brookhaven National Laboratory. The data were processed and scaled with HKL2000 (268) to 2.1 Å. A search model was generated from the structure of EscN from *E. coli* (PDB ID 2OBM) using the chainsaw algorithm (269,270), which was used to solve the structure of SsaN by molecular replacement using PHASER from the PHENIX software package (271). Model building and refinement was carried out through multiple iterations of Coot (272) and PHENIX-Refine until R values and geometry statistics reached suitable ranges (Table 3.1).

Molecular models for hexameric SsaN and SrcA-SsaN were generated using the structure-similarity matching algorithm within Coot (272,273). A hexamer of SsaN was modeled based on the F1 ATPase structure. SrcA was then modeled onto the surface of SsaN based on structural similarity between SrcA and the γ subunit of F1 ATP synthase. Protein interaction analysis for the model of SrcA-SsaN was performed using the protein interfaces, surfaces and assemblies program (PISA) (274).

RESULTS

SsaN is essential for virulence in an animal model of infection and for secretion of a subset of SPI-2 effectors

SsaN is predicted to be the T3SS-2 ATPase based upon its similarity to other characterized T3SS ATPases and by its enzymatic activity that has been demonstrated *in vitro* (168,176). We first confirmed the essential activity of this enzyme for bacterial infection fitness by competing a $\Delta ssaN$ mutant against wild-type bacteria in C57BL/6 mice. In these experiments, the competitive index (CI) for SsaN-deficient cells was less than 0.1 in the spleen, liver, and cecum (Figure 3.1A), indicating that the *ssaN* deletion strain was significantly attenuated during systemic infection.

Given that T3SS ATPases have been shown to be essential for effector secretion (150,152,172), we reasoned that the $\Delta ssaN$ strain was attenuated *in vivo* due to impaired release of SPI-2 effectors. To investigate this we tested the secretion of a panel of translocon and effector substrates in a wild-type and $\Delta ssaN$ background. As expected, SsaN was required for the secretion of needle and translocon components (Figure 3.1B), and the effectors encoded within the SPI-2 locus, SseF and SseG (Table 3.2). We confirmed that SsaN was responsible for this secretion defect by complementing the $\Delta ssaN$ strain with a wild-type copy of *ssaN* under the control of the *tac* promoter. Secretion of the translocon component, SseC, was partially restored in the complemented $\Delta ssaN$ strain (Figure 3.1C).

By contrast to the requirement of SsaN for the secretion of substrates encoded within the SPI-2 locus, SsaN displayed a mixed dispensability pattern for the secretion of

effectors encoded outside of the SPI-2 locus. In fact, a subset of effectors was secreted to near wild-type levels in the *ssaN* mutant (Figures 3.1B and D). To determine whether this subset of effectors was being secreted by the T3SS-1 in the absence of a functional T3SS-2, we constructed $\Delta invC$ and $\Delta ssaN\Delta invC$ strains and examined the secretion of PipB, PipB2, SseL, and SopD2 in these backgrounds. While these effectors could be secreted in the single $\Delta ssaN$ and $\Delta invC$ mutants, secretion was completely abolished in the $\Delta ssaN\Delta invC$ double mutant (Figure 3.1D and Table 3.2), indicating that a subset of SPI-2 effectors can be targeted to the T3SS-1 in the absence of SsaN.

Crystal structure of SsaN

We noted in our secretion profiles that all of the substrates encoded within the SPI-2 locus that required SsaN for secretion have known or putative chaperones. Given that T3SS ATPases have been proposed to function as a docking site for chaperone-effector complexes (167), we sought to define the molecular mechanism by which SsaN captures these complexes to initiate translocation. To do so, we solved the structure of a N-terminally truncated variant of SsaN, SsaN $_{\Delta 1-89}$, at a resolution of 2.1Å (PDB 4NPH). The N-terminally truncated variant of SsaN was needed to generate enough soluble protein for crystallization trials and its structure was determined by molecular replacement with the orthologous T3SS ATPase from enteropathogenic *E. coli*, EscN (150). A summary of the crystallographic data and refinement statistics are shown in Table 3.1. SsaN $_{\Delta 1-89}$ contains two domains, a central domain (residues 90-331) and a C-terminal domain (residues 332-433). The central domain is highly similar to other

ATPase catalytic domains with a mixed α/β Rossmann fold (275) containing 3 and 4 helices which buttress either side of a central nine-stranded parallel β -sheet. The C-terminal domain, for which there is currently no known function, is comprised of 5 helices (Figure 3.2A). ATPase domains from SsaN and F1 ATPases (PDB 1E79) (276) are strikingly similar and can be structurally aligned with a r.m.s deviation of ~ 1.9 Å for C α atoms spanning 225 residues. SsaN homologues form hexamers (155,158), and SsaN can be readily modeled into a hexamer conformation based on the structure of the F1 ATPase (Figure 3.2B). In addition to Walker boxes for both SsaN and EscN being highly conserved (Walker A at the end of $\alpha 2$ and Walker B within $\beta 9$), the arginine finger motif containing R352, which contributes to ATP binding and possibly hexamer formation (277), is also well conserved.

Despite SsaN and EscN sharing nearly identical secondary structure and aligning with a r.m.s deviation of 1.2 Å, two important differences are apparent. The first relates to alterations within the C-terminal domain (residues 377-393) (Figure 3.3A). A point mutation (V393P) introduced in this region of EscN to facilitate structure determination (150) results in a partial disruption and unraveling of $\alpha 10$ compared to SsaN. This difference is particularly interesting since it corresponds to a change leading to a secretion-deficient protein and occurs in a region predicted to be important for chaperone binding (150). The possibility that the structure of SsaN represents a secretion-competent conformation is further supported by the fact that SsaN and the F1 ATPase (but not EscN) adopt an identical bent helical structure for $\alpha 10$ (Figure 3.3B). Importantly, this helix in the F1 ATPase makes direct contact with the γ subunit of the ATPase synthase complex

(Figure 3.3B) further implicating this region as important for mediating protein-protein interactions. A second difference between SsaN (residues 268-283) and EscN results from partial unwinding of $\alpha 7$ and outward rotation of the loop joining helices 6 and 7 in SsaN (Figure 3.3C). This region within SsaN is largely unstructured, suggesting that in the absence of other binding partners and/or a N-terminal oligomerization domain, this region is able to adopt a number of conformations.

Placement of SrcA onto hexameric SsaN

Based on our crystal structure of SsaN, several initial models for SsaN-chaperone binding were constructed. We focused our analysis on the interaction between SsaN and the T3SS-2 multi-cargo chaperone, SrcA, for which structural information is available. During this process it was observed that the structure of SrcA retains some structural similarity to the γ subunit of the ATP synthase. Since the γ subunit directly interacts with the analogous $\alpha 10$ region in the F1 ATPase, a model for the SrcA-SsaN interaction was constructed based on structural similarity between SrcA and the γ subunit. Docking was performed using the secondary structure matching (SSM) algorithm within Coot (272,273). A single monomer of SrcA aligned with the γ subunit with a r.m.s deviation of 2.9 Å over 80 residues (Figure 3.4A). The resulting model for hexameric SsaN interacting with a dimer of SrcA (Figure 3.4B) covers a calculated (PISA) surface area of 1450 Å² involving asymmetric interactions with both subunits of SrcA and 4 out of 6 subunits from SsaN. Only two steric clashes involving main chain atoms within flexible loop regions were present. Regions within SsaN predicted to be important for mediating this

interaction include 385-397 and 401-405; however, 385-397 contributes the majority of the interaction with SrcA and involves 4 of 6 subunits within a SsaN hexamer (Figure 3.4B). In SrcA, the modeled regions include: chain A 25-28, 42-48, 85-88 and chain B 33-37, 64-79, 115-125 (Figures 3.4C and D). These interaction interfaces are more distributed compared to SsaN and involve multiple, weaker contacts.

Experimental validation of the chaperone-T3SS ATPase interface

The C-terminal region of T3SS ATPases has been implicated in chaperone binding (150,153,167); however, there has been limited work defining the precise chaperone interaction site. Based on our crystal structure of SsaN, we had identified two potential regions on SsaN that may mediate an interaction with a chaperone, residues 268-283 ($\alpha 6-7$) or 377-393 ($\alpha 10$). Given that our model of SrcA placed onto SsaN suggested that region 377-393 and not 268-283 would serve as the chaperone docking site, we first examined the contribution of these regions to chaperone docking *in vitro*. Given that T3SS ATPases can recognize both unladen chaperones (167,168) and chaperone-effector complexes (167,168), we focused our *in vitro* pull-down assays on the interaction between SsaN and unladen SrcA. As shown in Figure 3.5A, a deletion within residues 268-283 ($\Delta V273-E276$) did not disrupt binding of SsaN to SrcA. In contrast, mutation of V379 in the 377-393 region completely abolished the interaction (Figure 3.5A). This finding implicates region 377-393 of SsaN as the binding site for SrcA and confirms the importance of the C-terminal region of T3SS ATPases in chaperone docking.

Structural comparison of EscN-V393P and SsaN suggested that a V379P mutation on SsaN would introduce a disruption toward the end of $\alpha 10$ and the region connecting $\alpha 10$ to $\alpha 11$, making it unsuitable for SrcA binding. Since a proline for valine substitution within this helix is expected to indirectly disrupt the chaperone interaction site, we sought to more precisely define the chaperone binding region by examining the contribution of residues at the end of $\alpha 10$ (L381-L385) and in the loop connecting $\alpha 10$ to $\alpha 11$ (Q389) to SrcA binding. Mutation of the region L381-I385 (L381A/L382A/I385A mutant) on SsaN did not inhibit SrcA binding in the *in vitro* pull-down assay whereas a Q389K mutation reduced SrcA binding to SsaN to less than half of wild-type SsaN (Figure 3.5B). This result, which is in agreement with our model, implicates the loop region connecting $\alpha 10$ and $\alpha 11$ as the critical site for chaperone binding. The structural integrity of all SsaN variants was confirmed by measuring their ATPase activity as done previously for InvC variants (152). The ATPase activity of the SsaN variants was not different from wild-type; however, a Walker A motif mutant (K168E) was significantly impaired (Figure 3.5C). We further confirmed the structural integrity of the SsaN variants that were impaired for SrcA binding by circular dichroism (Figure 3.5D).

To validate the biological significance of the chaperone-T3SS ATPase interaction, we generated *Salmonella* strains in which the chromosomal copy of *ssaN* was replaced with *ssaN* containing either the V379P or Q389K mutation and competed these mutants against wild-type bacteria in mouse infections. The bacterial strain with the SsaN-V379P variant, which was incapable of chaperone binding *in vitro* (Figure 3.5A) but catalyzed ATP hydrolysis at wild-type levels (Figure 3.5C), was as defective as a *ssaN* deletion

mutant during host infection (Figure 3.5E). The SsaN-Q389K mutant, which was only partially impaired for SrcA binding *in vitro*, had statistically attenuated *in vivo* fitness (Figure 3.5E). However, the fitness defect for the SsaN-Q389K mutant was more similar to wild-type than the SsaN-V379P mutant. These data establish that chaperone-T3SS ATPase interactions are a key molecular interface for bacterial fitness in the host environment.

We next examined the contribution of residues N26, R27, W74, R117, E120 and H124 on SrcA to the chaperone-ATPase interface, as these residues were predicted to be important for SsaN binding based upon our model. The N26A/R27A and R117A/E120A/H124A mutants were some of the most impaired variants for SsaN binding while individual mutation of the residues in SrcA chain B (65-79; 115-125) had varying effects on the SrcA-SsaN interaction (Figure 3.6A). Since neither chain A nor chain B mutations were sufficient to completely abolish SrcA binding, likely because SrcA forms a dimer and both regions contact SsaN, we created SrcA variants harboring combined mutations in both chains A and B (N26A/R27A with R117A, E120A, or H124A). These SrcA variants were defective for interacting with SsaN (Figure 3.6B). Our model had predicted that introduction of these mutations in SrcA would have no effect on chaperone binding to effector cargo. To examine this experimentally and to verify that our combined mutants were still functional, we examined the binding of these SrcA mutants to the effector cargo PipB2. As shown in Figure 3.6C, all SrcA variants retained full functionality for binding to PipB2. Taken together, these findings define the

chaperone-T3SS ATPase interface and validate our structural model of the chaperone-SsaN interaction.

The universal importance of chaperone-T3SS ATPase interactions for effector secretion suggests that the C-terminal chaperone-binding domain in the ATPases may be highly conserved amongst Gram-negative pathogens. To investigate this, a sliding window approach was used to determine the conservation in the chaperone-binding domain of SsaN to seven orthologs in other Gram-negative bacteria. As shown in Table 3.3 and Figure 3.7, the chaperone-binding domain of SsaN is highly conserved with respect to the corresponding region in EscN (*E. coli*), CdsN (*Chlamydia*), PscN (*Pseudomonas*) and YscN (*Yersinia*). The level of conservation in this region is similar to the conserved Walker boxes involved in ATP hydrolysis whereas other regions of the proteins are less conserved (Figure 3.7). Taken together with the structural work, these experiments solidified the importance of the C-terminal region of SsaN in chaperone docking.

DISCUSSION

The interaction that occurs between chaperones and T3SS ATPases is critical for ensuring that effector substrates are efficiently delivered to the secretion apparatus for translocation. Despite its importance, there has been limited work defining the precise chaperone-T3SS ATPase interaction site. In this study, we employed a combination of structural and biochemical work to elucidate the binding site of the multi-cargo chaperone, SrcA, on the T3SS-2 ATPase, SsaN.

We first quantified the contribution of SsaN to virulence and effector secretion. The fitness defect observed for the *ssaN* mutant was in agreement with the strong virulence attenuation phenotypes that have been reported for other T3SS ATPase mutants (152,173); however, the dispensability of SsaN for the secretion of a subset of SPI-2 effectors was surprising considering that, to date, T3SS ATPases have been shown to be essential for effector secretion (150,152,172). Effectors for which SsaN was dispensable for secretion were found to be targeted to the T3SS-1, a finding which is not unprecedented as PipB2 has been shown to be translocated by both the T3SS-1 and T3SS-2 (278). Most importantly, the secretion pattern of effectors highlighted a difference in the targeting and recognition of SPI-2 effectors by the T3SSs. Many of the effectors encoded outside of the SPI-2 locus are not associated with chaperones and are secreted by both the T3SS-1 and T3SS-2. By contrast, all of the SPI-2 encoded translocator and effector substrates have an associated chaperone and are strictly reliant on the SPI-2 T3SS system for secretion. Chaperones may therefore play a crucial role in the targeting and recognition process.

A comparison of SsaN to the *E. coli* T3SS ATPase EscN revealed substantial similarity between the two structures with the most notable differences localized to the C-terminal region. The C-terminal region of T3SS ATPases had previously been implicated in chaperone binding, largely based on the demonstration that an InvC-L376P mutant is unable to bind a SicP-SptP complex (167). In the structural characterization of EscN, Zarivach *et al.* noted that the C-terminal region of EscN was shorter than that of the F1 ATPase, which led them to consider how chaperones might engage with EscN (150). The corresponding InvC-L376P mutation in EscN, EscN-V393P, mapped to the outer rim of their predicted chaperone-EscN interface and was also shown to impact effector secretion (150). Since the V393P mutation was suggested to affect an extended helical region in EscN (150), we sought to more precisely define the key residues involved in the chaperone-T3SS ATPase interaction. A model of SrcA interacting with hexameric SsaN was generated based on the structural similarity between SrcA and the γ subunit of the F1 ATP synthase (276). Although such a model can only be expected to provide rough estimates for a protein-protein interaction, the degree of surface complementarity and buried surface area suggested a feasible model for the chaperone-SsaN interaction, which we validated experimentally. Furthermore, the residues that we identified in SrcA as important for mediating an interaction with SsaN are similar to regions in the *E. coli* chaperone, CesAB, that were found by NMR analysis to be most affected upon binding with EscN in solution (258).

Our structural work and model of SrcA bound to SsaN raise interesting questions in regards to effector secretion. First, the high degree of sequence conservation of the

chaperone binding regions on T3SS ATPases suggests that this site is under selection. Despite this conservation, SsaN and EscN adopt alternate conformations in their chaperone docking sites with the end of $\alpha 10$ of SsaN being replaced by a coil between $\alpha 10$ and $\alpha 11$ in EscN. It is possible that these slight structural differences represent adapted conformations tailored to the chaperone and effector repertoire within a given species. Second, the residues that define the chaperone-T3SS ATPase interface facilitate only multiple, weak contact points between SsaN and SrcA. Also, the binding of the chaperone to the T3SS ATPase involves asymmetric interactions (different regions on the SrcA monomers within the dimer contact SsaN). Such an interaction may allow for greater flexibility in chaperone binding to and uncoupling from the T3SS ATPase before and during ATP hydrolysis, a process that must occur to energize chaperone dissociation and effector unfolding (167). Finally, assuming that the chaperone-bound T3SS ATPase is oriented to the membrane in the same manner as the F1 ATPase, it seems unlikely that an unfolded effector would be passed through the center of the T3SS ATPase hexameric channel. This is because the chaperone-ATPase interaction site is proximal to the inner membrane and not oriented toward the distal end of SsaN where the channel opening presents itself. Furthermore, in the flagellar T3SS that has many structural features in common with the virulence-associated T3SS, FliJ is similar to the γ subunit of the F_0F_1 ATP synthase and was shown to occupy the central channel of the hexameric ATPase FliI (162). Therefore, it seems more probable that an unfolded effector would be passed to another component of the export apparatus to facilitate the secretion process.

T3SS ATPases have been explored as targets for novel anti-virulence drugs (279); however, targeting the active site of these enzymes may be challenging due to their conservation with eukaryotic enzymes. Peptide mimetics have proven useful in blocking protein interactions in the chlamydial T3SS, specifically for the interaction of CdsL with the ATPase, CdsN (154). Since mutation of the chaperone-binding site on SsaN resulted in severe virulence defects, an alternative target may be the essential interaction between chaperones and the T3SS ATPase. Furthermore, the high degree of conservation in the chaperone binding region suggests that a peptide mimetic blocking the chaperone-T3SS ATPase interaction would likely be active against a wide range of Gram-negative pathogens.

ACKNOWLEDGMENTS

We are grateful to members of the Coombes lab for helpful discussion on this work and for comments on the manuscript, and to Colin Cooper for construction of the Δ *ssaN* strain and *pFLAG-SsaN*. We are grateful to Raquel Eband and Richard Eband for technical assistance with the CD analysis. This work was supported by grants from the Natural Sciences and Engineering Research Council of Canada, the Canadian Institutes of Health Research (MOP 82704), the Canada Foundation for Innovation, and a Canada Research Chair (to B.K.C.). S.E.A. is the recipient of a Canada Graduate Scholarship from the CIHR. B.R.T. is the recipient of an Ontario Graduate Scholarship.

FIGURE 3.1. *ssaN* contributes to pathogenesis in a murine model of typhoid and is required for the secretion of only a subset of SPI-2 effectors. (A) Competitive infections between wild-type and Δ *ssaN* strains in C57BL/6 mice were conducted with a 1:1 mixture of both strains and CI values were determined 72 hours post-infection. Each filled circle represents an individual mouse (n = 5) and the geometric means are indicated by the horizontal lines. (B) Representative images of effector substrates that required *ssaN* for secretion (left panels) and those that were secreted in the absence of *ssaN* (right panels). Wild-type and Δ *ssaN* strains were grown in LPM medium and proteins were detected in the whole cell lysate (pellet) and secreted fractions by western blot analysis. DnaK served as a loading control and confirmed that there was no whole cell contamination in the secreted fractions. (C) Complementation of the Δ *ssaN* strain with *pssaN* in the *Salmonella* secretion assay. Indicated fractions were probed with anti-DnaK and anti-SseC antibodies. (D) PipB2 effector secretion in T3SS-1 and T3SS-2 mutant backgrounds. Strains were grown under SPI-2 inducing conditions and whole cell lysate and secreted fractions were subjected to western blot analysis with anti-HA and anti-DnaK antibodies.

FIGURE 3.1

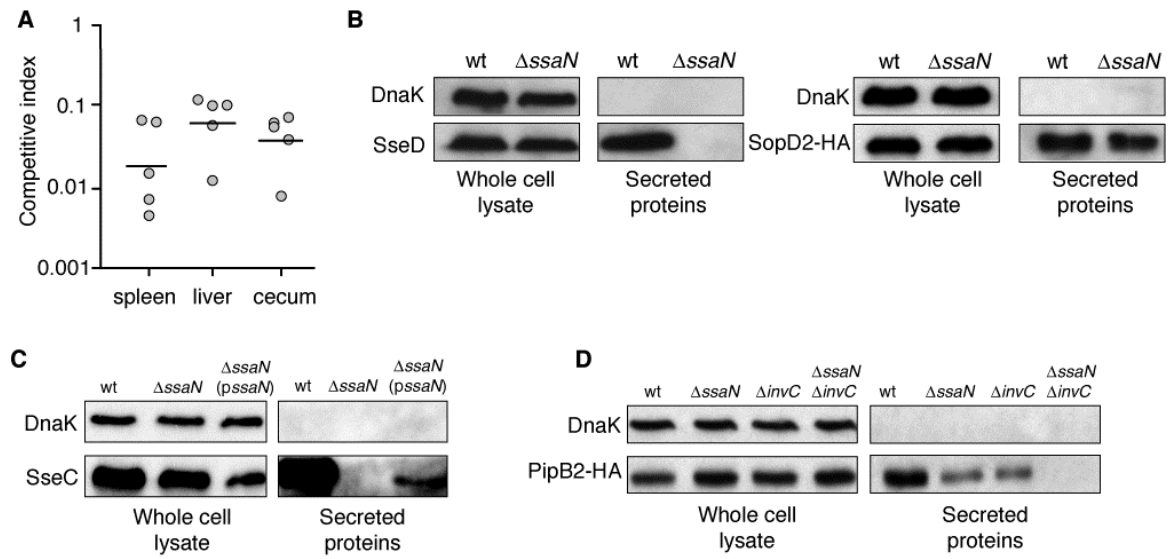


FIGURE 3.2. The structure of SsaN_{Δ1-89}. (A) Crystal structure of monomeric SsaN_{Δ1-89}. The dashed line indicates the disordered region that connects $\alpha 6$ and $\alpha 7$ which is missing in the structure. (B) SsaN modelled as a hexamer with each monomer represented by a different colour. The model is shown from the top view and at a 90° rotation. The structural figures are shown as stereo images.

FIGURE 3.2

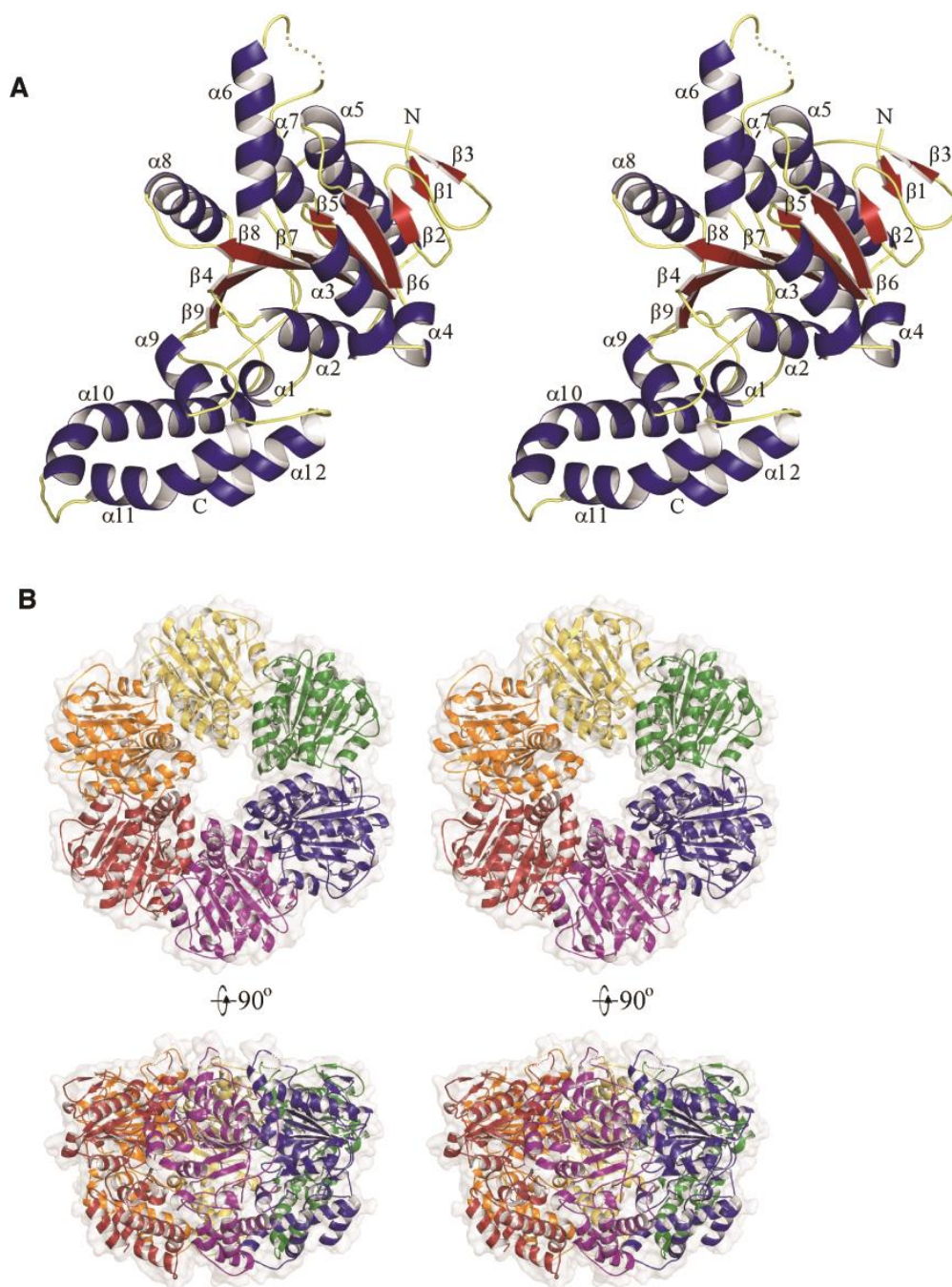


FIGURE 3.3. Structural differences between SsaN and EscN. (A) Disruption of the C-terminal $\alpha 10$ in EscN (blue) compared to SsaN (yellow). (B) SsaN (yellow) and the F1 ATPase (light grey) adopt an identical structure in $\alpha 10$ compared to EscN. (C) Difference between $\alpha 6$ and $\alpha 7$ of SsaN (yellow) and EscN (blue). The dashed line indicates the disordered region that is not modelled in the structure. The structural figures are shown as stereo images.

FIGURE 3.3

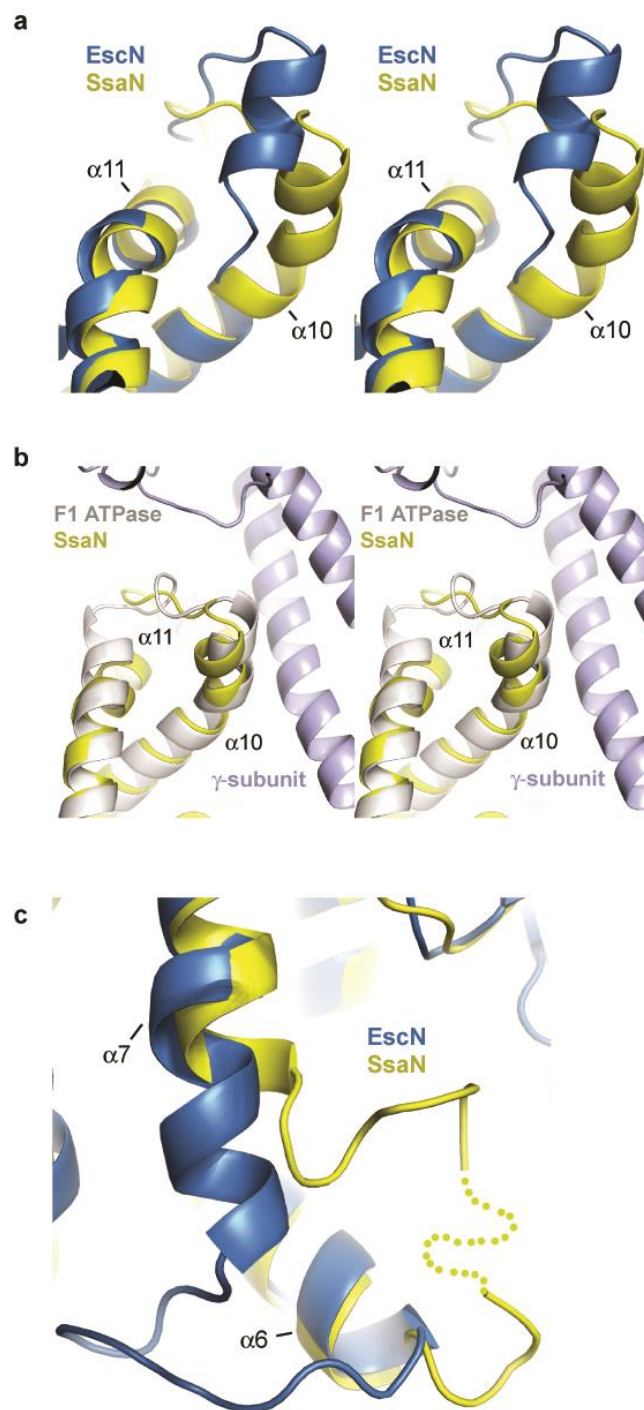


FIGURE 3.4. Structural model of the SrcA-SsaN interaction. (A) Dimeric SrcA aligned with the γ subunit (purple) of the F1 ATPase (light grey). (B) Model of the asymmetric interaction between dimeric SrcA and hexameric SsaN from the side view (left panel) and top view (right panel). Important interaction regions are shown in yellow for SrcA and purple for SsaN and are also indicated by the arrows. (C-D) Key amino acid residues that define the chaperone-T3SS ATPase interface for SsaN (purple) and SrcA (yellow). SrcA residues of interest on chain B (C) and chain A (D) are shown. Highlighted residues on SsaN and SrcA are those that were validated experimentally. The structural figures are shown as stereo images.

FIGURE 3.4

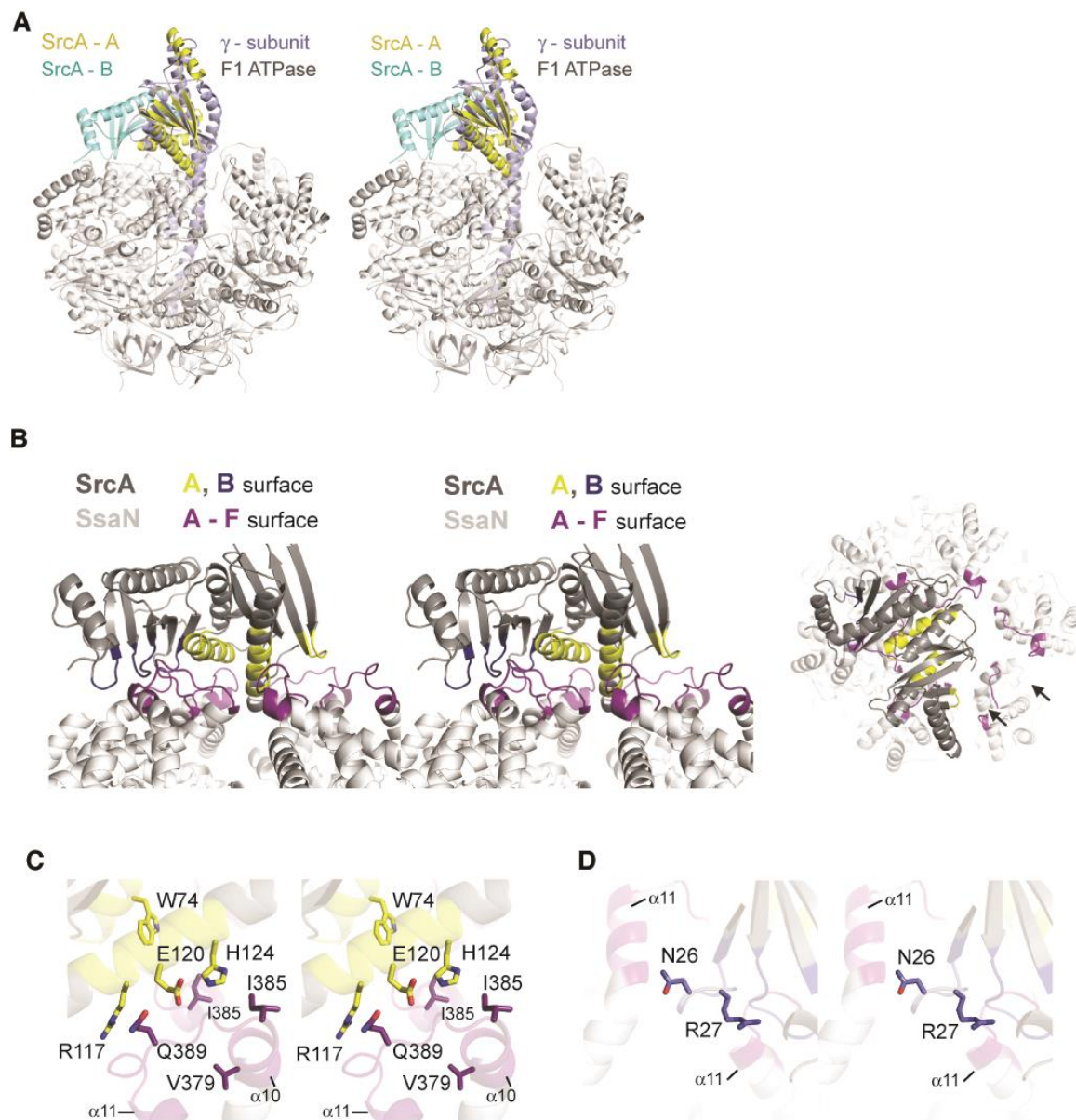


FIGURE 3.5. Identification of the chaperone binding region on SsaN. (A-B) Protein interaction studies were conducted with lysates over-expressing wild-type His-tagged SrcA and the indicated FLAG-tagged SsaN variants. Eluted proteins were analyzed by western immunoblotting with anti-His and anti-FLAG antibodies. wt, wild-type SsaN. Quantifications of normalized SsaN/SrcA ratios for input and elution fractions are shown. (C) Wild-type SsaN $_{\Delta 1-89}$ and variants were purified by Ni $^{2+}$ -affinity chromatography and their activity was assayed in a microplate assay using Biomol green. All assays were performed in triplicate. The asterisk denotes a *P*-value of < 0.05. (D) The secondary structures of wild-type SsaN $_{\Delta 1-89}$ and variants impaired for SrcA binding were determined by circular dichroism analysis. (E) Competitive infections between wild-type and *ssaN* mutants in C57BL/6 mice. Each filled circle or square represents an individual mouse (n = 5) and the geometric means are shown by the horizontal lines. *P* values are indicated.

FIGURE 3.5

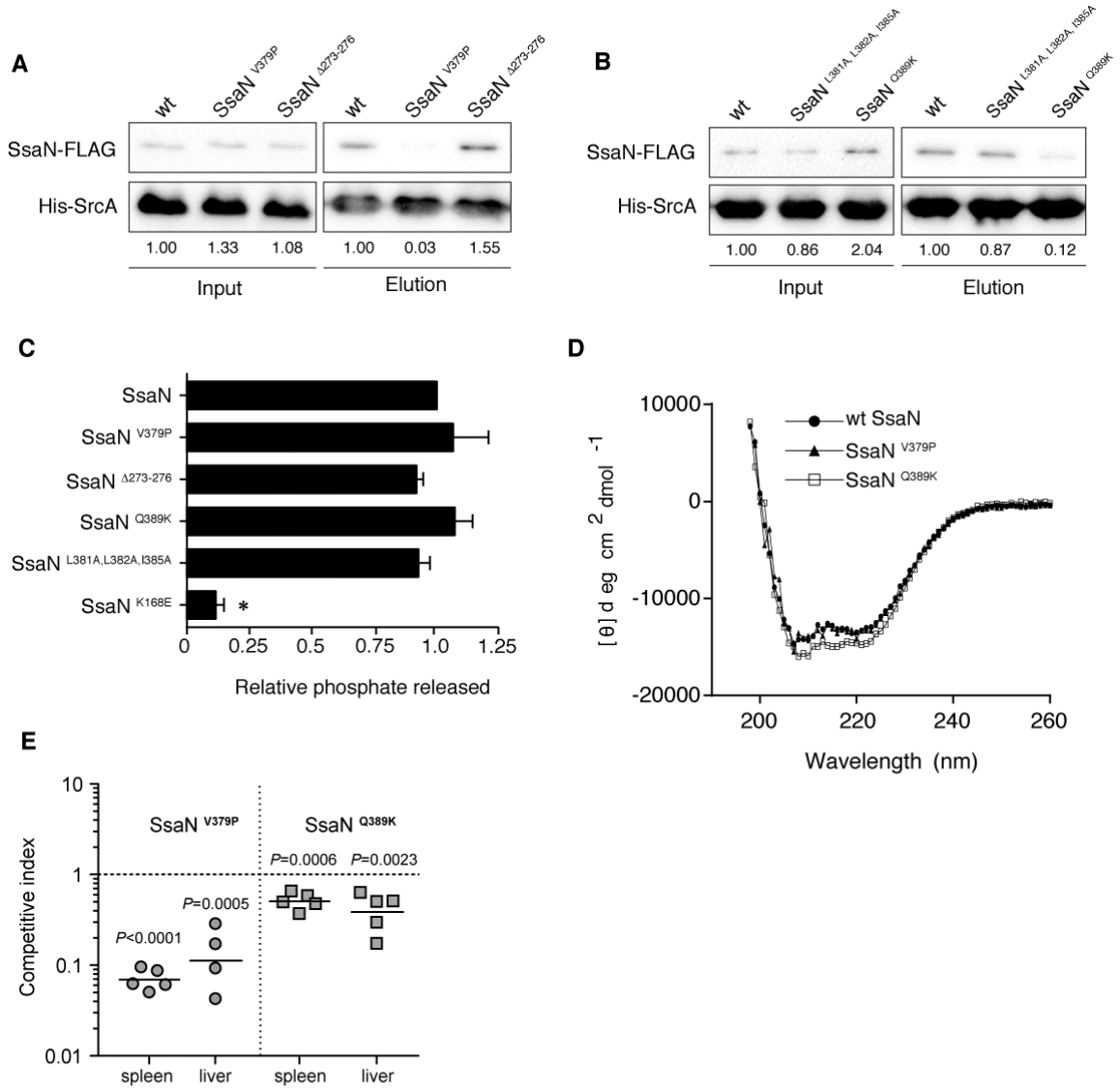


FIGURE 3.6. Key residues on SrcA that contribute to the chaperone-T3SS ATPase

interface. (A-B) Interactions of wild-type FLAG-tagged SsaN with the individual SrcA

chain A and B mutants (A) or combined chain mutants (B) were examined using an *in*

vitro pull-down assay. Eluted proteins were subjected to western blotting with the

indicated antibodies. wt, wild-type SrcA. Quantifications of normalized SsaN/SrcA ratios

for input and elution fractions are shown. (C) Protein interaction studies between the

indicated His-tagged SrcA mutants and wild-type FLAG-tagged PipB2. Proteins bound to

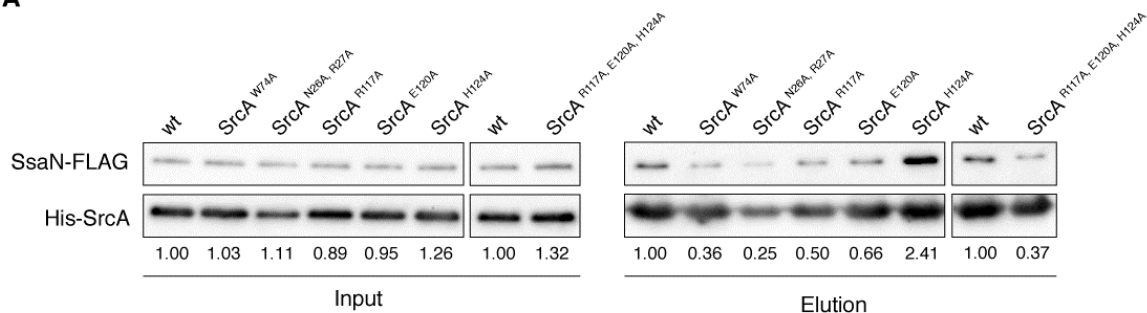
Ni-NTA agarose beads were eluted and subjected to western blot analysis with anti-His

and anti-FLAG antibodies. wt, wild-type SrcA. Quantifications of normalized

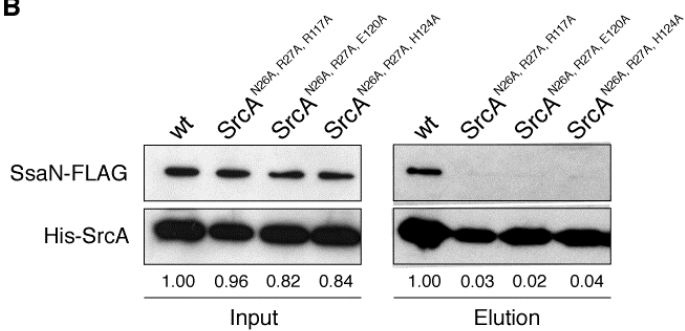
PipB2/SrcA ratios are shown.

FIGURE 3.6

A



B



C

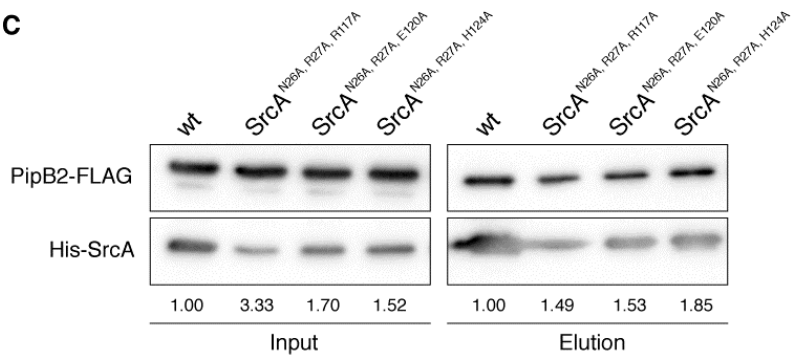


FIGURE 3.7. Conservation of the putative chaperone binding domain between SsaN and EscN. The sequences of SsaN and EscN were aligned and a sliding window approach (window size of 13) was used to determine the percentage of identity of SsaN and EscN across the entire protein. The windows encompassing the Walker A and Walker B boxes in both proteins, and the window starting at the extended helical region of the proposed chaperone binding domain are shown.

FIGURE 3.7

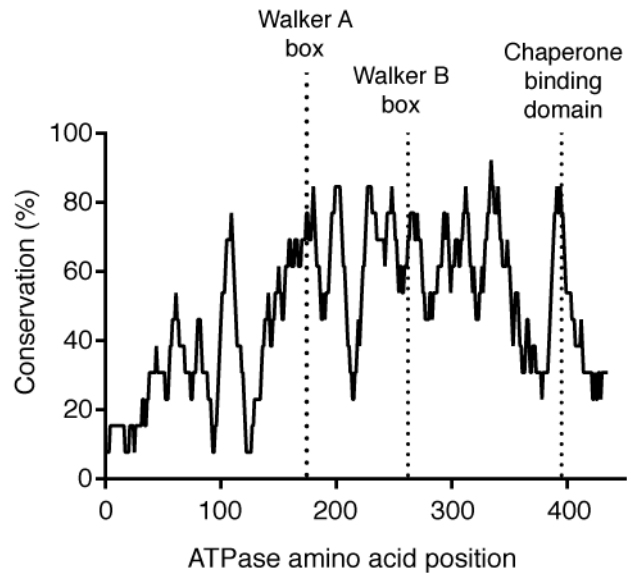


Table 3.1. Data Collection and Model Refinement Statistics

Data collection		Model and refinement	
Space group	C2	Resolution (Å) ^a	37.03 – 2.10
Cell parameters		<i>R</i> _{work} / <i>R</i> _{free} (%)	18.11/23.04
a,b,c (Å)	138.13, 76.31, 39.09	Reflections _{observed}	22,862
α, β, γ (°)	90, 103.701, 90	Reflections _{Rfree}	2,015
Molecules in ASU	1	No. atoms	
Resolution (Å) ^a	50.0 - 2.10	Protein	2,551
Unique reflections	22,889	Ligand/ion	0
Redundancy ^a	3.2 (3.2)	Water	125
Completeness (%) ^a	98.1 (98.5)	R.m.s.d. bond	
<i>I</i> /σ(<i>I</i>) ^a	11.1 (2.60)	Lengths (Å)	0.008
<i>R</i> _{merge} (%) ^a	9.7 (51.4)	Angles (°)	1.212
Wilson B Factor (Å ²)	29.03	Average B Factor (Å ²)	48.13
PDB 4NPH			

^a Statistics for the highest resolution shell are shown in parentheses

Table 3.2. SPI-2 effector secretion in Δ ssaN and Δ ssaN Δ invC strains

Secretion Substrate	Chaperone	Secretion in ΔssaN^a	Secretion in ΔssaNΔinvC^b
SseB	SseA(180), SsaE (182)	X	---
SseC	SrcA (177)	X	---
SseD	SseA (181)	X	---
SseF	SrcB (183)	X	---
SseG	SrcB	X	---
SseJ		X	---
PipB		Y	X
PipB2	SrcA (176)	Y	X
SseL	SrcA	Y	X
SopD2		Y	X

^aX, no detectable secretion; Y, denotes presence of effector substrate in secreted fraction

^b---, not tested

Table 3.3. Conservation of Chaperone Binding Domain amongst T3SS ATPases in Gram-Negative Pathogens

Protein	Chaperone Binding Domain Identity to SsaN^a (%)	Overall Identity to SsaN^b (%)
EscN (<i>E. coli</i>)	84.6	49.0
CdsN (<i>Chlamydia</i>)	76.9	46.8
PscN (<i>Pseudomonas</i>)	76.9	51.9
YscN (<i>Yersinia</i>)	76.9	52.1
BscN (<i>Bordetella</i>)	69.2	48.5
InvC (<i>Salmonella</i>)	46.2	41.8
FliI (Flagellar T3SS)	30.8	42.7

^a Percentages were determined by calculating the number of identical residues between the putative chaperone binding domain of SsaN and the corresponding regions in other T3SS ATPases (window size of 13)

^b Overall identity to SsaN indicates the total number of identical residues between the amino acid sequences of SsaN and other T3SS ATPases

Table 3.S1. Strains, plasmids and oligonucleotides used in this study

Strain, Plasmid or Oligonucleotide	Description	Reference or Source
Strains		
BKC1-1	SL1344, wild-type <i>S. enterica</i> sv. Typhimurium, Sm ^R	(280)
BKC6-10	SL1344 <i>ushA::Cm</i>	(129)
BKC32-53	SL1344 Δ <i>ssaN</i> ; Kan cassette excised, Sm ^R	This study
BKC32-54	SL1344 Δ <i>invC</i> ; Kan cassette excised, Sm ^R	This study
BKC32-55	SL1344 Δ <i>ssaNΔ<i>invC</i>; Kan cassette excised, Sm^R</i>	This study
BKC32-56	SL1344 <i>ssaN::ssaNV379P</i> , Sm ^R	This study
BKC32-57	SL1344 <i>ssaN::ssaNQ389K</i> , Sm ^R	This study
BKC1-14	DH5 α (<i>supE44</i> Δ <i>lacU169</i> (ϕ <i>lacZ</i> Δ <i>M15</i>) <i>hsdR17 recA1 endA1 gyrA96 thi-1 relA1</i>)	Lab strain
BKC4-45	DH5 α - λ <i>pir</i> (<i>supE44</i> Δ <i>lacU169</i> (ϕ <i>lacZ</i> Δ <i>M15</i>) <i>hsdR17 recA1 endA1 gyrA96 thi-1 relA1</i> λ <i>pir</i>)	Lab strain
BKC32-34	<i>E. coli</i> S17-1- λ <i>pir</i> (Tp ^R Sm ^R <i>recA</i> , <i>thi</i> , <i>pro</i> , <i>hsdR</i> -M+RP4: 2-Tc:Mu:Km Tn7 λ <i>pir</i>)	Lab strain
BKC8-37	<i>E. coli</i> BL21(DE3) strain used for protein over-expression (F ⁻ <i>ompT hsdS_B</i> (r_B^- m_B^- <i>tetA</i>))	Lab strain
Plasmids		
pKD4	oriR γ , Kan ^R cassette flanked by FRT sites (FLP recombinase target)	(242)
pDK46	RepA1019(Ts), λ , γ , β and <i>exo</i> expressed from <i>ParaBAD</i> , Amp ^R	(242)
pCP20	Plasmid expressing FLP recombinase, Amp ^R	(242)
pRE112	Suicide plasmid for allelic exchange, Cm ^R	(281)
pWSK129	Used to express HA-tagged effectors under their native promoters, Kan ^R	(282,283)
pACYC	Used to express HA-tagged effectors under their native promoters, Cm ^R	(284)
pFLAG-CTC	For expression of C-terminal FLAG-tagged constructs from P _{<i>tac</i>} , Amp ^R	Sigma
pFLAG-MAC	For expression of N-terminal FLAG-tagged constructs from P _{<i>tac</i>} , Amp ^R	Sigma
<i>psseF</i> -HA	pWSK129 expressing HA-tagged <i>sseF</i> under control of the <i>sseA</i> promoter, Kan ^R	Our collection
<i>psseG</i> -HA	pWSK129 expressing HA-tagged <i>sseG</i> under control of the <i>sseA</i> promoter, Kan ^R	Our collection
<i>psseJ</i> -HA	pWSK129 expressing HA-tagged <i>sseJ</i> under control of its native promoter, Kan ^R	This study
<i>ppipB</i> -HA	pACYC expressing HA-tagged <i>pipB</i> under control of its native promoter, Cm ^R	Our collection
<i>ppipB2</i> -HA	pWSK129 with HA-tagged <i>pipB2</i> under control of its native promoter, Kan ^R	Our collection
<i>psseL</i> -HA	pWSK129 expressing HA-tagged <i>sseL</i> under control of its native promoter, Kan ^R	Our collection
<i>psopD2</i> -HA	pACYC expressing HA-tagged <i>sopD2</i> under control of its native promoter, Cm ^R	Our collection
pRE112-	pRE112 with 1kb regions upstream and downstream of	This study

<i>ssaNV379P</i>	<i>ssaNV379P</i>	
pRE112- <i>ssaNQ389K</i>	pRE112 with 1kb regions upstream and downstream of <i>ssaNQ389K</i>	This study
<i>pssaN_{Δ1-89}</i>	pET3a carrying N-terminally truncated <i>ssaN</i> (<i>ssaN_{Δ1-89}</i>), Amp ^R	(176)
<i>pssaN_{Δ1-89}-V379P</i>	pET28b carrying N-terminally truncated <i>ssaNV379P</i> , Amp ^R	This study
<i>pssaN_{Δ1-89}-Δ273-276</i>	pET28b carrying N-terminally truncated <i>ssaNΔ273-276</i> , Amp ^R	This study
<i>pssaN_{Δ1-89}-L381A/L382A/I385A</i>	pET28b carrying N-terminally truncated <i>ssaNL381A/L382A/I385A</i> , Amp ^R	This study
<i>pssaN_{Δ1-89}-Q389K</i>	pET28b carrying N-terminally truncated <i>ssaNQ389K</i> , Amp ^R	This study
<i>pssaN</i>	pFLAG-CTC with wild-type <i>ssaN</i> (complementation studies), Amp ^R	This study
<i>pssaNV379P</i>	pFLAG-MAC with <i>ssaNV379P</i> , Amp ^R	This study
<i>pssaNΔ273-276</i>	pFLAG-MAC with <i>ssaNΔ273-276</i> , Amp ^R	This study
<i>pssaNL381A/L382A/I385A</i>	pFLAG-MAC with <i>ssaNL381A/L382A/I385A</i> , Amp ^R	This study
<i>pssaNQ389K</i>	pFLAG-MAC with <i>ssaNQ389K</i> , Amp ^R	This study
<i>pipB2</i>	pFLAG-CTC with <i>pipB2</i> , Amp ^R	This study
<i>srcA</i>	pET28b with wild-type <i>srcA</i> , Kan ^R	This study
<i>srcAN26A/R27A</i>	pET28b with <i>srcAN26A/R27A</i> , Kan ^R	This study
<i>srcAR117A/E120A/H124A</i>	pET28b with <i>srcAR117A/E120A/H124A</i> , Kan ^R	This study
<i>srcAN26A/R27A/R117A</i>	pET28b with <i>srcA</i> carrying mutations in both T3SS-ATPase binding domains, Kan ^R	This study
<i>srcAN26A/R27A/E120A</i>	pET28b with <i>srcA</i> carrying mutations in both T3SS-ATPase binding domains, Kan ^R	This study
<i>srcAN26A/R27A/H124A</i>	pET28b with <i>srcA</i> carrying mutations in both T3SS-ATPase binding domains, Kan ^R	This study
<i>srcAW74A</i>	pET28b with <i>srcAW74A</i> , Kan ^R	This study
<i>srcAR117A</i>	pET28b with <i>srcAR117A</i> , Kan ^R	This study
<i>srcAE120A</i>	pET28b with <i>srcAE120A</i> , Kan ^R	This study
<i>srcAH124A</i>	pET28b with <i>srcAH124A</i> , Kan ^R	This study

Oligonucleotides

<i>ssaNdel-F</i>	5'gaccttagcgaagaggagttggcggacaatgaagaatgaattgatgcagtgtaggctggagctgcttcg
<i>ssaNdel-R</i>	5'ctccagcaaagttccatgatcactcggtagtatttggtgtaattttccatatgaatattccttag
<i>ssaNdel-sc-F</i>	5'gtcacttctgtcgacaccgcgacg
<i>ssaNdel-sc-R</i>	5'gacactgctaaagcgcgctctgg
<i>invCdel-F</i>	5'cttaattctggtcagcgaatgcattcataccgctcaactgtcatcaaacatagaatattcctccttag
<i>invCdel-R</i>	5'caatatctggaagtttttagtcggtcgcctaatagatgaaaacacctgttaggctggagctgcttcg
<i>invCdel-sc-F</i>	5'ctgcacgcagcgtatctaataac
<i>invCdel-sc-R</i>	5'gaaattctaatgaccataatggaag
<i>psseJ-F</i>	5'gcgctgacacctaataaggccaaaagcatcgaag
<i>psseJ-R</i>	5'cgcatcttctcagtggaataatgatgagctataaaacttctc
<i>pRE112-ssaN-F</i>	5'gcgctctagaatggttcccggcgcgatgctcttaac
<i>pRE112-ssaN-F2</i>	5'gaccttagcgaagaggagttggcggacaatgaagaatgaattgatgcaac
<i>pRE112-ssaN-F3</i>	5'gaaaattaccacaaatactaccgagtgatgaaacttctgctggag
<i>pRE112-ssaN-R</i>	5'gcgcgagctcactgctgcaataacggcgccag

pRE112-ssaN-R2 5'ctccagcaaagtttccatgatcactcggtagtatttggtgaattttc
pRE112-ssaN-R3 5'gttgcataattcattcttcattgtccgccaactcctctcgctaaggtc
pFLAG-ssaN-F 5'gcgc**ctc**gagatgaagaatgaattgatgcaacgtc
pFLAG-ssaN-R 5'gcgc**gtac**ctcactcggtagtatttggtgtaa
ssaNV379P-F2 5'accaggag**ct**gaactgtaatacgcattggggaataccag
ssaNV379P-R2 5'ttaacagtt**agg**ctcctggtaaagcggcagaccgtc
ssaNΔ273-276-F2 5'gagaccgcgatccgccagggctatttag
ssaNΔ273-276-R2 5'tggcggatcgcggctctcctccggcg
ssaNL381A/L382 5'gttgaag**cg**caatacgc**gt**ggggaataaccagcaggagttgatacagatac
A/ I385A-F2
ssaNL381A/L382 5'tectcgctggtattcccc**agc**gcg**gtattg**cc**gct**tcaacctcctggtaaagc
A/ I385A-R2
ssaNQ389K-F2 5'gttgaactgtaatacgcattggggaata**caag**caggagttgatacagatactgaca
aagc
ssaNQ389K-R2 5'tectcg**ctt**gtattccc**aat**gcgtattaacagttcaacctcctggtaaagc
pFLAG-pipB2-F 5'gcgc**catat**gatggagcgtcactcgatagctg
pFLAG-pipB2-R 5'gcgc**gtac**caatatttctactataaaattcg
pET28b-srcA-F 5'ggg**catat**gtattcaagagccgatcgctta
pET28b-srcA-R 5'ggg**gatc**ctcacgtataatcggtatccagagttat
srcAN26A/R27A- 5'**cgccat**atgatgtattcaagagccgatcgcttattaagacagtttctactaaaataaat
F accgattcaattgtctttgacgaag**ccg**cattatgc
srcAR117A/E120 5'**cgcg**gatcctcacgtataatcggtatccagagttattcctttatcctgtaaaat**gg**cata
A/H124A-R cagatt**cg**cattgat**gca**ataactac
srcAW74A-F2 5'ctttgaattctcaatgctaatt**agc**gttgcagagaataatggaccac
srcAW74A-R2 5'gtgtccattattctctgcaaa**cg**ctaaattagcattgagaaattcaaaag
srcAR117A-R 5'**cgcg**gatcctcacgtataatcggtatccagagttattcctttatcctgtaaaatgtgatac
agattctccattgat**gca**ataactac
srcAE120A-R 5'**cgcg**gatcctcacgtataatcggtatccagagttattcctttatcctgtaaaatgtgatac
agatt**cg**cattgatctaaataactac
srcAH124A-R 5'**cgcg**gatcctcacgtataatcggtatccagagttattcctttatcctgtaaaat**gg**cata
cagattctccattgatctaaataactac

CHAPTER FOUR

DISCUSSION

DISCUSSION

Summary of Main Conclusions

Enteric pathogens have a profound impact on human health worldwide. Understanding the mechanisms by which these pathogens cause disease will aid in the development of novel strategies to combat them. The focus of our research group has centered on the roles of the O157:H7 serotype of STEC and *Salmonella enterica* species in human disease. The chapters within this work have described the characterization of two proteins associated with virulence-related functions, motility and type III secretion, in *E. coli* O157:H7 and *Salmonella enterica* serovar Typhimurium, respectively. Together, this work has contributed to the broader understanding of virulence strategies employed by enteric pathogens.

The O157:H7 serotype of EHEC is commonly associated with outbreaks and severe disease outcomes, but the basis for this enhanced virulence in human populations over other serotypes is unknown. The characterization of a highly virulent O157:H7 serotype with a seropathotype B strain, which is less frequently associated with outbreaks and HUS, revealed that there are four O-islands unique to seropathotype A strains (5). One of these O-islands, OI-1, had remained phenotypically uncharacterized. As such, we examined the gene products of this O-island (Figure 2.1) and identified a novel repressor of *E. coli* O157:H7 motility encoded in OI-1, *Z0021*. Deletion of *Z0021* was found to increase the motility of this pathogen (Figure 2.2) while over-expression of *Z0021* led to a decrease in the swimming phenotype (Figure 2.4). Through transcriptional reporter

assays, qRT-PCR and western blot analysis, and multi-copy suppression experiments (Figures 2.5 and 2.6), *Z0021* was found to exert its regulatory effect on EHEC motility prior to the activation of class II/III promoters in the flagellar cascade. This work was the first phenotypic characterization of the gene products of OI-1 and provided insight into the potential and unique virulence strategies of seropathotype A strains of EHEC.

The global impact of *Salmonella enterica* serovars on human health has been substantial. A key virulence-related trait of these pathogens is their ability to inject effector proteins into host cells through a T3SS. At the time this project was undertaken, the role of the SPI-2 encoded T3SS ATPase, SsaN, in type III secretion had not been addressed. We examined the contribution of SsaN to virulence and effector secretion (Figure 3.1) and uncovered a differential targeting phenotype for a subset of SPI-2 effectors. Furthermore, the structure of SsaN (Figure 3.2) facilitated the development of a model for a chaperone engaged with a T3SS ATPase (Figure 3.4). This model, which was validated experimentally (Figures 3.5 and 3.6), provided insight into the mechanism by which effector substrates are secreted by T3SSs and showed that the chaperone-T3SS ATPase interaction contributes to *Salmonella* pathogenesis.

Despite the advances these studies make to understanding bacterial virulence strategies, a number of unanswered questions remain: What is the role of OI-1 in EHEC pathogenesis? When are OI-1 gene products activated during the context of an infection? With what other proteins does SsaN interact at the base of the T3SS? Why is there a differential targeting pattern of SPI-2 effectors? These questions will be the focus of the following sections.

Future Directions for OI-1 and Z0021-Mediated Repression of Motility

The identification of four O-islands unique to seropathotype A strains of STEC laid the foundation for elucidating the basis of the greater virulence of these serotypes. While we characterized Z0021 as a motility repressor, the functions of the remaining gene products in OI-1 have yet to be determined. The remaining gene products have similarity to known adhesin (Z0020), usher (Z0022), chaperone (Z0023), and major fimbrial (Z0024) proteins based on BLAST analyses (5,27). As such, it would be worthwhile to determine whether OI-1 is capable of producing functional fimbriae. An approach similar to that of the characterization of the Lpf clusters of OI-141 and OI-154 may be useful for determining whether the gene products of OI-1 can assemble fimbriae at the cell surface and facilitate adherence to tissue culture cells (28,29). In addition to these genes, OI-1 also contains a gene of unknown function, Z0025. Z0025 contains pentapeptide repeats, similar to those found in other T3SS-associated effectors (285), and may be a putative non-LEE encoded effector protein. Given this annotation, it would be worthwhile to determine whether this protein is expressed under LEE-inducing conditions and if it is secreted. Based upon these results, a study examining the role of this putative effector protein in EHEC pathogenesis could be undertaken. In addition, the gene products of OI-47 have yet to be studied. This OI is unique from the other three seropathotype A specific OIs because it is predicted to contain putative virulence genes (5). Thus, a careful analysis of the gene products of OI-47 could contribute to the understanding of the unique virulence strategies of certain EHEC serotypes.

In an expression analysis of the 16 fimbrial operons in *E. coli* O157:H7, very few regions were activated under the experimental conditions tested (27). While the conditions examined were extensive (temperature, pH, various media, growth stages, etc.), only four promoter regions showed activity in these *in vitro* assays (27). These findings suggest that either the signals that activate these operons *in vivo* cannot yet be recreated *in vitro*, the expression of these operons is tightly regulated and limited during host infection, or that these operons are simply not expressed. The promoter region of OI-1 showed no activity in these *in vitro* experiments (27). While it would be worthwhile and informative to determine the conditions that activate OI-1 expression, this may only be possible in *in vivo* based experiments. Nevertheless, determining the timing of OI-1 expression during infection may provide insight into the role of this O-island in EHEC pathogenesis.

In addition to these phenotypic approaches to further understand the role of OI-1 in EHEC pathogenesis, a more biochemical study could aim to precisely define the mechanism of Z0021-mediated repression of motility. While we showed that Z0021 exerts its regulatory role prior to the activation of class II promoters, its mechanism of repression is not yet known. An *in vitro* approach could be undertaken to determine whether Z0021 prevents the formation of a FlhD₄C₂ complex or whether Z0021 prevents FlhD₄C₂ from binding to class II promoters. Notably, over-expression of Z0021 in various Gram-negative pathogens results in a significant decrease in motility (Uma Silphaduang, unpublished data), likely due to the high conservation of FlhD and FlhC amongst bacteria. Thus, understanding the precise mechanism of Z0021-mediated repression

would be useful and may lead to the development of novel strategies that aim to target flagellar expression. Also, given the lack of similarity of Z0021 to other proteins, any structural information that could be obtained on Z0021 could contribute to understanding the mechanism by which it represses motility. Together, these phenotypic and biochemical studies may further our knowledge of the pathogenesis and virulence strategies employed by *E. coli* O157:H7.

Future Directions Addressing the Role of SsaN in Type III Secretion and Beyond

The work presented on the *Salmonella enterica* T3SS-2 ATPase, SsaN, enhances our understanding of type III secretion in a number of Gram-negative pathogens; however, many questions still remain. Most notably, the interaction partners of T3SS ATPases in both the cytosol and at the membrane have yet to be fully elucidated. While it is known that T3SS ATPases form a complex with a FliH and FliJ homologues in the bacterial cytoplasm (163,286), work on the T2SS ATPase from *Xanthomonas campestris* has shown that ATPases associated with secretion systems can alternate between a cytoplasmic or membrane-bound state depending upon the secretion state of the channel (287). Given this work, it is intriguing to speculate that T3SS ATPases also cycle between the cytoplasm (prior to the secretion of an effector substrate) and the membrane (during effector translocation). If this proves to be true, perhaps T3SS ATPase monomers bind to chaperone or chaperone-effector complexes in the cytoplasm. This scenario would allow for new ATPase monomers, perhaps laden with cargo, to readily associate with an active secretion channel to more rapidly facilitate effector translocation, and would also allow

for T3SS ATPase monomers to be recycled back to the cytoplasm once an effector has been secreted.

At the membrane, T3SS ATPases are linked to the C-ring protein through an interaction with a YscL family member (163). Aside from a yeast two-hybrid analysis on the *Yersinia* T3SS, there has been limited work further delineating the interactions of T3SS components at the membrane. As such, a detailed understanding of T3SS assembly remains elusive. Future work that aims to determine the precise interaction partners of T3SS ATPases at the membrane will also provide definitive evidence of the orientation of these ATPases at the membrane. Genetic experiments on the SPI-1 encoded T3SS ATPase, InvC, have suggested that the N-terminal regions of T3SS ATPases are oriented toward the membrane (152). Subsequent studies highlighting the structural similarity between T3SSs and the F_0F_1 ATPase instead suggest that the C-terminal regions of T3SS ATPases face the membrane (162). Future experiments that define the orientation of T3SS ATPases at the membrane will provide insight into whether effector substrates are unfolded and passed through the central channel of hexameric T3SS ATPases or are instead passed to another component of the secretion apparatus to facilitate the translocation process.

The differential targeting of SPI-2 effectors to the T3SS-1 and T3SS-2 was unexpected; however, the finding that effectors encoded outside of the SPI-2 locus are targeted to both T3SSs for secretion has been noted in previous works. Further experimentation will be needed to determine whether the differential pattern in secretion for the effectors examined in our work also extends to effector translocation. Some

effectors such as PipB2, SspH1, SteA, SteB, and SlrP have been shown to be translocated by both the T3SS-1 and T3SS-2 (58). To date, the basis for this differential targeting has not been determined. One possibility is that genomic location plays a role in dictating effector targeting. For instance, SseF and SseG are encoded within the SPI-2 locus and are strictly dependent on the T3SS-2 for secretion. Other effectors encoded outside of SPI-2 can be secreted by the T3SS-1 or T3SS-2. Perhaps the evolution of these effectors outside of the SPI-2 locus has given them less specificity for the T3SS-2. However, since SseJ is only secreted by the T3SS-2, the differential targeting of effectors is likely more complex than simply the genomic location of the effector.

It is intriguing to speculate that differences in the secretion signals of SPI-2 effectors play a role in dictating specificity; however, in the absence of a well-defined secretion signal this possibility is merely speculative. Studies examining the role of secretion signals in governing T3SS specificity have found that SPI-1 effectors lacking their chaperone binding domains can be secreted by the flagellar T3SS (185). It would be worthwhile to determine whether swapping the N-terminal region of an effector that is strictly dependent on the T3SS-2 for secretion with the N-terminal region of a more promiscuous effector will allow for the T3SS-2 dependent effector to be secreted by both the T3SS-1 and T3SS-2. Such experimentation examining the role of secretion signals in the differential targeting of effectors may ultimately aid in defining a precise secretion signal. Another possibility to explain the differential targeting of effectors is that the function of the effector contributes to secretion specificity. For instance, perhaps the SPI-2 effectors that are secreted early in the infection process can be secreted by either the

T3SS-1 or the T3SS-2 while effectors that are required at a later stage of infection are only secreted by the T3SS-2. Given that the precise functions of a number of secretion substrates have yet to be elucidated, it is unclear whether effector function contributes to the differential targeting of SPI-2 effectors. Despite the large repertoire of effectors identified to date, the difficulty in identifying new secretion substrates also makes it likely that future work will uncover a greater number of effectors associated with the SPI-2 encoded T3SS.

In addition to the potential identification of more effector substrates, there are also likely a greater number of chaperones that have yet to be characterized for the T3SS-2. To date, only five chaperones have been identified for the T3SS-2 despite over thirty effector substrates being secreted by this system. The identification of these chaperones was greatly facilitated by their genomic location and proximity to their secretion substrates. In the absence of readily identifiable T3SS-2 specific chaperones, perhaps a general chaperone remains to be uncovered that can bind to a number of T3SS-2 effectors and maintain them in a secretion-competent state. This scenario would not be unprecedented as HpaB from *Xanthomonas* has been shown to function as a general chaperone for at least five effector substrates (288). Thus, despite the substantial advances that have been made with respect to understanding T3SSs, it is clear that there is still much to be learned.

Concluding Remarks

The work presented within this thesis has sought to address a broad aim of understanding the pathogenesis and virulence strategies of a subset of enteric pathogens.

This aim was achieved by elucidating the functions of two virulence-associated proteins involved in motility and type III secretion in *E. coli* O157:H7 and *Salmonella enterica* serovar Typhimurium, respectively. As the number of diseases caused by Gram-negative pathogens continues to rise, further compounded by the prevalence of antibiotic resistance, there is a pressing need to develop novel strategies to combat these pathogens. The development of treatment strategies that target key virulence mechanisms of pathogens can only be achieved through a deep understanding of these processes. This work represents the tip of the iceberg in fully appreciating the breadth of virulence strategies that pathogens have evolved to evade host defenses.

REFERENCES

1. Kaper, J.B., Nataro, J.P. & Mobley, H.L. Pathogenic *Escherichia coli*. *Nat Rev Microbiol* **2**, 123-40 (2004).
2. Nataro, J.P. & Kaper, J.B. Diarrheagenic *Escherichia coli*. *Clin Microbiol Rev* **11**, 142-201 (1998).
3. Whittam, T.S. *et al.* Clonal relationships among *Escherichia coli* strains that cause hemorrhagic colitis and infantile diarrhea. *Infect Immun* **61**, 1619-29 (1993).
4. Zhou, Z. *et al.* Derivation of *Escherichia coli* O157:H7 from its O55:H7 precursor. *PLoS One* **5**, e8700 (2010).
5. Shen, S., Mascarenhas, M., Morgan, R., Rahn, K. & Karmali, M.A. Identification of four fimbria-encoding genomic islands that are highly specific for verocytotoxin-producing *Escherichia coli* serotype O157 strains. *J Clin Microbiol* **43**, 3840-50 (2005).
6. Karmali, M.A. *et al.* Association of genomic O island 122 of *Escherichia coli* EDL 933 with verocytotoxin-producing *Escherichia coli* seropathotypes that are linked to epidemic and/or serious disease. *J Clin Microbiol* **41**, 4930-40 (2003).
7. Abuladze, T. *et al.* Bacteriophages reduce experimental contamination of hard surfaces, tomato, spinach, broccoli, and ground beef by *Escherichia coli* O157:H7. *Appl Environ Microbiol* **74**, 6230-8 (2008).
8. Scaletsky, I.C. *et al.* Diffusely adherent *Escherichia coli* as a cause of acute diarrhea in young children in Northeast Brazil: a case-control study. *J Clin Microbiol* **40**, 645-8 (2002).
9. Frank, C. *et al.* Epidemic profile of Shiga-toxin-producing *Escherichia coli* O104:H4 outbreak in Germany. *N Engl J Med* **365**, 1771-80 (2011).
10. Munera, D. *et al.* Autotransporters but not pAA are critical for rabbit colonization by Shiga toxin-producing *Escherichia coli* O104:H4. *Nat Commun* **5**, 3080 (2014).
11. Qadri, F., Svennerholm, A.M., Faruque, A.S. & Sack, R.B. Enterotoxigenic *Escherichia coli* in developing countries: epidemiology, microbiology, clinical features, treatment, and prevention. *Clin Microbiol Rev* **18**, 465-83 (2005).
12. Akiba, M., Kusumoto, M. & Iwata, T. Rapid identification of *Salmonella enterica* serovars, Typhimurium, Choleraesuis, Infantis, Hadar, Enteritidis, Dublin and Gallinarum, by multiplex PCR. *J Microbiol Methods* **85**, 9-15 (2011).
13. Majowicz, S.E. *et al.* The global burden of nontyphoidal *Salmonella* gastroenteritis. *Clin Infect Dis* **50**, 882-9 (2010).
14. Haraga, A., Ohlson, M.B. & Miller, S.I. Salmonellae interplay with host cells. *Nat Rev Microbiol* **6**, 53-66 (2008).
15. Crump, J.A., Luby, S.P. & Mintz, E.D. The global burden of typhoid fever. *Bull World Health Organ* **82**, 346-53 (2004).
16. Lloyd, A.L., Henderson, T.A., Vigil, P.D. & Mobley, H.L. Genomic islands of uropathogenic *Escherichia coli* contribute to virulence. *J Bacteriol* **191**, 3469-81 (2009).

17. Ochman, H., Lawrence, J.G. & Groisman, E.A. Lateral gene transfer and the nature of bacterial innovation. *Nature* **405**, 299-304 (2000).
18. Schmidt, H. & Hensel, M. Pathogenicity islands in bacterial pathogenesis. *Clin Microbiol Rev* **17**, 14-56 (2004).
19. Thomas, C.M. & Nielsen, K.M. Mechanisms of, and barriers to, horizontal gene transfer between bacteria. *Nat Rev Microbiol* **3**, 711-21 (2005).
20. Perna, N.T. *et al.* Genome sequence of enterohaemorrhagic *Escherichia coli* O157:H7. *Nature* **409**, 529-33 (2001).
21. Hayashi, T. *et al.* Complete genome sequence of enterohemorrhagic *Escherichia coli* O157:H7 and genomic comparison with a laboratory strain K-12. *DNA Res* **8**, 11-22 (2001).
22. Elliott, S.J. *et al.* The complete sequence of the locus of enterocyte effacement (LEE) from enteropathogenic *Escherichia coli* E2348/69. *Mol Microbiol* **28**, 1-4 (1998).
23. McDaniel, T.K., Jarvis, K.G., Donnenberg, M.S. & Kaper, J.B. A genetic locus of enterocyte effacement conserved among diverse enterobacterial pathogens. *Proc Natl Acad Sci U S A* **92**, 1664-8 (1995).
24. Sperandio, V., Mellies, J.L., Nguyen, W., Shin, S. & Kaper, J.B. Quorum sensing controls expression of the type III secretion gene transcription and protein secretion in enterohemorrhagic and enteropathogenic *Escherichia coli*. *Proc Natl Acad Sci U S A* **96**, 15196-201 (1999).
25. Karch, H. *et al.* A genomic island, termed high-pathogenicity island, is present in certain non-O157 Shiga toxin-producing *Escherichia coli* clonal lineages. *Infect Immun* **67**, 5994-6001 (1999).
26. Shimizu, T., Ohta, Y. & Noda, M. Shiga toxin 2 is specifically released from bacterial cells by two different mechanisms. *Infect Immun* **77**, 2813-23 (2009).
27. Low, A.S. *et al.* Analysis of fimbrial gene clusters and their expression in enterohaemorrhagic *Escherichia coli* O157:H7. *Environ Microbiol* **8**, 1033-47 (2006).
28. Torres, A.G. *et al.* Identification and characterization of *lpfABCC'DE*, a fimbrial operon of enterohemorrhagic *Escherichia coli* O157:H7. *Infect Immun* **70**, 5416-27 (2002).
29. Torres, A.G., Kanack, K.J., Tutt, C.B., Popov, V. & Kaper, J.B. Characterization of the second long polar (LP) fimbriae of *Escherichia coli* O157:H7 and distribution of LP fimbriae in other pathogenic *E. coli* strains. *FEMS Microbiol Lett* **238**, 333-44 (2004).
30. Sabbagh, S.C., Forest, C.G., Lepage, C., Leclerc, J.M. & Daigle, F. So similar, yet so different: uncovering distinctive features in the genomes of *Salmonella enterica* serovars Typhimurium and Typhi. *FEMS Microbiol Lett* **305**, 1-13 (2010).
31. Janakiraman, A. & Slauch, J.M. The putative iron transport system SitABCD encoded on SPI1 is required for full virulence of *Salmonella typhimurium*. *Mol Microbiol* **35**, 1146-55 (2000).

32. Mills, D.M., Bajaj, V. & Lee, C.A. A 40 kb chromosomal fragment encoding *Salmonella typhimurium* invasion genes is absent from the corresponding region of the *Escherichia coli* K-12 chromosome. *Mol Microbiol* **15**, 749-59 (1995).
33. Ellermeier, C.D.S., J.M. The Prokaryotes. Vol. 6 (ed. Dworkin, M.F., S.) 123-158 (Springer, 2006).
34. Shea, J.E., Hensel, M., Gleeson, C. & Holden, D.W. Identification of a virulence locus encoding a second type III secretion system in *Salmonella typhimurium*. *Proc Natl Acad Sci U S A* **93**, 2593-7 (1996).
35. Ochman, H., Soncini, F.C., Solomon, F. & Groisman, E.A. Identification of a pathogenicity island required for *Salmonella* survival in host cells. *Proc Natl Acad Sci U S A* **93**, 7800-4 (1996).
36. Cirillo, D.M., Valdivia, R.H., Monack, D.M. & Falkow, S. Macrophage-dependent induction of the *Salmonella* pathogenicity island 2 type III secretion system and its role in intracellular survival. *Mol Microbiol* **30**, 175-88 (1998).
37. Hensel, M., Hinsley, A.P., Nikolaus, T., Sawers, G. & Berks, B.C. The genetic basis of tetrathionate respiration in *Salmonella typhimurium*. *Mol Microbiol* **32**, 275-87 (1999).
38. Hensel, M., Nikolaus, T. & Egelseer, C. Molecular and functional analysis indicates a mosaic structure of *Salmonella* pathogenicity island 2. *Mol Microbiol* **31**, 489-98 (1999).
39. Marcus, S.L., Brumell, J.H., Pfeifer, C.G. & Finlay, B.B. *Salmonella* pathogenicity islands: big virulence in small packages. *Microbes Infect* **2**, 145-56 (2000).
40. Nguyen, Y. & Sperandio, V. Enterohemorrhagic *E. coli* (EHEC) pathogenesis. *Front Cell Infect Microbiol* **2**, 90 (2012).
41. Thevenot, J. *et al.* Enterohemorrhagic *Escherichia coli* O157:H7 survival in an in vitro model of the human large intestine and interactions with probiotic yeasts and resident microbiota. *Appl Environ Microbiol* **79**, 1058-64 (2013).
42. Gomes, T.A. *et al.* Adhesin-encoding genes from shiga toxin-producing *Escherichia coli* are more prevalent in atypical than in typical enteropathogenic *E. coli*. *J Clin Microbiol* **49**, 3334-7 (2011).
43. Rendon, M.A. *et al.* Commensal and pathogenic *Escherichia coli* use a common pilus adherence factor for epithelial cell colonization. *Proc Natl Acad Sci U S A* **104**, 10637-42 (2007).
44. Tatsuno, I. *et al.* *toxB* gene on pO157 of enterohemorrhagic *Escherichia coli* O157:H7 is required for full epithelial cell adherence phenotype. *Infect Immun* **69**, 6660-9 (2001).
45. Torres, A.G. *et al.* Outer membrane protein A of *Escherichia coli* O157:H7 stimulates dendritic cell activation. *Infect Immun* **74**, 2676-85 (2006).
46. Liu, H., Magoun, L., Luperchio, S., Schauer, D.B. & Leong, J.M. The Tir-binding region of enterohaemorrhagic *Escherichia coli* intimin is sufficient to trigger actin condensation after bacterial-induced host cell signalling. *Mol Microbiol* **34**, 67-81 (1999).

47. Luo, Y. *et al.* Crystal structure of enteropathogenic *Escherichia coli* intimin-receptor complex. *Nature* **405**, 1073-7 (2000).
48. Deng, W. *et al.* A comprehensive proteomic analysis of the type III secretome of *Citrobacter rodentium*. *J Biol Chem* **285**, 6790-800 (2010).
49. Tobe, T. *et al.* An extensive repertoire of type III secretion effectors in *Escherichia coli* O157 and the role of lambdoid phages in their dissemination. *Proc Natl Acad Sci U S A* **103**, 14941-6 (2006).
50. Endo, Y. *et al.* Site of action of a Vero toxin (VT2) from *Escherichia coli* O157:H7 and of Shiga toxin on eukaryotic ribosomes. RNA N-glycosidase activity of the toxins. *Eur J Biochem* **171**, 45-50 (1988).
51. Goldwater, P.N. & Bettelheim, K.A. Treatment of enterohemorrhagic *Escherichia coli* (EHEC) infection and hemolytic uremic syndrome (HUS). *BMC Med* **10**, 12 (2012).
52. Grif, K., Dierich, M.P., Karch, H. & Allerberger, F. Strain-specific differences in the amount of Shiga toxin released from enterohemorrhagic *Escherichia coli* O157 following exposure to subinhibitory concentrations of antimicrobial agents. *Eur J Clin Microbiol Infect Dis* **17**, 761-6 (1998).
53. Jones, B.D., Ghorri, N. & Falkow, S. *Salmonella typhimurium* initiates murine infection by penetrating and destroying the specialized epithelial M cells of the Peyer's patches. *J Exp Med* **180**, 15-23 (1994).
54. Galan, J.E. Molecular genetic bases of *Salmonella* entry into host cells. *Mol Microbiol* **20**, 263-71 (1996).
55. Jepson, M.A., Collares-Buzato, C.B., Clark, M.A., Hirst, B.H. & Simmons, N.L. Rapid disruption of epithelial barrier function by *Salmonella typhimurium* is associated with structural modification of intercellular junctions. *Infect Immun* **63**, 356-9 (1995).
56. Hensel, M. *et al.* Genes encoding putative effector proteins of the type III secretion system of *Salmonella* pathogenicity island 2 are required for bacterial virulence and proliferation in macrophages. *Mol Microbiol* **30**, 163-74 (1998).
57. Buckner, M.M., Croxen, M.A., Arena, E.T. & Finlay, B.B. A comprehensive study of the contribution of *Salmonella enterica* serovar Typhimurium SPI2 effectors to bacterial colonization, survival, and replication in typhoid fever, macrophage, and epithelial cell infection models. *Virulence* **2**, 208-16 (2011).
58. Figueira, R. & Holden, D.W. Functions of the *Salmonella* pathogenicity island 2 (SPI-2) type III secretion system effectors. *Microbiology* **158**, 1147-61 (2012).
59. Varma, J.K. *et al.* Hospitalization and antimicrobial resistance in *Salmonella* outbreaks, 1984-2002. *Emerg Infect Dis* **11**, 943-6 (2005).
60. McLaughlin, L.M. *et al.* The *Salmonella* SPI2 effector SseI mediates long-term systemic infection by modulating host cell migration. *PLoS Pathog* **5**, e1000671 (2009).
61. Dhanoa, A. & Fatt, Q.K. Non-typhoidal *Salmonella* bacteraemia: epidemiology, clinical characteristics and its' association with severe immunosuppression. *Ann Clin Microbiol Antimicrob* **8**, 15 (2009).

62. Chevance, F.F. & Hughes, K.T. Coordinating assembly of a bacterial macromolecular machine. *Nat Rev Microbiol* **6**, 455-65 (2008).
63. Wadhams, G.H. & Armitage, J.P. Making sense of it all: bacterial chemotaxis. *Nat Rev Mol Cell Biol* **5**, 1024-37 (2004).
64. Kamp, H.D. & Higgins, D.E. A protein thermometer controls temperature-dependent transcription of flagellar motility genes in *Listeria monocytogenes*. *PLoS Pathog* **7**, e1002153 (2011).
65. Blair, D.F. How bacteria sense and swim. *Annu Rev Microbiol* **49**, 489-522 (1995).
66. Davey, M.E. & O'Toole G, A. Microbial biofilms: from ecology to molecular genetics. *Microbiol Mol Biol Rev* **64**, 847-67 (2000).
67. Tasteyre, A., Barc, M.C., Collignon, A., Boureau, H. & Karjalainen, T. Role of FliC and FliD flagellar proteins of *Clostridium difficile* in adherence and gut colonization. *Infect Immun* **69**, 7937-40 (2001).
68. Pratt, L.A. & Kolter, R. Genetic analysis of *Escherichia coli* biofilm formation: roles of flagella, motility, chemotaxis and type I pili. *Mol Microbiol* **30**, 285-93 (1998).
69. Kirov, S.M. Bacteria that express lateral flagella enable dissection of the multifunctional roles of flagella in pathogenesis. *FEMS Microbiol Lett* **224**, 151-9 (2003).
70. Erhardt, M., Namba, K. & Hughes, K.T. Bacterial nanomachines: the flagellum and type III injectisome. *Cold Spring Harb Perspect Biol* **2**, a000299 (2010).
71. Terashima, H., Kojima, S. & Homma, M. Flagellar motility in bacteria structure and function of flagellar motor. *Int Rev Cell Mol Biol* **270**, 39-85 (2008).
72. Chilcott, G.S. & Hughes, K.T. Coupling of flagellar gene expression to flagellar assembly in *Salmonella enterica* serovar typhimurium and *Escherichia coli*. *Microbiol Mol Biol Rev* **64**, 694-708 (2000).
73. Liu, X. & Matsumura, P. The FlhD/FlhC complex, a transcriptional activator of the *Escherichia coli* flagellar class II operons. *J Bacteriol* **176**, 7345-51 (1994).
74. Wang, S., Fleming, R.T., Westbrook, E.M., Matsumura, P. & McKay, D.B. Structure of the *Escherichia coli* FlhDC complex, a prokaryotic heteromeric regulator of transcription. *J Mol Biol* **355**, 798-808 (2006).
75. Ohnishi, K., Kutsukake, K., Suzuki, H. & Iino, T. Gene *fliA* encodes an alternative sigma factor specific for flagellar operons in *Salmonella typhimurium*. *Mol Gen Genet* **221**, 139-47 (1990).
76. Liu, X. & Matsumura, P. An alternative sigma factor controls transcription of flagellar class-III operons in *Escherichia coli*: gene sequence, overproduction, purification and characterization. *Gene* **164**, 81-4 (1995).
77. Gillen, K.L. & Hughes, K.T. Transcription from two promoters and autoregulation contribute to the control of expression of the *Salmonella typhimurium* flagellar regulatory gene *flgM*. *J Bacteriol* **175**, 7006-15 (1993).
78. Aldridge, P.D. *et al.* The flagellar-specific transcription factor, sigma28, is the Type III secretion chaperone for the flagellar-specific anti-sigma28 factor FlgM. *Genes Dev* **20**, 2315-26 (2006).

79. Toker, A.S., Kihara, M. & Macnab, R.M. Deletion analysis of the FlhM flagellar switch protein of *Salmonella typhimurium*. *J Bacteriol* **178**, 7069-79 (1996).
80. Lowder, B.J., Duyvesteyn, M.D. & Blair, D.F. FliG subunit arrangement in the flagellar rotor probed by targeted cross-linking. *J Bacteriol* **187**, 5640-7 (2005).
81. Minamino, T. & Macnab, R.M. Components of the *Salmonella* flagellar export apparatus and classification of export substrates. *J Bacteriol* **181**, 1388-94 (1999).
82. Waters, R.C., O'Toole, P.W. & Ryan, K.A. The FliK protein and flagellar hook-length control. *Protein Sci* **16**, 769-80 (2007).
83. Samatey, F.A. *et al.* Structure of the bacterial flagellar hook and implication for the molecular universal joint mechanism. *Nature* **431**, 1062-8 (2004).
84. Hirano, T., Yamaguchi, S., Oosawa, K. & Aizawa, S. Roles of FliK and FlhB in determination of flagellar hook length in *Salmonella typhimurium*. *J Bacteriol* **176**, 5439-49 (1994).
85. Wurpel, D.J., Beatson, S.A., Totsika, M., Petty, N.K. & Schembri, M.A. Chaperone-usher fimbriae of *Escherichia coli*. *PLoS One* **8**, e52835 (2013).
86. Waksman, G. & Hultgren, S.J. Structural biology of the chaperone-usher pathway of pilus biogenesis. *Nat Rev Microbiol* **7**, 765-74 (2009).
87. Nuccio, S.P. & Baumler, A.J. Evolution of the chaperone/usher assembly pathway: fimbrial classification goes Greek. *Microbiol Mol Biol Rev* **71**, 551-75 (2007).
88. Orndorff, P.E. & Falkow, S. Organization and expression of genes responsible for type 1 piliation in *Escherichia coli*. *J Bacteriol* **159**, 736-44 (1984).
89. Zeiner, S.A., Dwyer, B.E. & Clegg, S. FimA, FimF, and FimH are necessary for assembly of type 1 fimbriae on *Salmonella enterica* serovar Typhimurium. *Infect Immun* **80**, 3289-96 (2012).
90. Krogfelt, K.A. & Klemm, P. Investigation of minor components of *Escherichia coli* type 1 fimbriae: protein chemical and immunological aspects. *Microb Pathog* **4**, 231-8 (1988).
91. Krogfelt, K.A., Bergmans, H. & Klemm, P. Direct evidence that the FimH protein is the mannose-specific adhesin of *Escherichia coli* type 1 fimbriae. *Infect Immun* **58**, 1995-8 (1990).
92. Sauer, F.G., Remaut, H., Hultgren, S.J. & Waksman, G. Fiber assembly by the chaperone-usher pathway. *Biochim Biophys Acta* **1694**, 259-67 (2004).
93. Klemm, P. FimC, a chaperone-like periplasmic protein of *Escherichia coli* involved in biogenesis of type 1 fimbriae. *Res Microbiol* **143**, 831-8 (1992).
94. Jones, C.H. *et al.* FimC is a periplasmic PapD-like chaperone that directs assembly of type 1 pili in bacteria. *Proc Natl Acad Sci U S A* **90**, 8397-401 (1993).
95. Valenski, M.L., Harris, S.L., Spears, P.A., Horton, J.R. & Orndorff, P.E. The Product of the *fimI* gene is necessary for *Escherichia coli* type 1 pilus biosynthesis. *J Bacteriol* **185**, 5007-11 (2003).
96. Connell, I. *et al.* Type 1 fimbrial expression enhances *Escherichia coli* virulence for the urinary tract. *Proc Natl Acad Sci U S A* **93**, 9827-32 (1996).

97. Abraham, J.M., Freitag, C.S., Clements, J.R. & Eisenstein, B.I. An invertible element of DNA controls phase variation of type 1 fimbriae of *Escherichia coli*. *Proc Natl Acad Sci U S A* **82**, 5724-7 (1985).
98. van der Woude, M.W. & Baumler, A.J. Phase and antigenic variation in bacteria. *Clin Microbiol Rev* **17**, 581-611, table of contents (2004).
99. Klemm, P. Two regulatory *fim* genes, *fimB* and *fimE*, control the phase variation of type 1 fimbriae in *Escherichia coli*. *EMBO J* **5**, 1389-93 (1986).
100. McClain, M.S., Blomfield, I.C. & Eisenstein, B.I. Roles of *fimB* and *fimE* in site-specific DNA inversion associated with phase variation of type 1 fimbriae in *Escherichia coli*. *J Bacteriol* **173**, 5308-14 (1991).
101. Kuwahara, H., Myers, C.J. & Samoilov, M.S. Temperature control of fimbriation circuit switch in uropathogenic *Escherichia coli*: quantitative analysis via automated model abstraction. *PLoS Comput Biol* **6**, e1000723 (2010).
102. O'Gara, J.P. & Dorman, C.J. Effects of local transcription and H-NS on inversion of the *fim* switch of *Escherichia coli*. *Mol Microbiol* **36**, 457-66 (2000).
103. Kawula, T.H. & Orndorff, P.E. Rapid site-specific DNA inversion in *Escherichia coli* mutants lacking the histonelike protein H-NS. *J Bacteriol* **173**, 4116-23 (1991).
104. Tinker, J.K., Hancox, L.S. & Clegg, S. FimW is a negative regulator affecting type 1 fimbrial expression in *Salmonella enterica* serovar typhimurium. *J Bacteriol* **183**, 435-42 (2001).
105. Clegg, S., Hancox, L.S. & Yeh, K.S. *Salmonella typhimurium* fimbrial phase variation and FimA expression. *J Bacteriol* **178**, 542-5 (1996).
106. Tinker, J.K. & Clegg, S. Characterization of FimY as a coactivator of type 1 fimbrial expression in *Salmonella enterica* serovar Typhimurium. *Infect Immun* **68**, 3305-13 (2000).
107. Shaikh, N., Holt, N.J., Johnson, J.R. & Tarr, P.I. Fim operon variation in the emergence of Enterohemorrhagic *Escherichia coli*: an evolutionary and functional analysis. *FEMS Microbiol Lett* **273**, 58-63 (2007).
108. Bajaj, V., Lucas, R.L., Hwang, C. & Lee, C.A. Co-ordinate regulation of *Salmonella typhimurium* invasion genes by environmental and regulatory factors is mediated by control of *hila* expression. *Mol Microbiol* **22**, 703-14 (1996).
109. Song, M. *et al.* ppGpp-dependent stationary phase induction of genes on *Salmonella* pathogenicity island 1. *J Biol Chem* **279**, 34183-90 (2004).
110. Schechter, L.M., Damrauer, S.M. & Lee, C.A. Two AraC/XylS family members can independently counteract the effect of repressing sequences upstream of the *hila* promoter. *Mol Microbiol* **32**, 629-42 (1999).
111. Ellermeier, C.D. & Slauch, J.M. RtsA and RtsB coordinately regulate expression of the invasion and flagellar genes in *Salmonella enterica* serovar Typhimurium. *J Bacteriol* **185**, 5096-108 (2003).
112. Golubeva, Y.A., Sadik, A.Y., Ellermeier, J.R. & Slauch, J.M. Integrating global regulatory input into the *Salmonella* pathogenicity island 1 type III secretion system. *Genetics* **190**, 79-90 (2012).

113. Darwin, K.H. & Miller, V.L. The putative invasion protein chaperone SicA acts together with InvF to activate the expression of *Salmonella typhimurium* virulence genes. *Mol Microbiol* **35**, 949-60 (2000).
114. Darwin, K.H. & Miller, V.L. Type III secretion chaperone-dependent regulation: activation of virulence genes by SicA and InvF in *Salmonella typhimurium*. *EMBO J* **20**, 1850-62 (2001).
115. Fabrega, A. & Vila, J. *Salmonella enterica* serovar Typhimurium skills to succeed in the host: virulence and regulation. *Clin Microbiol Rev* **26**, 308-41 (2013).
116. Olekhovich, I.N. & Kadner, R.J. Role of nucleoid-associated proteins Hha and H-NS in expression of *Salmonella enterica* activators HilD, HilC, and RtsA required for cell invasion. *J Bacteriol* **189**, 6882-90 (2007).
117. Baxter, M.A., Fahlen, T.F., Wilson, R.L. & Jones, B.D. HilE interacts with HilD and negatively regulates *hilA* transcription and expression of the *Salmonella enterica* serovar Typhimurium invasive phenotype. *Infect Immun* **71**, 1295-305 (2003).
118. Deiwick, J., Nikolaus, T., Erdogan, S. & Hensel, M. Environmental regulation of *Salmonella* pathogenicity island 2 gene expression. *Mol Microbiol* **31**, 1759-73 (1999).
119. Coombes, B.K., Brown, N.F., Valdez, Y., Brumell, J.H. & Finlay, B.B. Expression and secretion of *Salmonella* pathogenicity island-2 virulence genes in response to acidification exhibit differential requirements of a functional type III secretion apparatus and SsaL. *J Biol Chem* **279**, 49804-15 (2004).
120. Hensel, M. *et al.* Functional analysis of *ssaJ* and the *ssaK/U* operon, 13 genes encoding components of the type III secretion apparatus of *Salmonella* Pathogenicity Island 2. *Mol Microbiol* **24**, 155-67 (1997).
121. Osborne, S.E. & Coombes, B.K. Transcriptional priming of *Salmonella* Pathogenicity Island-2 precedes cellular invasion. *PLoS One* **6**, e21648 (2011).
122. Carroll, R.K. *et al.* Structural and functional analysis of the C-terminal DNA binding domain of the *Salmonella typhimurium* SPI-2 response regulator SsrB. *J Biol Chem* **284**, 12008-19 (2009).
123. Tomljenovic-Berube, A.M., Mulder, D.T., Whiteside, M.D., Brinkman, F.S. & Coombes, B.K. Identification of the regulatory logic controlling *Salmonella* pathoadaptation by the SsrA-SsrB two-component system. *PLoS Genet* **6**, e1000875 (2010).
124. Bijlsma, J.J. & Groisman, E.A. The PhoP/PhoQ system controls the intramacrophage type three secretion system of *Salmonella enterica*. *Mol Microbiol* **57**, 85-96 (2005).
125. Lee, A.K., Detweiler, C.S. & Falkow, S. OmpR regulates the two-component system SsrA-SsrB in *Salmonella* pathogenicity island 2. *J Bacteriol* **182**, 771-81 (2000).
126. Linehan, S.A., Rytönen, A., Yu, X.J., Liu, M. & Holden, D.W. SlyA regulates function of *Salmonella* pathogenicity island 2 (SPI-2) and expression of SPI-2-associated genes. *Infect Immun* **73**, 4354-62 (2005).

127. Lim, S., Kim, B., Choi, H.S., Lee, Y. & Ryu, S. Fis is required for proper regulation of *ssaG* expression in *Salmonella enterica* serovar Typhimurium. *Microb Pathog* **41**, 33-42 (2006).
128. Kelly, A. *et al.* A global role for Fis in the transcriptional control of metabolism and type III secretion in *Salmonella enterica* serovar Typhimurium. *Microbiology* **150**, 2037-53 (2004).
129. Coombes, B.K., Wickham, M.E., Lowden, M.J., Brown, N.F. & Finlay, B.B. Negative regulation of *Salmonella* pathogenicity island 2 is required for contextual control of virulence during typhoid. *Proc Natl Acad Sci U S A* **102**, 17460-5 (2005).
130. Silphaduang, U., Mascarenhas, M., Karmali, M. & Coombes, B.K. Repression of intracellular virulence factors in *Salmonella* by the Hha and YdgT nucleoid-associated proteins. *J Bacteriol* **189**, 3669-73 (2007).
131. Abby, S.S. & Rocha, E.P. The non-flagellar type III secretion system evolved from the bacterial flagellum and diversified into host-cell adapted systems. *PLoS Genet* **8**, e1002983 (2012).
132. Diepold, A. *et al.* Deciphering the assembly of the *Yersinia* type III secretion injectisome. *EMBO J* **29**, 1928-40 (2010).
133. Wagner, S. *et al.* Organization and coordinated assembly of the type III secretion export apparatus. *Proc Natl Acad Sci U S A* **107**, 17745-50 (2010).
134. Burkinshaw, B.J. & Strynadka, N.C. Assembly and structure of the T3SS. *Biochim Biophys Acta* **1843**, 1649-63 (2014).
135. Cornelis, G.R. & Van Gijsegem, F. Assembly and function of type III secretory systems. *Annu Rev Microbiol* **54**, 735-74 (2000).
136. Buttner, D. Protein export according to schedule: architecture, assembly, and regulation of type III secretion systems from plant- and animal-pathogenic bacteria. *Microbiol Mol Biol Rev* **76**, 262-310 (2012).
137. Hartmann, N. & Buttner, D. The inner membrane protein HrcV from *Xanthomonas spp.* is involved in substrate docking during type III secretion. *Mol Plant Microbe Interact* **26**, 1176-89 (2013).
138. Schulz, S. & Buttner, D. Functional characterization of the type III secretion substrate specificity switch protein HpaC from *Xanthomonas campestris pv. vesicatoria*. *Infect Immun* **79**, 2998-3011 (2011).
139. Yu, X.J., McGourty, K., Liu, M., Unsworth, K.E. & Holden, D.W. pH sensing by intracellular *Salmonella* induces effector translocation. *Science* **328**, 1040-3 (2010).
140. Yu, X.J., Liu, M., Matthews, S. & Holden, D.W. Tandem translation generates a chaperone for the *Salmonella* type III secretion system protein SsaQ. *J Biol Chem* **286**, 36098-107 (2011).
141. Spreter, T. *et al.* A conserved structural motif mediates formation of the periplasmic rings in the type III secretion system. *Nat Struct Mol Biol* **16**, 468-76 (2009).

142. Chakravorty, D., Rohde, M., Jager, L., Deiwick, J. & Hensel, M. Formation of a novel surface structure encoded by *Salmonella* Pathogenicity Island 2. *EMBO J* **24**, 2043-52 (2005).
143. Journet, L., Agrain, C., Broz, P. & Cornelis, G.R. The needle length of bacterial injectisomes is determined by a molecular ruler. *Science* **302**, 1757-60 (2003).
144. Monjaras Feria, J. *et al.* Role of EscP (Orf16) in injectisome biogenesis and regulation of type III protein secretion in enteropathogenic *Escherichia coli*. *J Bacteriol* **194**, 6029-45 (2012).
145. Nikolaus, T. *et al.* SseBCD proteins are secreted by the type III secretion system of *Salmonella* pathogenicity island 2 and function as a translocon. *J Bacteriol* **183**, 6036-45 (2001).
146. Holzer, S.U. & Hensel, M. Functional dissection of translocon proteins of the *Salmonella* pathogenicity island 2-encoded type III secretion system. *BMC Microbiol* **10**, 104 (2010).
147. Freeman, J.A., Rappl, C., Kuhle, V., Hensel, M. & Miller, S.I. SpiC is required for translocation of *Salmonella* pathogenicity island 2 effectors and secretion of translocon proteins SseB and SseC. *J Bacteriol* **184**, 4971-80 (2002).
148. Kimbrough, T.G. & Miller, S.I. Assembly of the type III secretion needle complex of *Salmonella typhimurium*. *Microbes Infect* **4**, 75-82 (2002).
149. Andrade, A., Pardo, J.P., Espinosa, N., Perez-Hernandez, G. & Gonzalez-Pedrajo, B. Enzymatic characterization of the enteropathogenic *Escherichia coli* type III secretion ATPase EscN. *Arch Biochem Biophys* **468**, 121-7 (2007).
150. Zarivach, R., Vuckovic, M., Deng, W., Finlay, B.B. & Strynadka, N.C. Structural analysis of a prototypical ATPase from the type III secretion system. *Nat Struct Mol Biol* **14**, 131-7 (2007).
151. Blaylock, B., Riordan, K.E., Missiakas, D.M. & Schneewind, O. Characterization of the *Yersinia enterocolitica* type III secretion ATPase YscN and its regulator, YscL. *J Bacteriol* **188**, 3525-34 (2006).
152. Akeda, Y. & Galan, J.E. Genetic analysis of the *Salmonella enterica* type III secretion-associated ATPase InvC defines discrete functional domains. *J Bacteriol* **186**, 2402-12 (2004).
153. Stone, C.B., Johnson, D.L., Bulir, D.C., Gilchrist, J.D. & Mahony, J.B. Characterization of the putative type III secretion ATPase CdsN (Cpn0707) of *Chlamydomonas pneumoniae*. *J Bacteriol* **190**, 6580-8 (2008).
154. Stone, C.B. *et al.* Chlamydia Pneumoniae CdsL Regulates CdsN ATPase Activity, and Disruption with a Peptide Mimetic Prevents Bacterial Invasion. *Front Microbiol* **2**, 21 (2011).
155. Pozidis, C. *et al.* Type III protein translocase: HrcN is a peripheral ATPase that is activated by oligomerization. *J Biol Chem* **278**, 25816-24 (2003).
156. Lorenz, C. & Buttner, D. Functional characterization of the type III secretion ATPase HrcN from the plant pathogen *Xanthomonas campestris pv. vesicatoria*. *J Bacteriol* **191**, 1414-28 (2009).

157. Imada, K., Minamino, T., Tahara, A. & Namba, K. Structural similarity between the flagellar type III ATPase FliI and F1-ATPase subunits. *Proc Natl Acad Sci U S A* **104**, 485-90 (2007).
158. Claret, L., Calder, S.R., Higgins, M. & Hughes, C. Oligomerization and activation of the FliI ATPase central to bacterial flagellum assembly. *Mol Microbiol* **48**, 1349-55 (2003).
159. Fan, F. & Macnab, R.M. Enzymatic characterization of FliI. An ATPase involved in flagellar assembly in *Salmonella typhimurium*. *J Biol Chem* **271**, 31981-8 (1996).
160. Auvray, F., Ozin, A.J., Claret, L. & Hughes, C. Intrinsic membrane targeting of the flagellar export ATPase FliI: interaction with acidic phospholipids and FliH. *J Mol Biol* **318**, 941-50 (2002).
161. Muller, S.A. *et al.* Double hexameric ring assembly of the type III protein translocase ATPase HrcN. *Mol Microbiol* **61**, 119-25 (2006).
162. Ibuki, T. *et al.* Common architecture of the flagellar type III protein export apparatus and F- and V-type ATPases. *Nat Struct Mol Biol* **18**, 277-82 (2011).
163. Jackson, M.W. & Plano, G.V. Interactions between type III secretion apparatus components from *Yersinia pestis* detected using the yeast two-hybrid system. *FEMS Microbiol Lett* **186**, 85-90 (2000).
164. Minamino, T. & MacNab, R.M. FliH, a soluble component of the type III flagellar export apparatus of *Salmonella*, forms a complex with FliI and inhibits its ATPase activity. *Mol Microbiol* **37**, 1494-503 (2000).
165. Lane, M.C., O'Toole, P.W. & Moore, S.A. Molecular basis of the interaction between the flagellar export proteins FliI and FliH from *Helicobacter pylori*. *J Biol Chem* **281**, 508-17 (2006).
166. Romo-Castillo, M. *et al.* EscO, a Functional and Structural Analog of the Flagellar FliJ Protein, Is a Positive Regulator of EscN ATPase Activity of the Enteropathogenic *Escherichia coli* Injectisome. *J Bacteriol* **196**, 2227-2241 (2014).
167. Akeda, Y. & Galan, J.E. Chaperone release and unfolding of substrates in type III secretion. *Nature* **437**, 911-5 (2005).
168. Yoshida, Y. *et al.* Functional Characterization of the Type III Secretion ATPase SsaN Encoded by *Salmonella* Pathogenicity Island 2. *PLoS One* **9**, e94347 (2014).
169. Sorg, J.A., Blaylock, B. & Schneewind, O. Secretion signal recognition by YscN, the *Yersinia* type III secretion ATPase. *Proc Natl Acad Sci U S A* **103**, 16490-5 (2006).
170. Wilharm, G. *et al.* *Yersinia enterocolitica* type III secretion depends on the proton motive force but not on the flagellar motor components MotA and MotB. *Infect Immun* **72**, 4004-9 (2004).
171. Minamino, T. & Namba, K. Distinct roles of the FliI ATPase and proton motive force in bacterial flagellar protein export. *Nature* **451**, 485-8 (2008).
172. Woestyn, S., Allaoui, A., Wattiau, P. & Cornelis, G.R. YscN, the putative energizer of the *Yersinia* Yop secretion machinery. *J Bacteriol* **176**, 1561-9 (1994).

173. Bozue, J. *et al.* A *Yersinia pestis* YscN ATPase mutant functions as a live attenuated vaccine against bubonic plague in mice. *FEMS Microbiol Lett* **332**, 113-21 (2012).
174. Thomas, N.A., Ma, I., Prasad, M.E. & Rafuse, C. Expanded roles for multicargo and class 1B effector chaperones in type III secretion. *J Bacteriol* **194**, 3767-73 (2012).
175. Fu, Y. & Galan, J.E. Identification of a specific chaperone for SptP, a substrate of the centisome 63 type III secretion system of *Salmonella typhimurium*. *J Bacteriol* **180**, 3393-9 (1998).
176. Cooper, C.A. *et al.* Structural and biochemical characterization of SrcA, a multicargo type III secretion chaperone in *Salmonella* required for pathogenic association with a host. *PLoS Pathog* **6**, e1000751 (2010).
177. Cooper, C.A., Mulder, D.T., Allison, S.E., Pilar, A.V. & Coombes, B.K. The SseC translocon component in *Salmonella enterica* serovar Typhimurium is chaperoned by SscA. *BMC Microbiol* **13**, 221 (2013).
178. Quinaud, M. *et al.* The PscE-PscF-PscG complex controls type III secretion needle biogenesis in *Pseudomonas aeruginosa*. *J Biol Chem* **280**, 36293-300 (2005).
179. Feldman, M.F. & Cornelis, G.R. The multitasking type III chaperones: all you can do with 15 kDa. *FEMS Microbiol Lett* **219**, 151-8 (2003).
180. Zurawski, D.V. & Stein, M.A. SseA acts as the chaperone for the SseB component of the *Salmonella* Pathogenicity Island 2 translocon. *Mol Microbiol* **47**, 1341-51 (2003).
181. Ruiz-Albert, J., Mundy, R., Yu, X.J., Beuzon, C.R. & Holden, D.W. SseA is a chaperone for the SseB and SseD translocon components of the *Salmonella* pathogenicity-island-2-encoded type III secretion system. *Microbiology* **149**, 1103-11 (2003).
182. Miki, T., Shibagaki, Y., Danbara, H. & Okada, N. Functional characterization of SsaE, a novel chaperone protein of the type III secretion system encoded by *Salmonella* pathogenicity island 2. *J Bacteriol* **191**, 6843-54 (2009).
183. Dai, S. & Zhou, D. Secretion and function of *Salmonella* SPI-2 effector SseF require its chaperone, SscB. *J Bacteriol* **186**, 5078-86 (2004).
184. Boonyom, R., Karavolos, M.H., Bulmer, D.M. & Khan, C.M. *Salmonella* pathogenicity island 1 (SPI-1) type III secretion of SopD involves N- and C-terminal signals and direct binding to the InvC ATPase. *Microbiology* **156**, 1805-14 (2010).
185. Lee, S.H. & Galan, J.E. *Salmonella* type III secretion-associated chaperones confer secretion-pathway specificity. *Mol Microbiol* **51**, 483-95 (2004).
186. Anderson, D.M., Fouts, D.E., Collmer, A. & Schneewind, O. Reciprocal secretion of proteins by the bacterial type III machines of plant and animal pathogens suggests universal recognition of mRNA targeting signals. *Proc Natl Acad Sci U S A* **96**, 12839-43 (1999).
187. Anderson, D.M. & Schneewind, O. A mRNA signal for the type III secretion of Yop proteins by *Yersinia enterocolitica*. *Science* **278**, 1140-3 (1997).

188. Anderson, D.M. & Schneewind, O. *Yersinia enterocolitica* type III secretion: an mRNA signal that couples translation and secretion of YopQ. *Mol Microbiol* **31**, 1139-48 (1999).
189. Niemann, G.S. *et al.* RNA type III secretion signals that require Hfq. *J Bacteriol* **195**, 2119-25 (2013).
190. Lloyd, S.A., Norman, M., Rosqvist, R. & Wolf-Watz, H. *Yersinia* YopE is targeted for type III secretion by N-terminal, not mRNA, signals. *Mol Microbiol* **39**, 520-31 (2001).
191. Lloyd, S.A., Sjostrom, M., Andersson, S. & Wolf-Watz, H. Molecular characterization of type III secretion signals via analysis of synthetic N-terminal amino acid sequences. *Mol Microbiol* **43**, 51-9 (2002).
192. Waterman, S.R. & Holden, D.W. Functions and effectors of the *Salmonella* pathogenicity island 2 type III secretion system. *Cell Microbiol* **5**, 501-11 (2003).
193. Hardt, W.D., Chen, L.M., Schuebel, K.E., Bustelo, X.R. & Galan, J.E. *S. typhimurium* encodes an activator of Rho GTPases that induces membrane ruffling and nuclear responses in host cells. *Cell* **93**, 815-26 (1998).
194. Bakshi, C.S. *et al.* Identification of SopE2, a *Salmonella* secreted protein which is highly homologous to SopE and involved in bacterial invasion of epithelial cells. *J Bacteriol* **182**, 2341-4 (2000).
195. Zhou, D., Chen, L.M., Hernandez, L., Shears, S.B. & Galan, J.E. A *Salmonella* inositol polyphosphatase acts in conjunction with other bacterial effectors to promote host cell actin cytoskeleton rearrangements and bacterial internalization. *Mol Microbiol* **39**, 248-59 (2001).
196. Hayward, R.D. & Koronakis, V. Direct nucleation and bundling of actin by the SipC protein of invasive *Salmonella*. *EMBO J* **18**, 4926-34 (1999).
197. Zhou, D., Mooseker, M.S. & Galan, J.E. Role of the *S. typhimurium* actin-binding protein SipA in bacterial internalization. *Science* **283**, 2092-5 (1999).
198. Liao, A.P. *et al.* *Salmonella* type III effector AvrA stabilizes cell tight junctions to inhibit inflammation in intestinal epithelial cells. *PLoS One* **3**, e2369 (2008).
199. Hersh, D. *et al.* The *Salmonella* invasin SipB induces macrophage apoptosis by binding to caspase-1. *Proc Natl Acad Sci U S A* **96**, 2396-401 (1999).
200. Guiney, D.G. The role of host cell death in *Salmonella* infections. *Curr Top Microbiol Immunol* **289**, 131-50 (2005).
201. Zhang, Y., Higashide, W.M., McCormick, B.A., Chen, J. & Zhou, D. The inflammation-associated *Salmonella* SopA is a HECT-like E3 ubiquitin ligase. *Mol Microbiol* **62**, 786-93 (2006).
202. Brumell, J.H., Perrin, A.J., Goosney, D.L. & Finlay, B.B. Microbial pathogenesis: new niches for *Salmonella*. *Curr Biol* **12**, R15-7 (2002).
203. Brumell, J.H., Tang, P., Mills, S.D. & Finlay, B.B. Characterization of *Salmonella*-induced filaments (Sifs) reveals a delayed interaction between *Salmonella*-containing vacuoles and late endocytic compartments. *Traffic* **2**, 643-53 (2001).

204. Boucrot, E., Henry, T., Borg, J.P., Gorvel, J.P. & Meresse, S. The intracellular fate of *Salmonella* depends on the recruitment of kinesin. *Science* **308**, 1174-8 (2005).
205. Knodler, L.A. *et al.* *Salmonella* type III effectors PipB and PipB2 are targeted to detergent-resistant microdomains on internal host cell membranes. *Mol Microbiol* **49**, 685-704 (2003).
206. Henry, T. *et al.* The *Salmonella* effector protein PipB2 is a linker for kinesin-1. *Proc Natl Acad Sci U S A* **103**, 13497-502 (2006).
207. Schroeder, N. *et al.* The virulence protein SopD2 regulates membrane dynamics of *Salmonella*-containing vacuoles. *PLoS Pathog* **6**, e1001002 (2010).
208. Miao, E.A. & Miller, S.I. A conserved amino acid sequence directing intracellular type III secretion by *Salmonella typhimurium*. *Proc Natl Acad Sci U S A* **97**, 7539-44 (2000).
209. Lossi, N.S., Rolhion, N., Magee, A.I., Boyle, C. & Holden, D.W. The *Salmonella* SPI-2 effector SseJ exhibits eukaryotic activator-dependent phospholipase A and glycerophospholipid : cholesterol acyltransferase activity. *Microbiology* **154**, 2680-8 (2008).
210. Haraga, A. & Miller, S.I. A *Salmonella enterica* serovar typhimurium translocated leucine-rich repeat effector protein inhibits NF-kappa B-dependent gene expression. *Infect Immun* **71**, 4052-8 (2003).
211. Bernal-Bayard, J. & Ramos-Morales, F. *Salmonella* type III secretion effector SlrP is an E3 ubiquitin ligase for mammalian thioredoxin. *J Biol Chem* **284**, 27587-95 (2009).
212. Miao, E.A. *et al.* *Salmonella* effectors translocated across the vacuolar membrane interact with the actin cytoskeleton. *Mol Microbiol* **48**, 401-15 (2003).
213. Kujat Choy, S.L. *et al.* SseK1 and SseK2 are novel translocated proteins of *Salmonella enterica* serovar typhimurium. *Infect Immun* **72**, 5115-25 (2004).
214. Brown, N.F. *et al.* *Salmonella* phage ST64B encodes a member of the SseK/NleB effector family. *PLoS One* **6**, e17824 (2011).
215. Saini, S., Brown, J.D., Aldridge, P.D. & Rao, C.V. FliZ Is a posttranslational activator of FlhD4C2-dependent flagellar gene expression. *J Bacteriol* **190**, 4979-88 (2008).
216. Lin, D., Rao, C.V. & Slauch, J.M. The *Salmonella* SPI1 type three secretion system responds to periplasmic disulfide bond status via the flagellar apparatus and the RcsCDB system. *J Bacteriol* **190**, 87-97 (2008).
217. Saini, S., Slauch, J.M., Aldridge, P.D. & Rao, C.V. Role of cross talk in regulating the dynamic expression of the flagellar *Salmonella* pathogenicity island 1 and type 1 fimbrial genes. *J Bacteriol* **192**, 5767-77 (2010).
218. Clegg, S. & Hughes, K.T. FimZ is a molecular link between sticking and swimming in *Salmonella enterica* serovar Typhimurium. *J Bacteriol* **184**, 1209-13 (2002).
219. Li, X., Rasko, D.A., Lockett, C.V., Johnson, D.E. & Mobley, H.L. Repression of bacterial motility by a novel fimbrial gene product. *EMBO J* **20**, 4854-62 (2001).

220. Simms, A.N. & Mobley, H.L. PapX, a P fimbrial operon-encoded inhibitor of motility in uropathogenic *Escherichia coli*. *Infect Immun* **76**, 4833-41 (2008).
221. Reiss, D.J. & Mobley, H.L. Determination of target sequence bound by PapX, repressor of bacterial motility, in *flhD* promoter using systematic evolution of ligands by exponential enrichment (SELEX) and high throughput sequencing. *J Biol Chem* **286**, 44726-38 (2011).
222. Chubiz, J.E., Golubeva, Y.A., Lin, D., Miller, L.D. & Slauch, J.M. FliZ regulates expression of the *Salmonella* pathogenicity island 1 invasion locus by controlling HilD protein activity in *Salmonella enterica* serovar typhimurium. *J Bacteriol* **192**, 6261-70 (2010).
223. Pescaretti Mde, L., Lopez, F.E., Morero, R.D. & Delgado, M.A. Transcriptional autoregulation of the RcsCDB phosphorelay system in *Salmonella enterica* serovar Typhimurium. *Microbiology* **156**, 3513-21 (2010).
224. Iyoda, S., Kamidoi, T., Hirose, K., Kutsukake, K. & Watanabe, H. A flagellar gene *fliZ* regulates the expression of invasion genes and virulence phenotype in *Salmonella enterica* serovar Typhimurium. *Microb Pathog* **30**, 81-90 (2001).
225. Kage, H., Takaya, A., Ohya, M. & Yamamoto, T. Coordinated regulation of expression of *Salmonella* pathogenicity island 1 and flagellar type III secretion systems by ATP-dependent ClpXP protease. *J Bacteriol* **190**, 2470-8 (2008).
226. Takaya, A., Kubota, Y., Isogai, E. & Yamamoto, T. Degradation of the HilC and HilD regulator proteins by ATP-dependent Lon protease leads to downregulation of *Salmonella* pathogenicity island 1 gene expression. *Mol Microbiol* **55**, 839-52 (2005).
227. Saini, S., Pearl, J.A. & Rao, C.V. Role of FimW, FimY, and FimZ in regulating the expression of type I fimbriae in *Salmonella enterica* serovar Typhimurium. *J Bacteriol* **191**, 3003-10 (2009).
228. Bustamante, V.H. *et al.* HilD-mediated transcriptional cross-talk between SPI-1 and SPI-2. *Proc Natl Acad Sci U S A* **105**, 14591-6 (2008).
229. Deiwick, J. *et al.* Mutations in *Salmonella* pathogenicity island 2 (SPI2) genes affecting transcription of SPI1 genes and resistance to antimicrobial agents. *J Bacteriol* **180**, 4775-80 (1998).
230. Kuhle, V. & Hensel, M. Cellular microbiology of intracellular *Salmonella enterica*: functions of the type III secretion system encoded by *Salmonella* pathogenicity island 2. *Cell Mol Life Sci* **61**, 2812-26 (2004).
231. Karmali, M.A. *et al.* The association between idiopathic hemolytic uremic syndrome and infection by verotoxin-producing *Escherichia coli*. *J Infect Dis* **151**, 775-82 (1985).
232. Karmali, M.A. Infection by verocytotoxin-producing *Escherichia coli*. *Clin Microbiol Rev* **2**, 15-38 (1989).
233. Coombes, B.K., Gilmour, M.W. & Goodman, C.D. The evolution of virulence in non-O157 shiga toxin-producing *Escherichia coli*. *Front Microbiol* **2**, 90 (2011).
234. Karmali, M.A., Petric, M., Lim, C., Fleming, P.C. & Steele, B.T. *Escherichia coli* cytotoxin, haemolytic-uraemic syndrome, and haemorrhagic colitis. *Lancet* **2**, 1299-1300 (1983).

235. Griffin, P.M. & Tauxe, R.V. The epidemiology of infections caused by *Escherichia coli* O157:H7, other enterohemorrhagic *E. coli*, and the associated hemolytic uremic syndrome. *Epidemiol Rev* **13**, 60-98 (1991).
236. Karch, H., Bielaszewska, M., Bitzan, M. & Schmidt, H. Epidemiology and diagnosis of Shiga toxin-producing *Escherichia coli* infections. *Diagn Microbiol Infect Dis* **34**, 229-43 (1999).
237. Coombes, B.K. *et al.* Molecular analysis as an aid to assess the public health risk of non-O157 Shiga toxin-producing *Escherichia coli* strains. *Appl Environ Microbiol* **74**, 2153-60 (2008).
238. Baumler, A.J. & Heffron, F. Identification and sequence analysis of *lpfABCDE*, a putative fimbrial operon of *Salmonella typhimurium*. *J Bacteriol* **177**, 2087-97 (1995).
239. Doughty, S. *et al.* Identification of a novel fimbrial gene cluster related to long polar fimbriae in locus of enterocyte effacement-negative strains of enterohemorrhagic *Escherichia coli*. *Infect Immun* **70**, 6761-9 (2002).
240. Macnab, R.M. Flagella and motility. In Neidhardt, F. (ed.), *Escherichia coli and Salmonella: Cellular and Molecular Biology*. pp. 123–145. (American Society for Microbiology, Washington, DC, 1996).
241. Akerley, B.J., Cotter, P.A. & Miller, J.F. Ectopic expression of the flagellar regulon alters development of the Bordetella-host interaction. *Cell* **80**, 611-20 (1995).
242. Datsenko, K.A. & Wanner, B.L. One-step inactivation of chromosomal genes in *Escherichia coli* K-12 using PCR products. *Proc Natl Acad Sci U S A* **97**, 6640-5 (2000).
243. Beeston, A.L. & Surette, M.G. pfs-dependent regulation of autoinducer 2 production in *Salmonella enterica* serovar Typhimurium. *J Bacteriol* **184**, 3450-6 (2002).
244. Guzman, L.M., Belin, D., Carson, M.J. & Beckwith, J. Tight regulation, modulation, and high-level expression by vectors containing the arabinose PBAD promoter. *J Bacteriol* **177**, 4121-30 (1995).
245. Pearson, M.M. & Mobley, H.L. Repression of motility during fimbrial expression: identification of 14 *mrpJ* gene paralogues in *Proteus mirabilis*. *Mol Microbiol* **69**, 548-58 (2008).
246. Sauer, F.G., Mulvey, M.A., Schilling, J.D., Martinez, J.J. & Hultgren, S.J. Bacterial pili: molecular mechanisms of pathogenesis. *Curr Opin Microbiol* **3**, 65-72 (2000).
247. Mulvey, M.A. *et al.* Induction and evasion of host defenses by type 1-piliated uropathogenic *Escherichia coli*. *Science* **282**, 1494-7 (1998).
248. Roe, A.J., Currie, C., Smith, D.G. & Gally, D.L. Analysis of type 1 fimbriae expression in verotoxigenic *Escherichia coli*: a comparison between serotypes O157 and O26. *Microbiology* **147**, 145-52 (2001).
249. Mahajan, A. *et al.* An investigation of the expression and adhesin function of H7 flagella in the interaction of *Escherichia coli* O157 : H7 with bovine intestinal epithelium. *Cell Microbiol* **11**, 121-37 (2009).

250. Tomoyasu, T. *et al.* The ClpXP ATP-dependent protease regulates flagellum synthesis in *Salmonella enterica* serovar typhimurium. *J Bacteriol* **184**, 645-53 (2002).
251. Kitagawa, R., Takaya, A. & Yamamoto, T. Dual regulatory pathways of flagellar gene expression by ClpXP protease in enterohaemorrhagic *Escherichia coli*. *Microbiology* **157**, 3094-103 (2011).
252. Takaya, A. *et al.* YdiV: a dual function protein that targets FlhDC for ClpXP-dependent degradation by promoting release of DNA-bound FlhDC complex. *Mol Microbiol* **83**, 1268-84 (2012).
253. Wada, T. *et al.* EAL domain protein YdiV acts as an anti-FlhD4C2 factor responsible for nutritional control of the flagellar regulon in *Salmonella enterica* serovar Typhimurium. *J Bacteriol* **193**, 1600-11 (2011).
254. Stafford, G.P., Ogi, T. & Hughes, C. Binding and transcriptional activation of non-flagellar genes by the *Escherichia coli* flagellar master regulator FlhD2C2. *Microbiology* **151**, 1779-88 (2005).
255. Cornelis, G.R. The type III secretion injectisome. *Nat Rev Microbiol* **4**, 811-25 (2006).
256. Thomas, N.A. *et al.* CesT is a multi-effector chaperone and recruitment factor required for the efficient type III secretion of both LEE- and non-LEE-encoded effectors of enteropathogenic *Escherichia coli*. *Mol Microbiol* **57**, 1762-79 (2005).
257. Gauthier, A. & Finlay, B.B. Translocated intimin receptor and its chaperone interact with ATPase of the type III secretion apparatus of enteropathogenic *Escherichia coli*. *J Bacteriol* **185**, 6747-55 (2003).
258. Chen, L. *et al.* Substrate-activated conformational switch on chaperones encodes a targeting signal in type III secretion. *Cell Rep* **3**, 709-15 (2013).
259. Coburn, B., Grassl, G.A. & Finlay, B.B. *Salmonella*, the host and disease: a brief review. *Immunol Cell Biol* **85**, 112-8 (2007).
260. Majowicz, S.E. *et al.* The global burden of nontyphoidal *Salmonella* gastroenteritis. *Clin Infect Dis* **50**, 882-9 (2010).
261. Lilic, M., Vujanac, M. & Stebbins, C.E. A common structural motif in the binding of virulence factors to bacterial secretion chaperones. *Mol Cell* **21**, 653-64 (2006).
262. Stebbins, C.E. & Galan, J.E. Maintenance of an unfolded polypeptide by a cognate chaperone in bacterial type III secretion. *Nature* **414**, 77-81 (2001).
263. Luo, Y. *et al.* Structural and biochemical characterization of the type III secretion chaperones CesT and SigE. *Nat Struct Biol* **8**, 1031-6 (2001).
264. Darwin, K.H., Robinson, L.S. & Miller, V.L. SigE is a chaperone for the *Salmonella enterica* serovar Typhimurium invasion protein SigD. *J Bacteriol* **183**, 1452-4 (2001).
265. Coombes, B.K., Brown, N.F., Kujat-Choy, S., Vallance, B.A. & Finlay, B.B. SseA is required for translocation of *Salmonella* pathogenicity island-2 effectors into host cells. *Microbes Infect* **5**, 561-70 (2003).
266. Tucker, S.C. & Galan, J.E. Complex function for SicA, a *Salmonella enterica* serovar typhimurium type III secretion-associated chaperone. *J Bacteriol* **182**, 2262-8 (2000).

267. Moraes, T.F., Spreter, T. & Strynadka, N.C. Piecing together the type III injectisome of bacterial pathogens. *Curr Opin Struct Biol* **18**, 258-66 (2008).
268. Otwinowski, Z., & Minor, W. *Processing of X-ray diffraction data collected in oscillation mode*. In *Methods in Enzymology: Macromolecular Crystallography, Part A*, Carter CWJ, Sweet RM Eds., Academic Press, New York (1997).
269. Stein, N. CHAINSAW: a program for mutating pdb files used as templates in molecular replacement. *J. Appl. Cryst.* **41**, 641-643 (2008).
270. Winn, M.D. *et al.* Overview of the CCP4 suite and current developments. *Acta Crystallogr D Biol Crystallogr* **67**, 235-42 (2011).
271. Adams, P.D. *et al.* PHENIX: building new software for automated crystallographic structure determination. *Acta Crystallogr D Biol Crystallogr* **58**, 1948-54 (2002).
272. Emsley, P. & Cowtan, K. Coot: model-building tools for molecular graphics. *Acta Crystallogr D Biol Crystallogr* **60**, 2126-32 (2004).
273. Krissinel, E. & Henrick, K. Secondary-structure matching (SSM), a new tool for fast protein structure alignment in three dimensions. *Acta Crystallogr D Biol Crystallogr* **60**, 2256-68 (2004).
274. Krissinel, E. & Henrick, K. Inference of macromolecular assemblies from crystalline state. *J Mol Biol* **372**, 774-97 (2007).
275. Walker, J.E., Saraste, M., Runswick, M.J. & Gay, N.J. Distantly related sequences in the alpha- and beta-subunits of ATP synthase, myosin, kinases and other ATP-requiring enzymes and a common nucleotide binding fold. *EMBO J* **1**, 945-51 (1982).
276. Gibbons, C., Montgomery, M.G., Leslie, A.G. & Walker, J.E. The structure of the central stalk in bovine F(1)-ATPase at 2.4 Å resolution. *Nat Struct Biol* **7**, 1055-61 (2000).
277. Lee, S. *et al.* The structure of ClpB: a molecular chaperone that rescues proteins from an aggregated state. *Cell* **115**, 229-40 (2003).
278. Baison-Olmo, F., Cardenal-Munoz, E. & Ramos-Morales, F. PipB2 is a substrate of the *Salmonella* pathogenicity island 1-encoded type III secretion system. *Biochem Biophys Res Commun* **423**, 240-6 (2012).
279. Swietnicki, W. *et al.* Identification of small-molecule inhibitors of Yersinia pestis Type III secretion system YscN ATPase. *PLoS One* **6**, e19716 (2011).
280. Wray, C. & Sojka, W.J. Experimental *Salmonella typhimurium* infection in calves. *Res Vet Sci* **25**, 139-43 (1978).
281. Edwards, R.A., Keller, L.H. & Schifferli, D.M. Improved allelic exchange vectors and their use to analyze 987P fimbria gene expression. *Gene* **207**, 149-57 (1998).
282. Coombes, B.K. *et al.* Genetic and molecular analysis of GogB, a phage-encoded type III-secreted substrate in *Salmonella enterica* serovar typhimurium with autonomous expression from its associated phage. *J Mol Biol* **348**, 817-30 (2005).
283. Wang, R.F. & Kushner, S.R. Construction of versatile low-copy-number vectors for cloning, sequencing and gene expression in *Escherichia coli*. *Gene* **100**, 195-9 (1991).

284. Chang, A.C. & Cohen, S.N. Construction and characterization of amplifiable multicopy DNA cloning vehicles derived from the P15A cryptic miniplasmid. *J Bacteriol* **134**, 1141-56 (1978).
285. Knodler, L.A. & Steele-Mortimer, O. The *Salmonella* effector PipB2 affects late endosome/lysosome distribution to mediate Sif extension. *Mol Biol Cell* **16**, 4108-23 (2005).
286. Minamino, T. & MacNab, R.M. Interactions among components of the *Salmonella* flagellar export apparatus and its substrates. *Mol Microbiol* **35**, 1052-64 (2000).
287. Chen, Y.L. & Hu, N.T. Function-related positioning of the type II secretion ATPase of *Xanthomonas campestris* *pv. campestris*. *PLoS One* **8**, e59123 (2013).
288. Buttner, D., Gurlebeck, D., Noel, L.D. & Bonas, U. HpaB from *Xanthomonas campestris* *pv. vesicatoria* acts as an exit control protein in type III-dependent protein secretion. *Mol Microbiol* **54**, 755-68 (2004).